

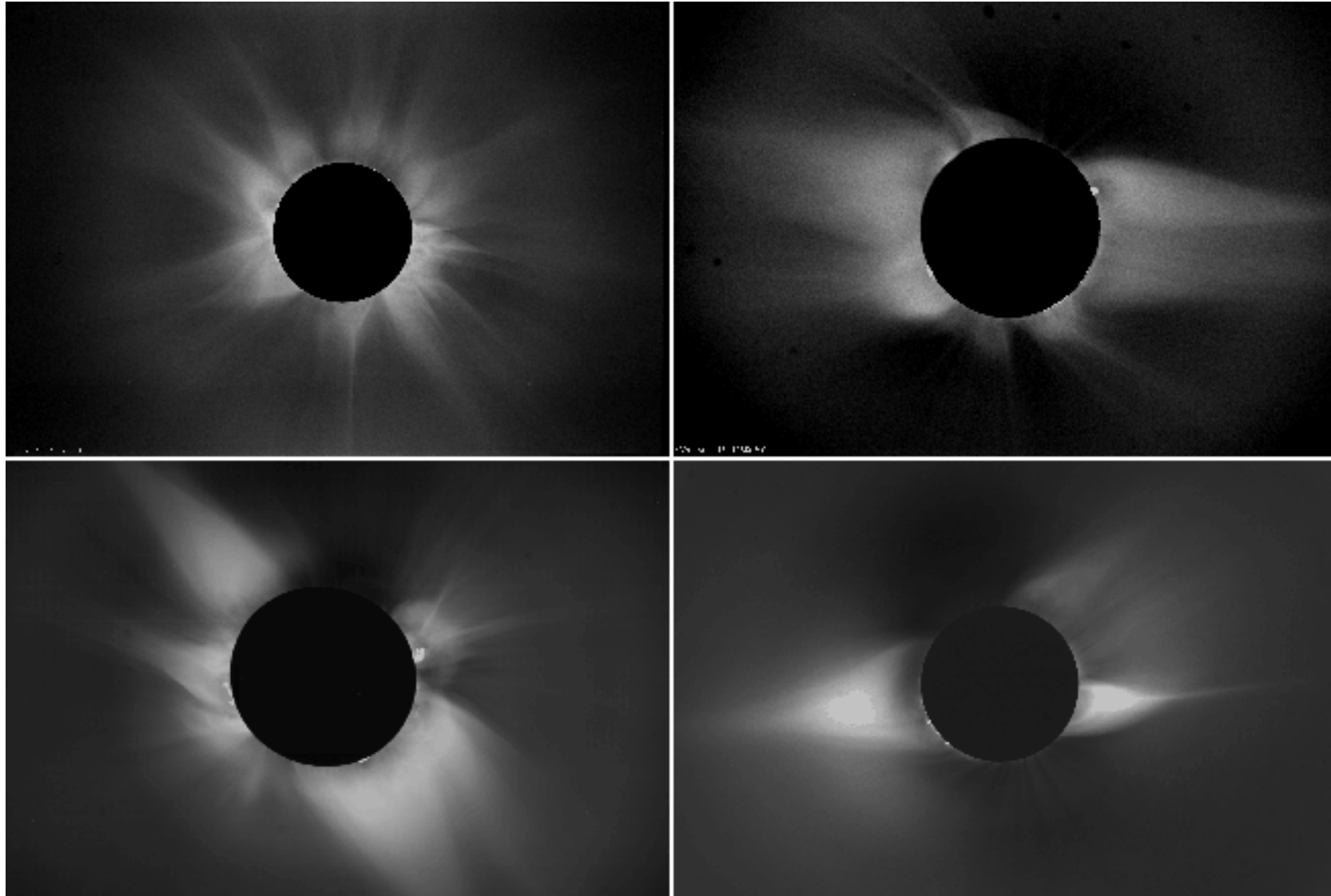
Coronagraphs

ATI 2016 - Lecture 12

Matthew Kenworthy // Leiden Observatory

Solar Corona

Solar eclipses revealed wealth of structure in outer layers of Sun



<http://celebrating200years.noaa.gov/breakthroughs/coronagraph/welcome.html>

Bernard Lyot



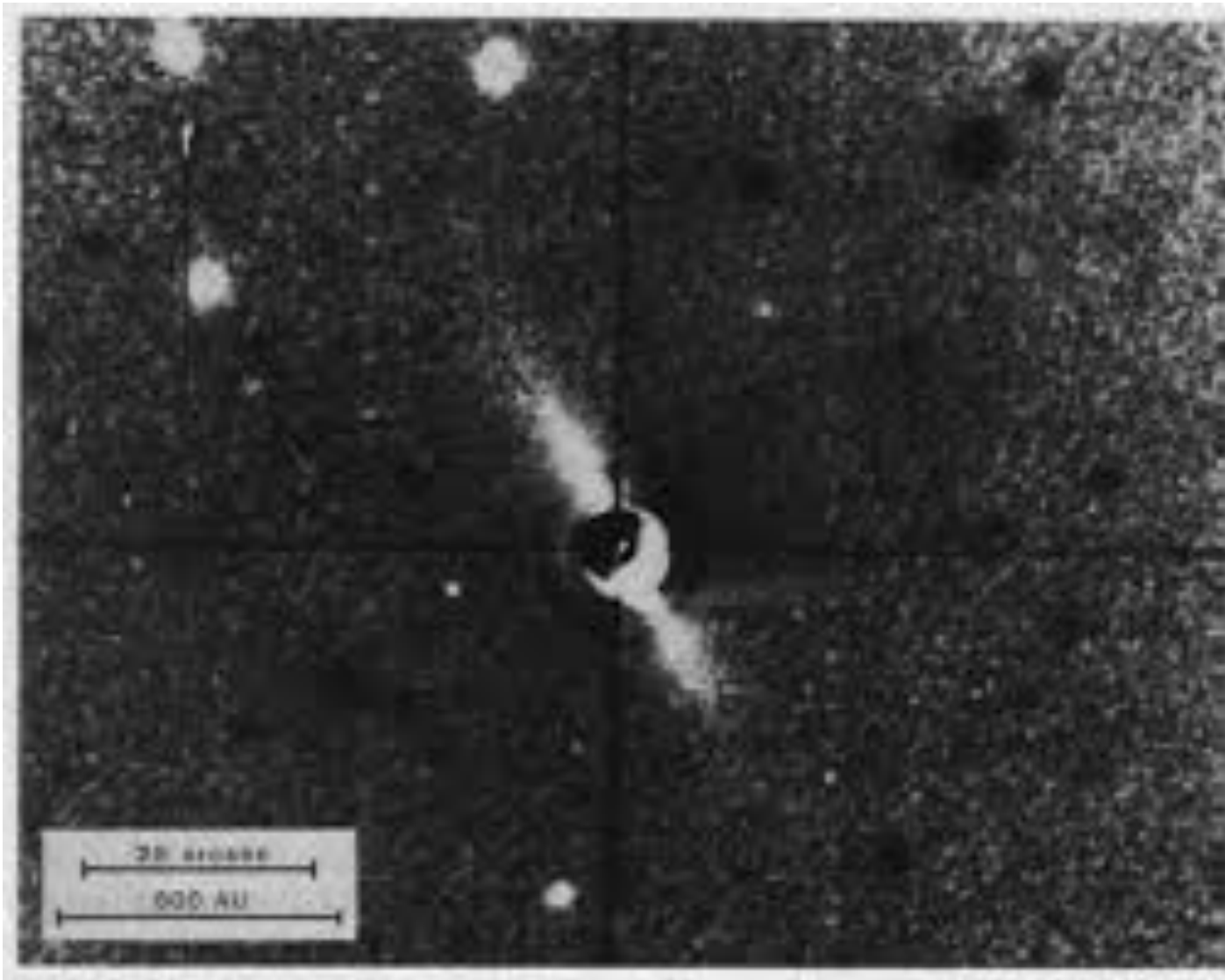
**Bernard Lyot sitting at his
Coronagraph at the Pic du Midi
observatory in France ca. 1939.**

**French astronomer and
instrument maker**

**Wanted to study the Sun's corona
without waiting for an eclipse**

**Invented the CORONAGRAPH in
1939 to block sunlight and take
photos of the corona.**

First circumstellar disk imaged in 1984



Smith and Terrile 1984

Fomalhaut Debris Disk

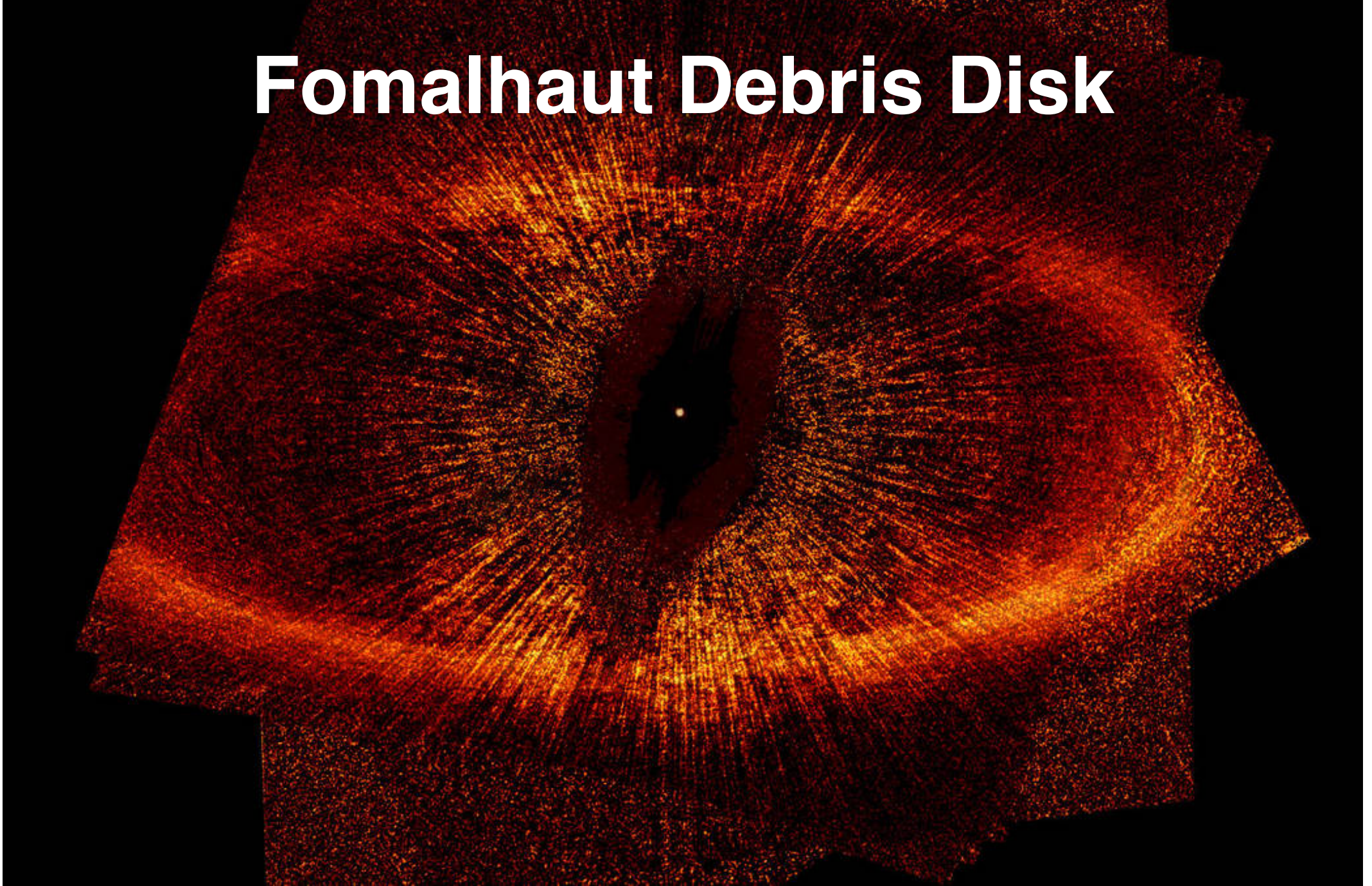
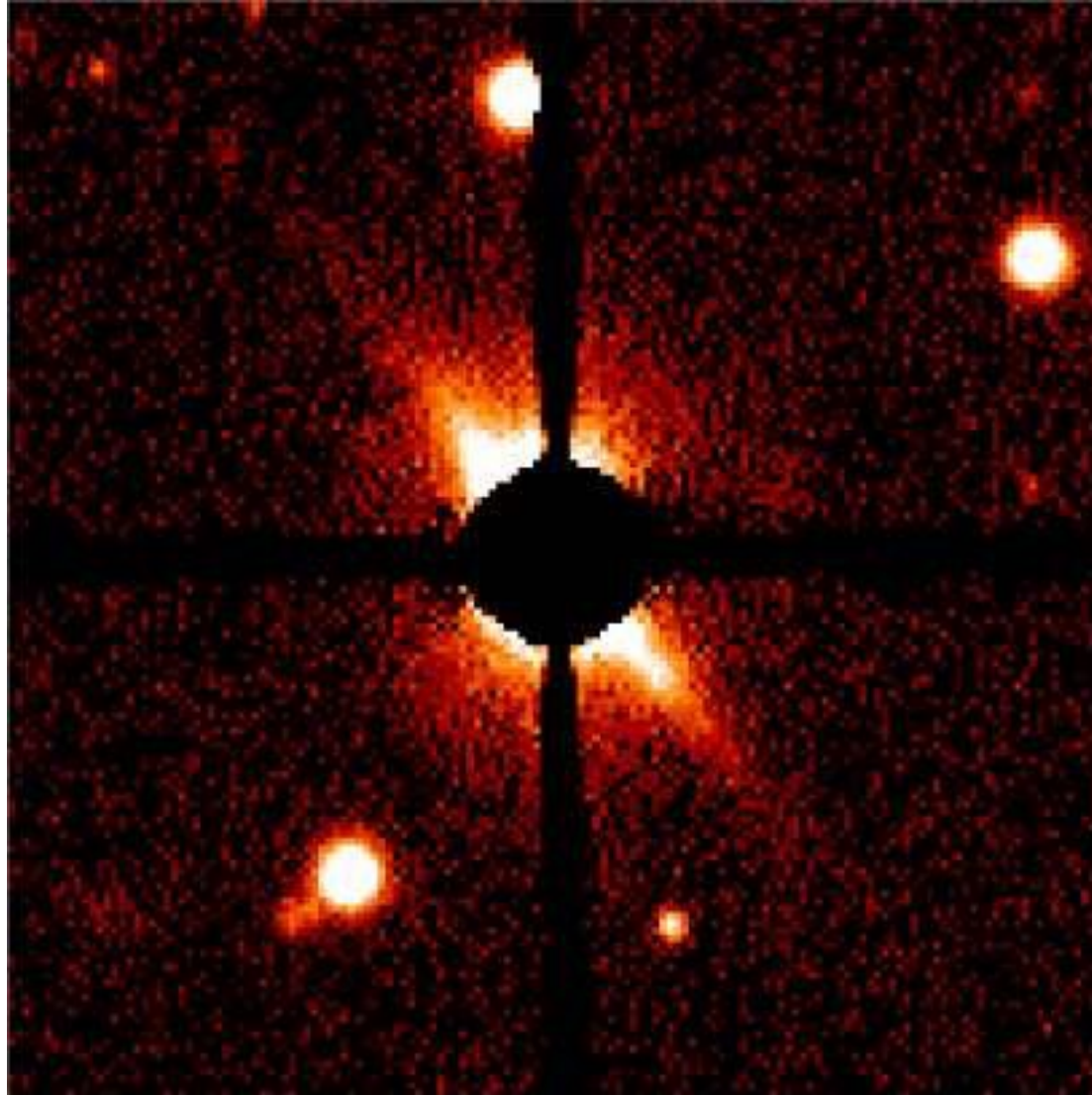


Image Credit: NASA, ESA, P. Kalas and J. Graham (University of California, Berkeley) and M. Clampin (NASA/GSFC)

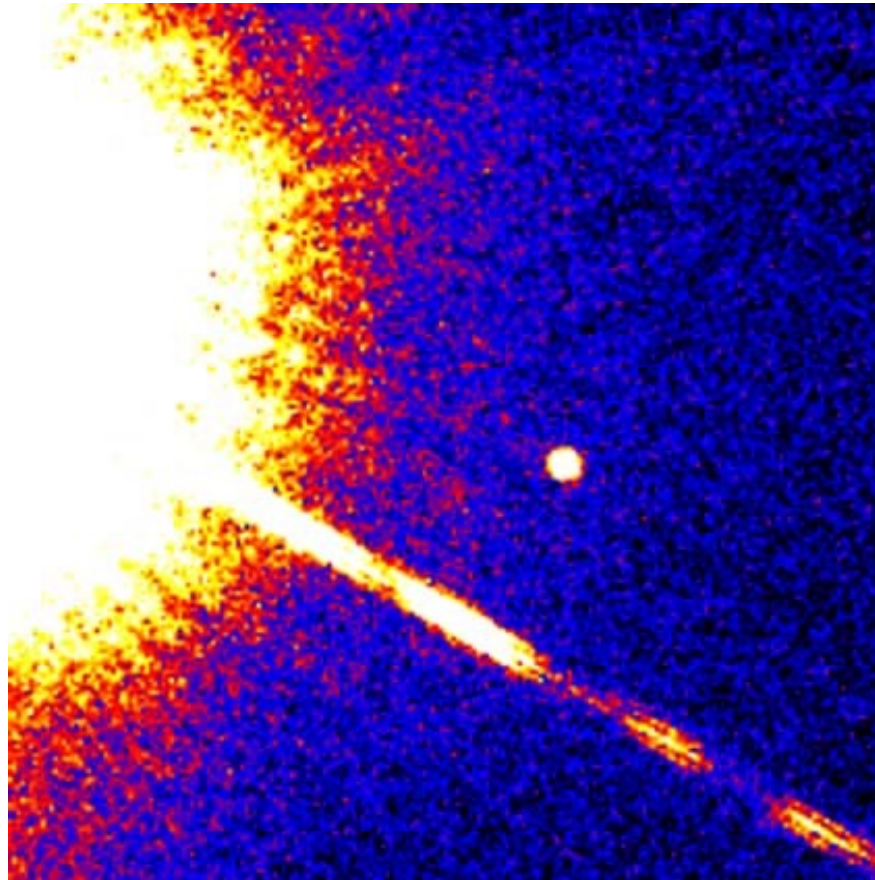
AU Mic



Paul Kalas 1990

First Brown Dwarf

Discovered in 1994 from Palomar 60 inch telescope

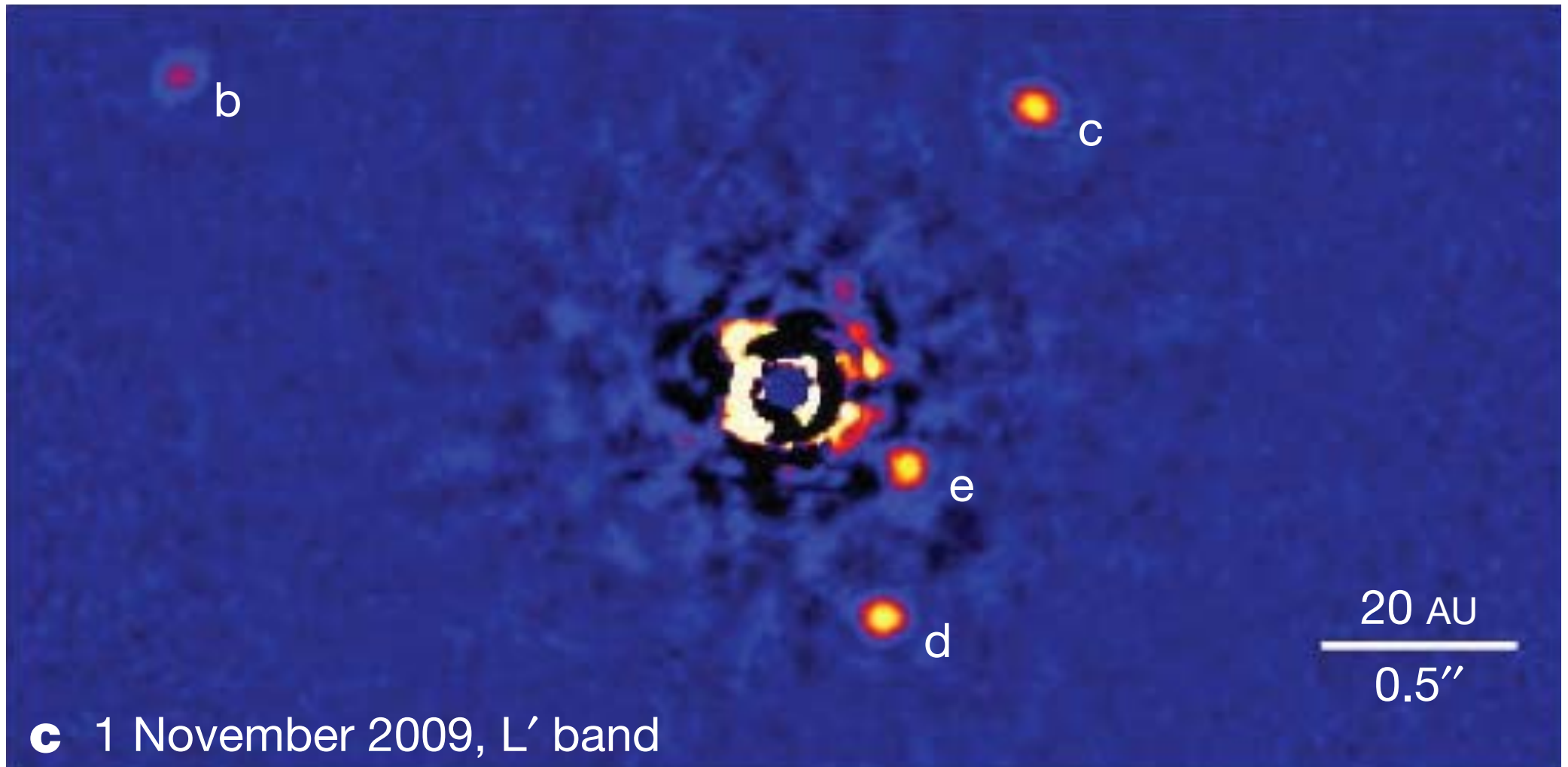


Gliese 229B - taken with HST

Credit: S. Kulkarni (Caltech), D.Golimowski (JHU) and NASA

...to planets

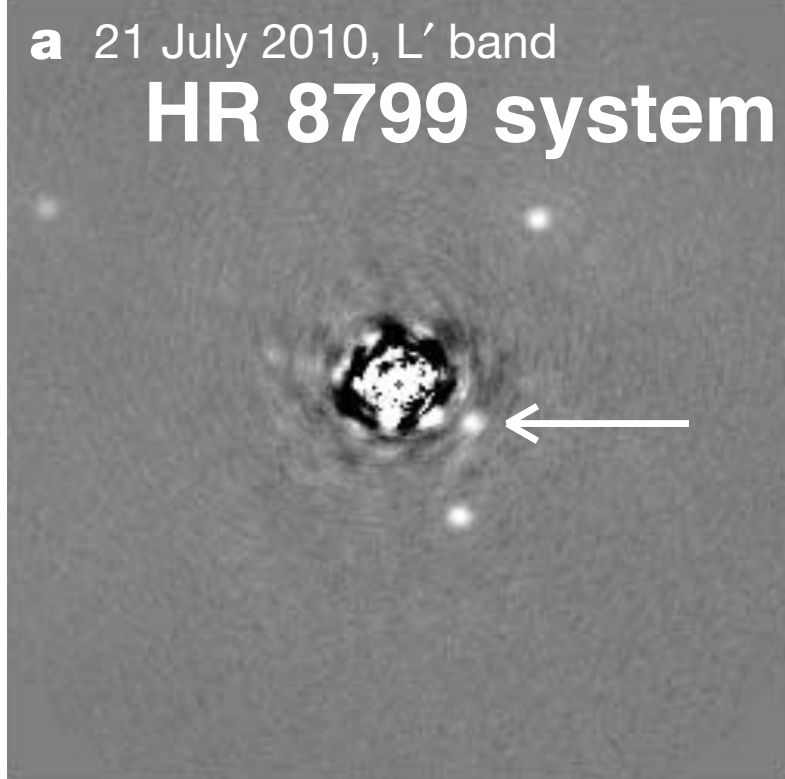
HR 8799



Marois et al. (2010)

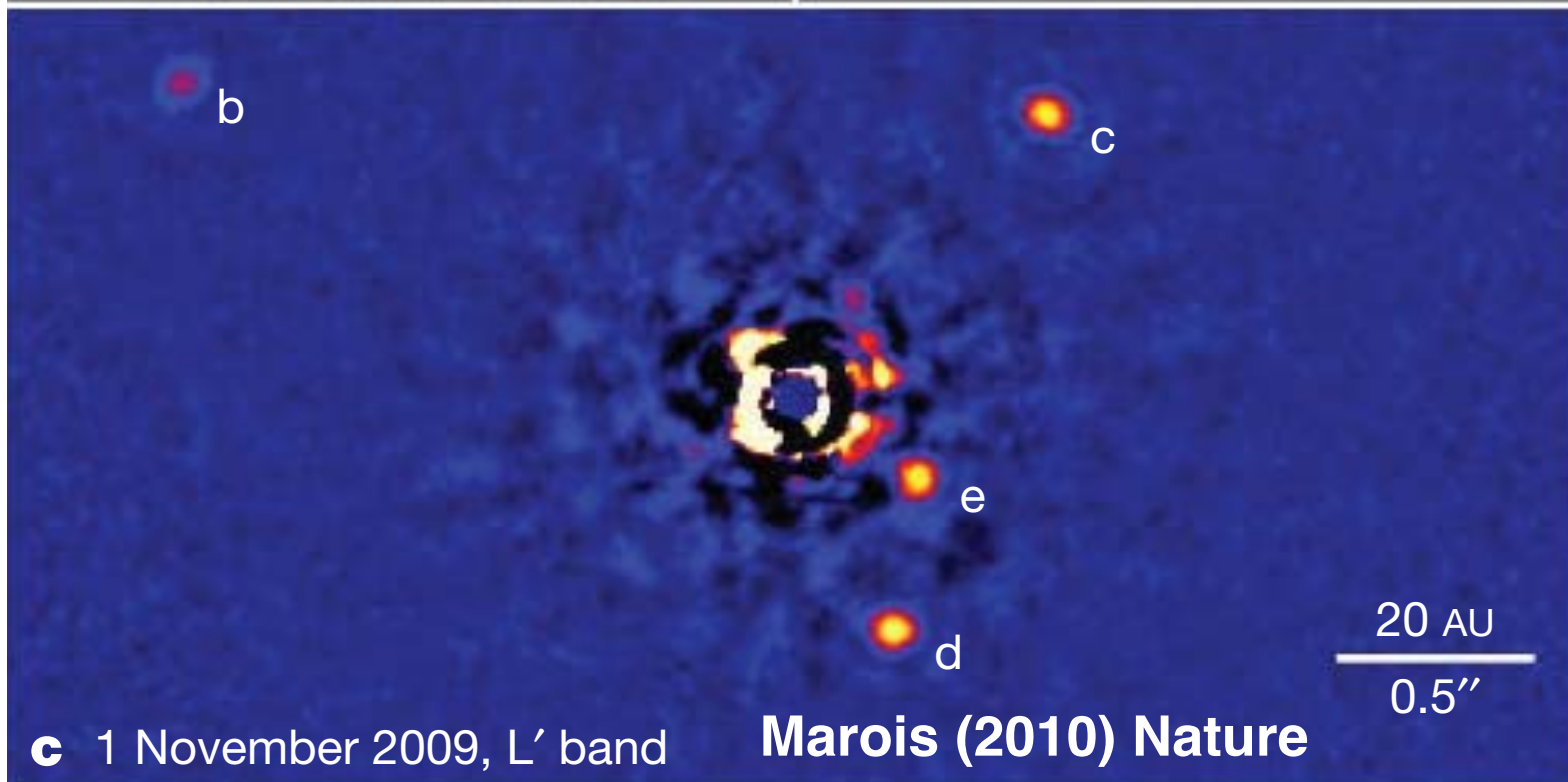
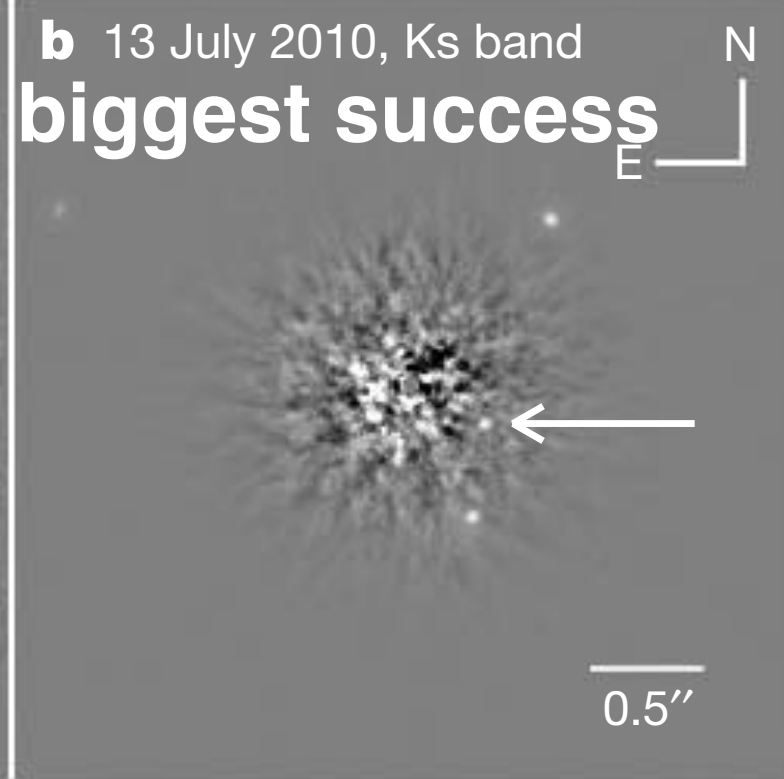
a 21 July 2010, L' band

HR 8799 system



b 13 July 2010, Ks band

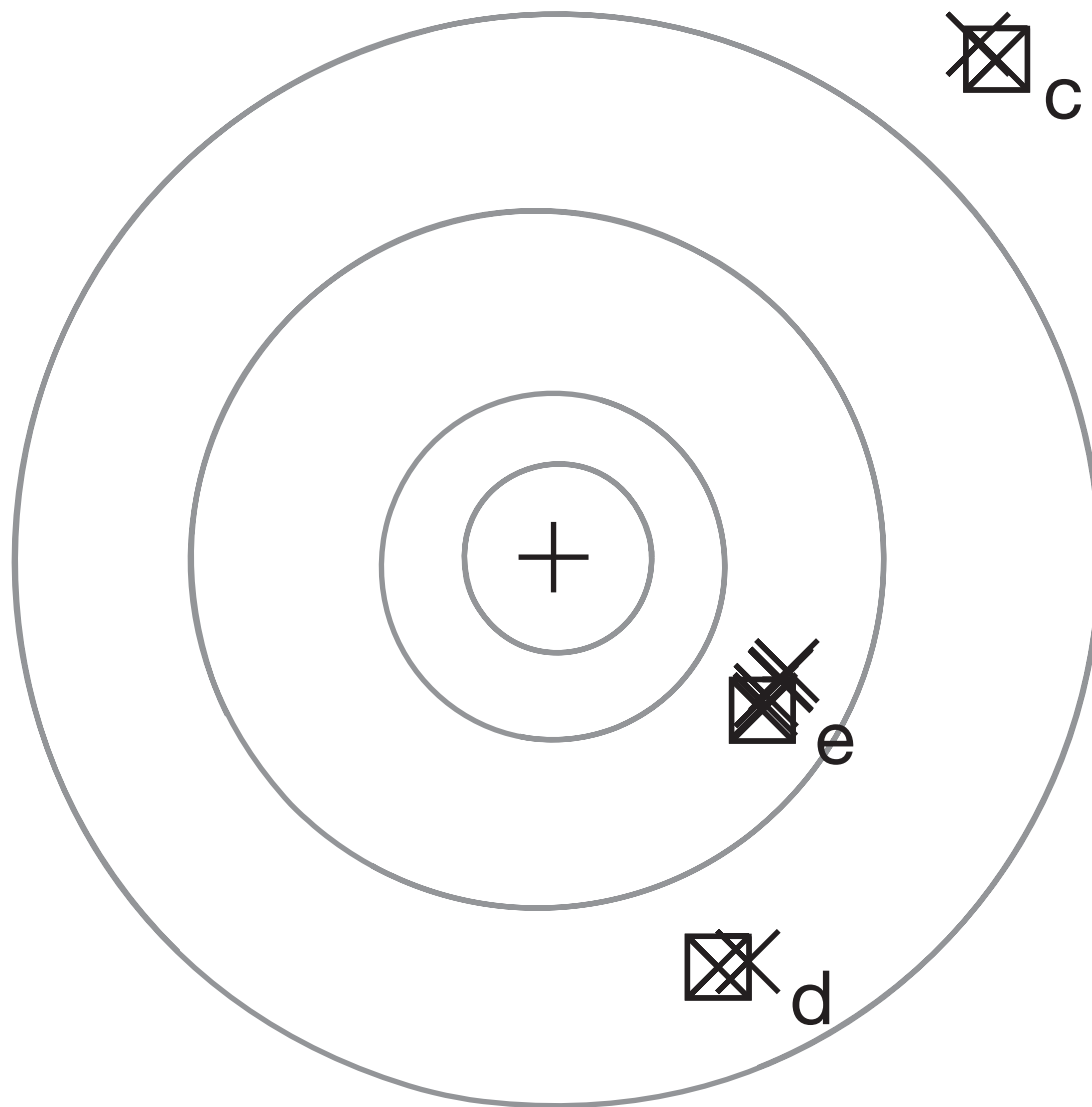
biggest success



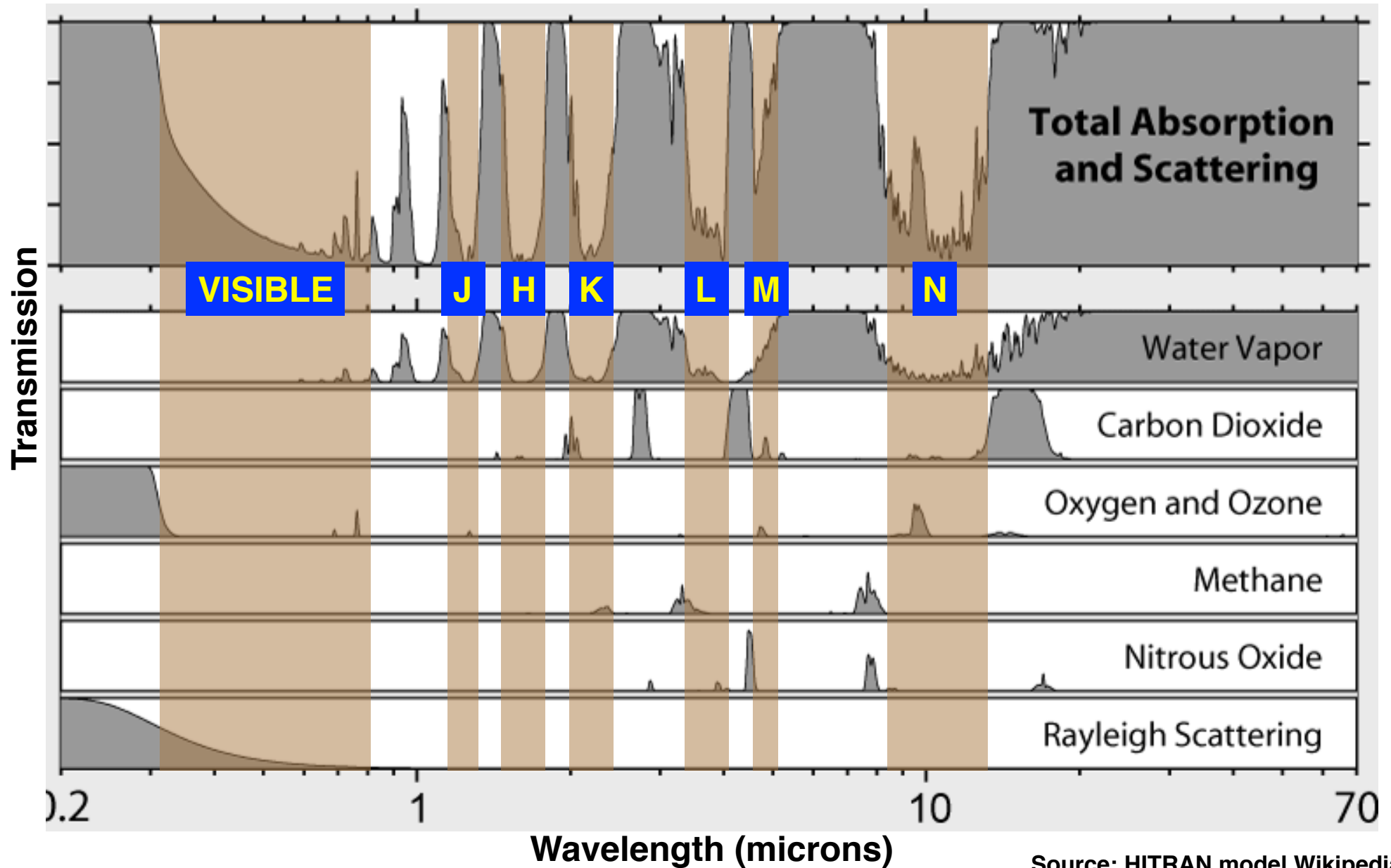
c 1 November 2009, L' band

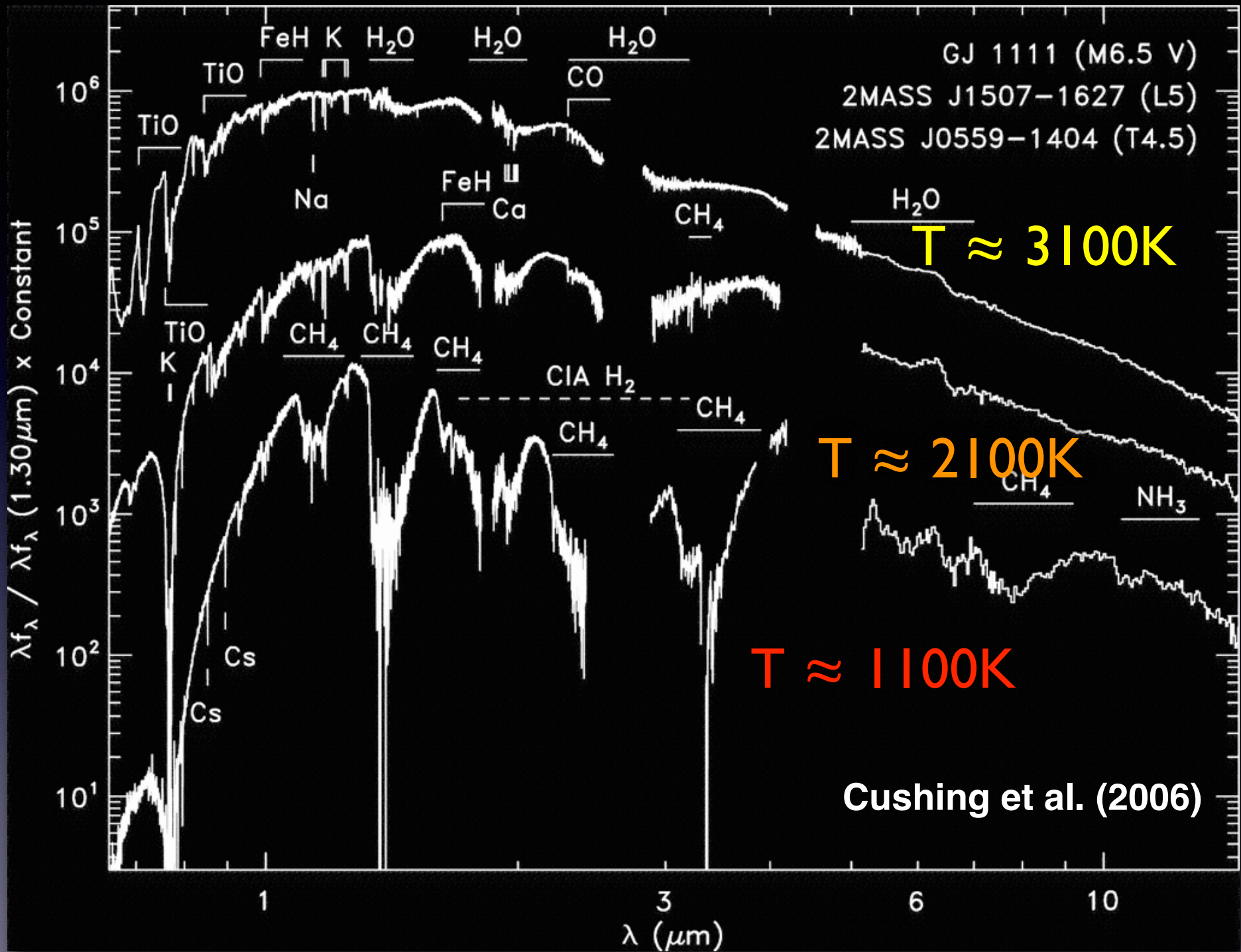
Marois (2010) Nature

Orbital Motion seen over several years

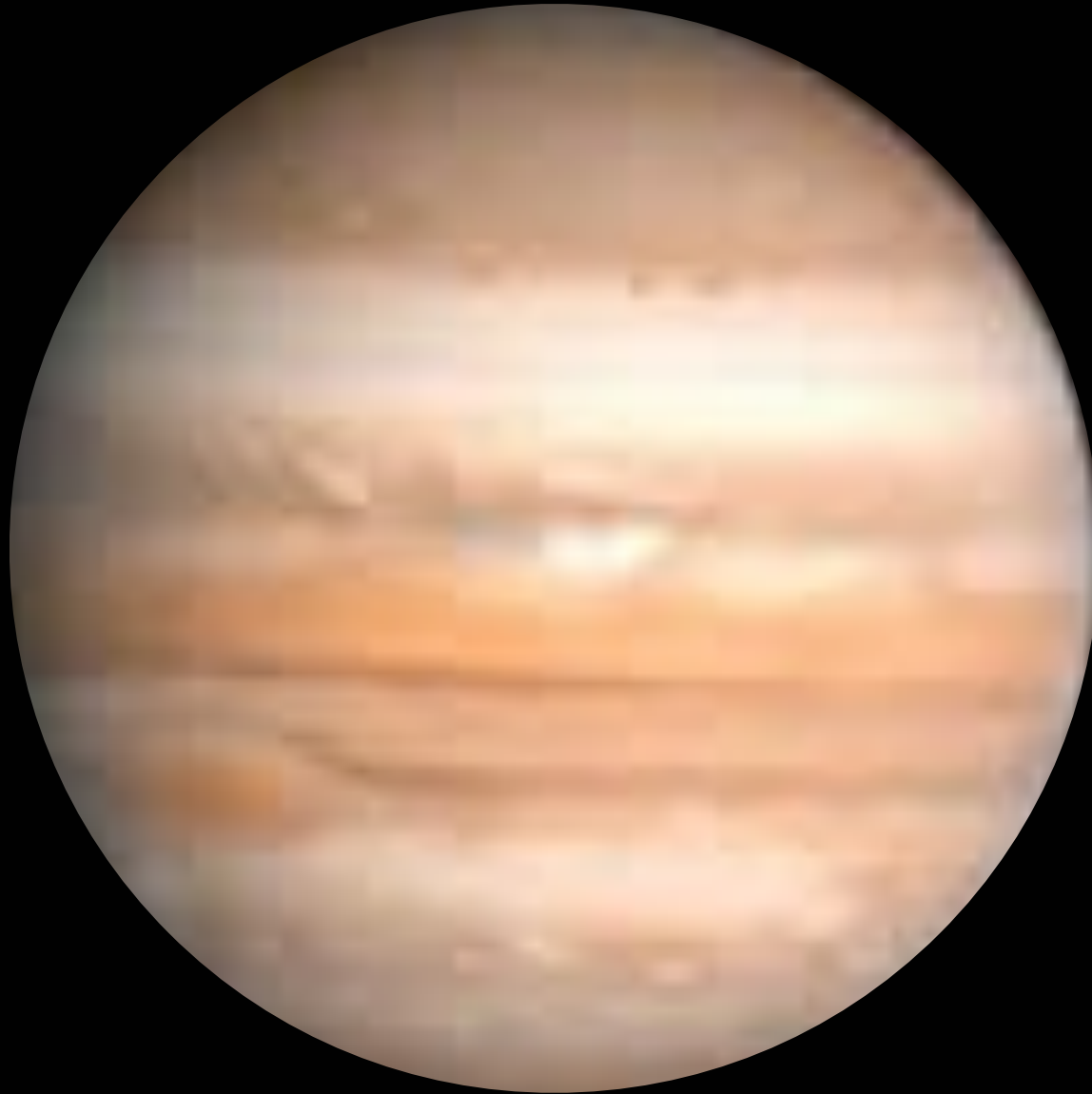


Atmospheric Transmission

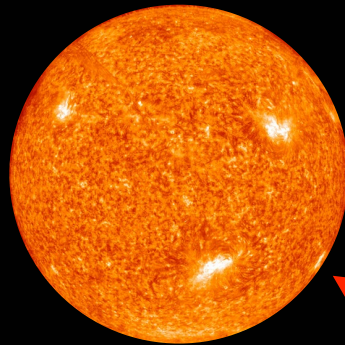




We'd like to see...



10^9 to 10^6 times brighter



1 arcsec or less



**both are unresolved sources
(maybe not the star though...)**



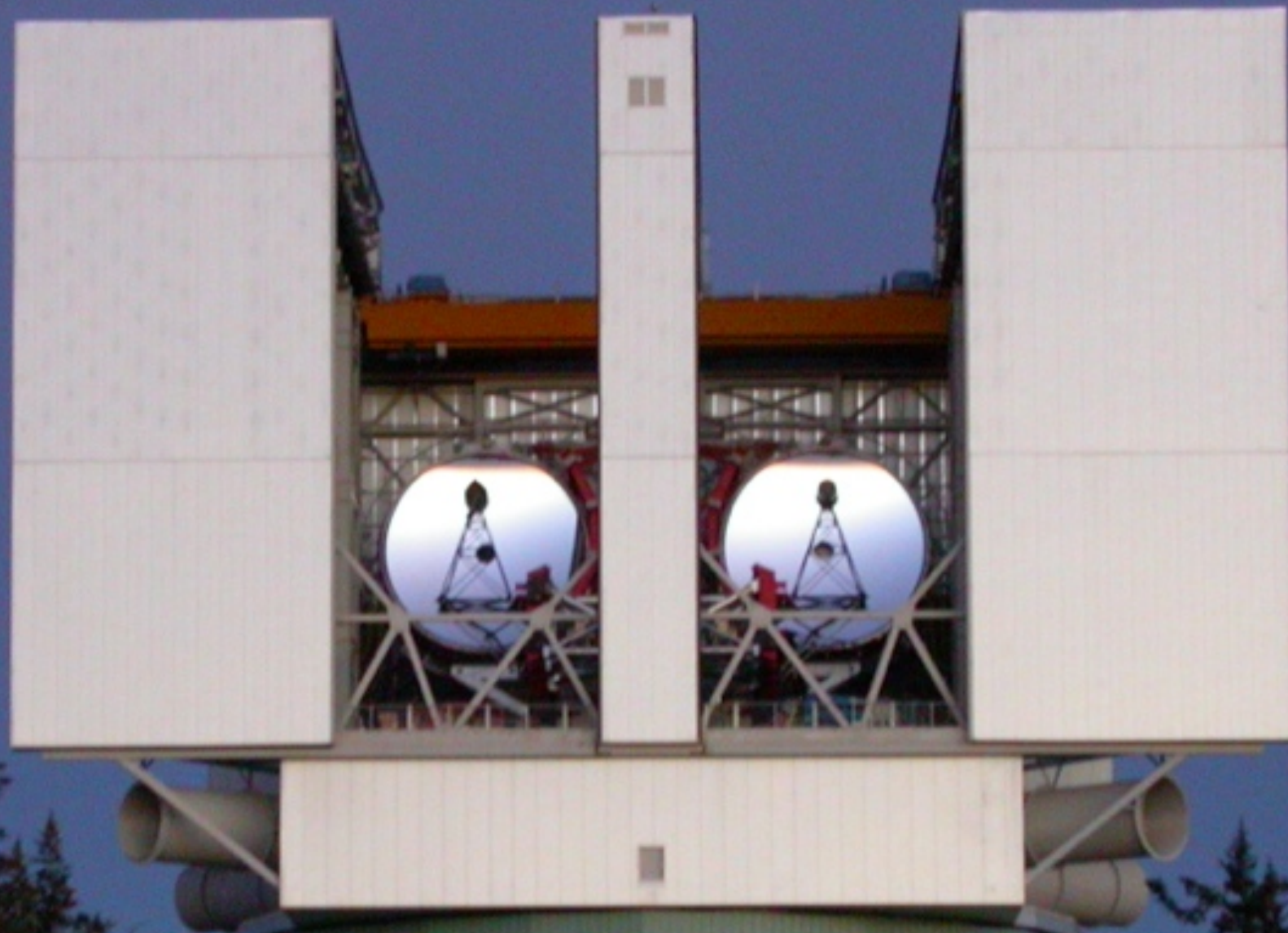
Telescopes - VLT in Chile



Large Binocular Telescope



Large Binocular Telescope



The Lingo

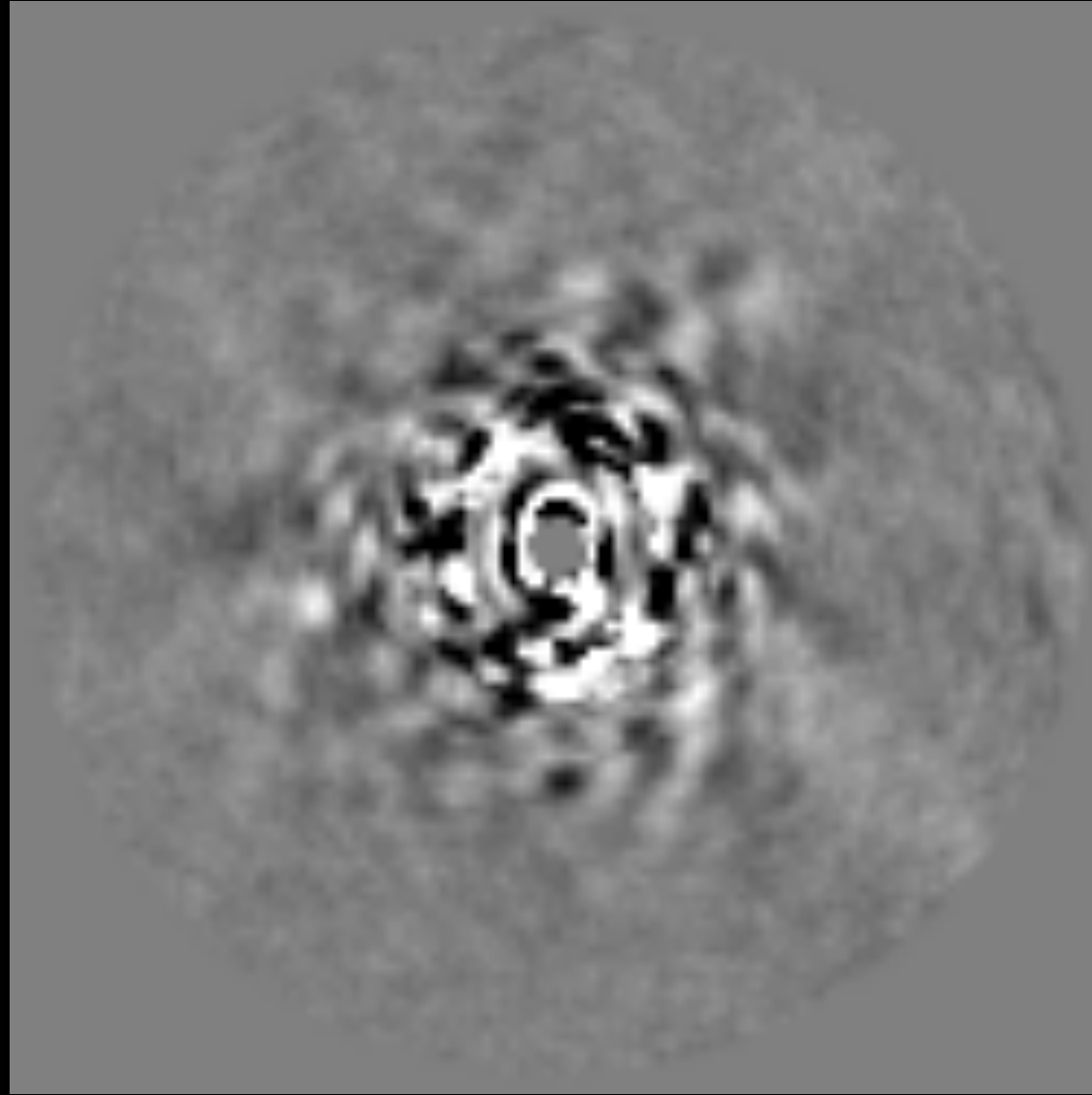
Inner Working Angle (IWA) and **Outer Working Angle (OWA)**:
Specify in units of λ/D the range of angles that the coronagraph effectively works with $>50\%$ planet transmission

Contrast (specified in delta magnitudes or number of decades):
this is the RAW contrast as seen in the PSF.
Space based coronagraphs aim for 10 decades, ground based for 5 to 6 decades.

Null order (specified as 2nd, 3rd, 4th, 5th....):
expresses how sensitive the coronagraph is to tip tilt error with the star
Higher orders are more immune to tip tilt, but have larger IWAs

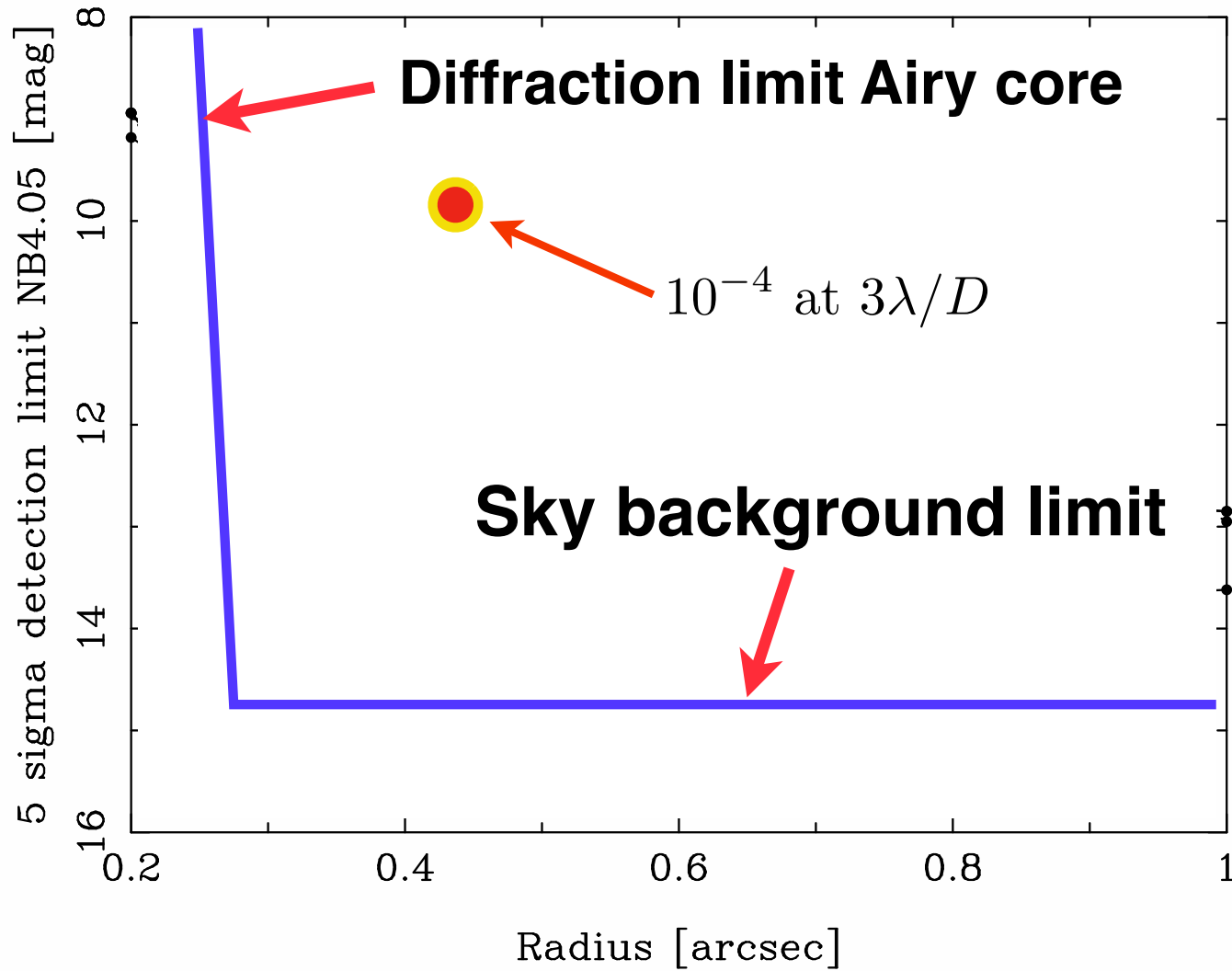
(adapted from Olivier Guyon's slides)

**Subtracting off a reference image leaves
“speckles”**



the telescope and camera “flex”

An ideal contrast curve



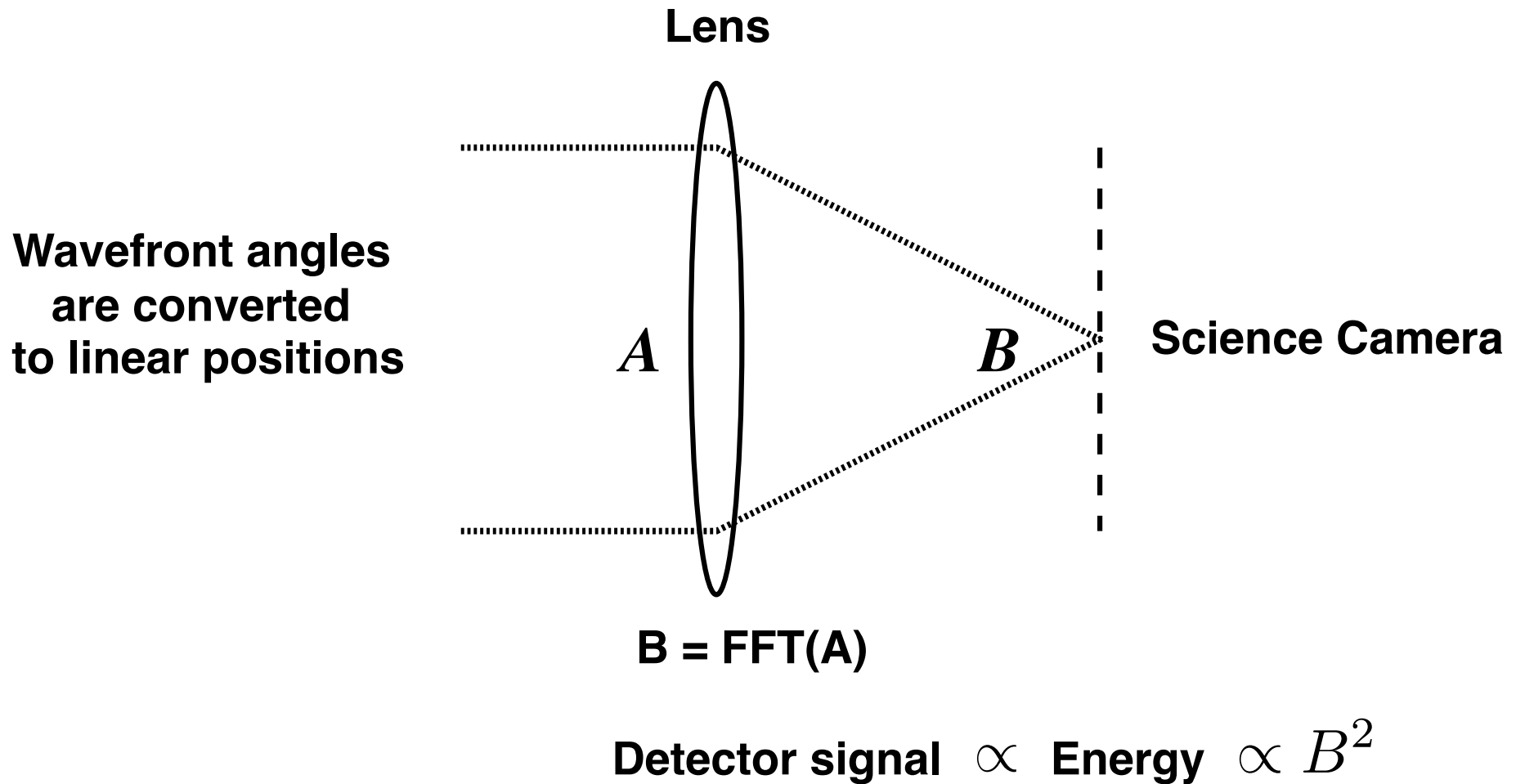
Coronagraphs are angular filters



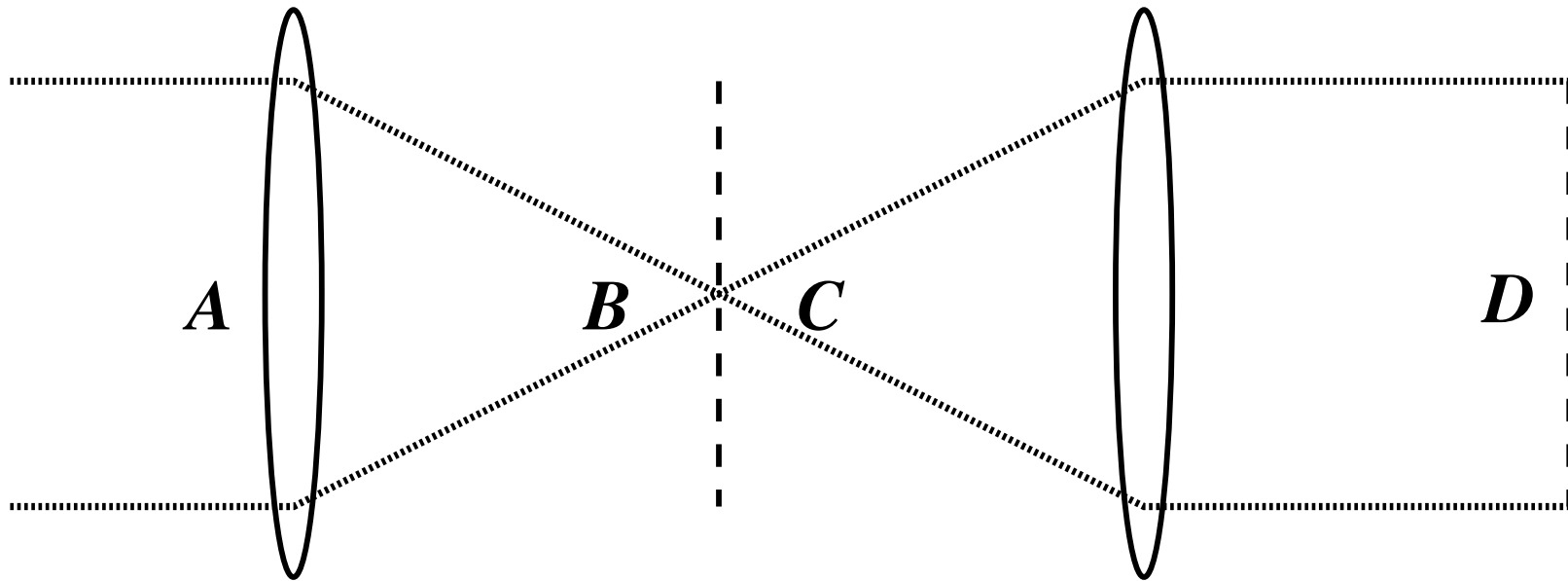
They apodize the telescope PSF

(“apodization” is Greek for ‘chopping off the foot’)

Lenses are Fourier Transform machines

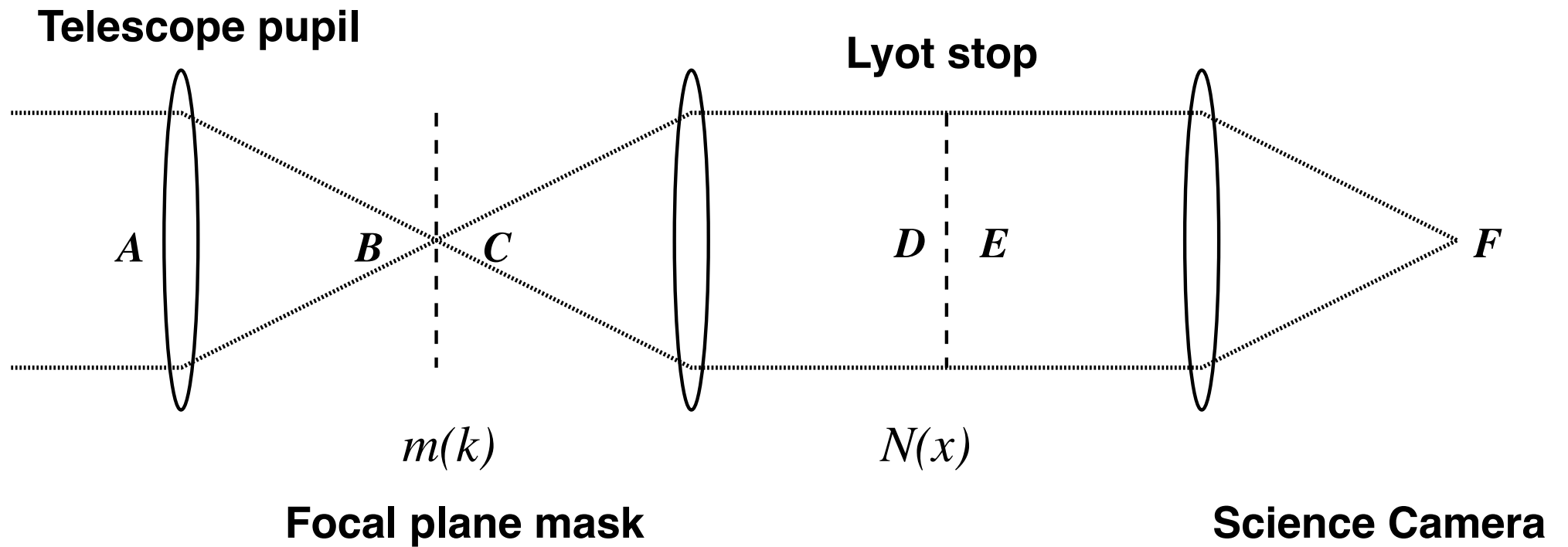


...and you go from Pupil Plane to Image Plane and back again

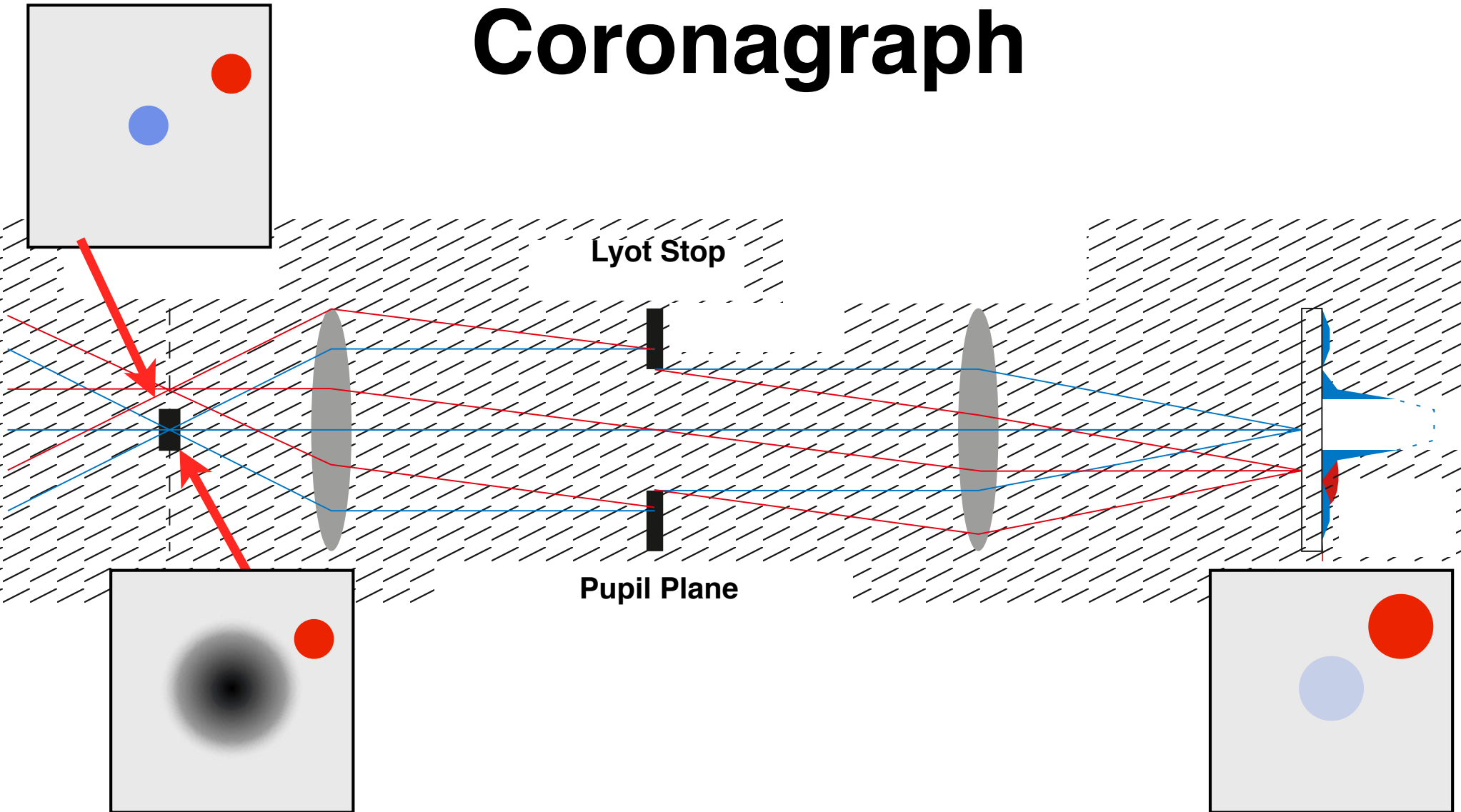


Pupil Plane \Rightarrow FFT \Rightarrow Focal Plane \Rightarrow IFFT \Rightarrow Pupil Plane

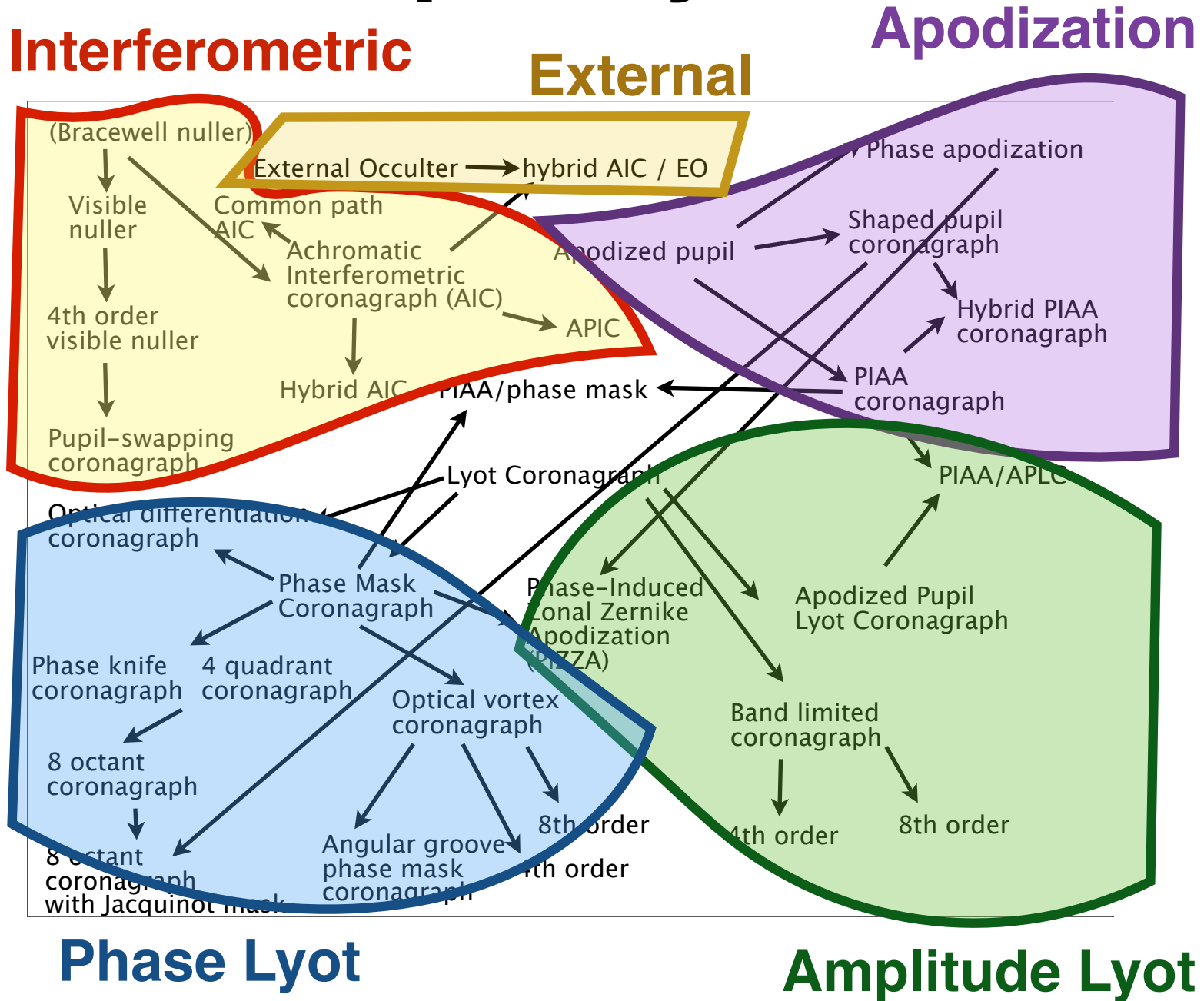
Layout of a basic coronagraph



Classical/Apodized Lyot Coronagraph



Can be split by method



Phase Lyot - 4 Quadrant Phase Mask (4QPM)

PHASE CORONAGRAPH WITH FOUR QUADRANTS. I. 148

Phase shift

2nd order null

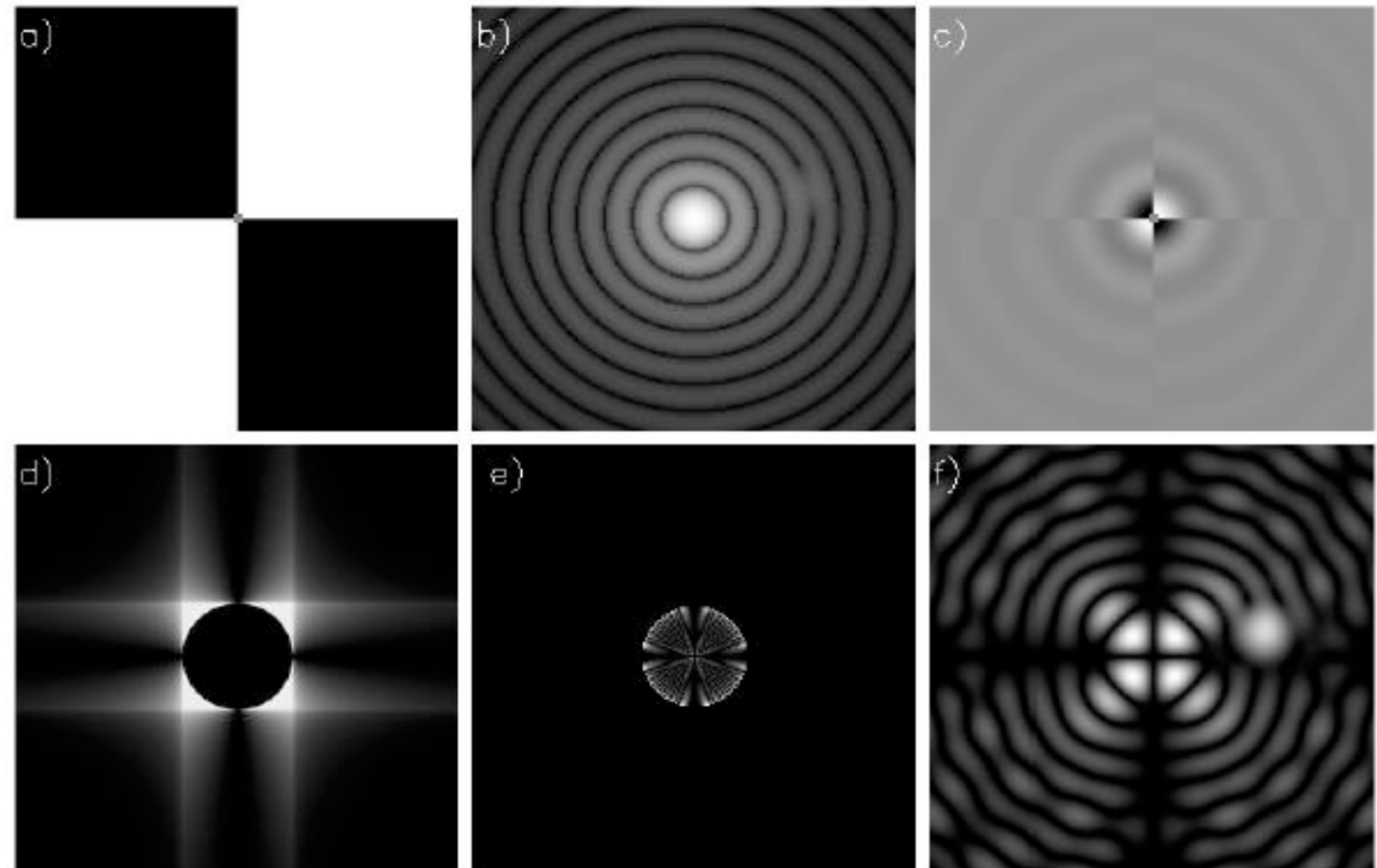
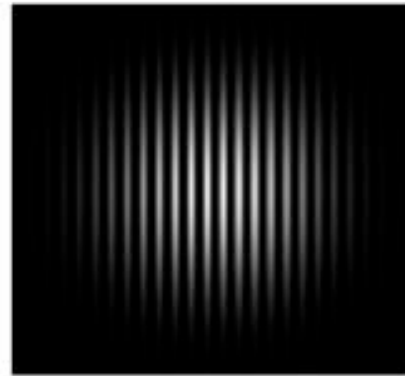


FIG. 2.—Numerical simulation illustrating the principle of the four-quadrant coronagraph. A companion 15 mag fainter (flux ratio of 10^6) is located λ/D away from the star. The individual images show (a) the shape of the phase mask (white for 0 phase shift, black for π phase shift), (b) the Airy pattern played in intensity, (c) the complex amplitude of the star phase shifted by the mask, (d) the exit pupil, (e) the exit pupil through the Lyot stop (95% of the pupil diameter), and (f) the coronagraphic image where the companion is clearly visible. Images are displayed with nonlinear scale.

Amplitude Lyot - Band Limited Mask Lyot (BL4, BL8)

A focal plane mask that moves star light into thin crescents at edge of pupil

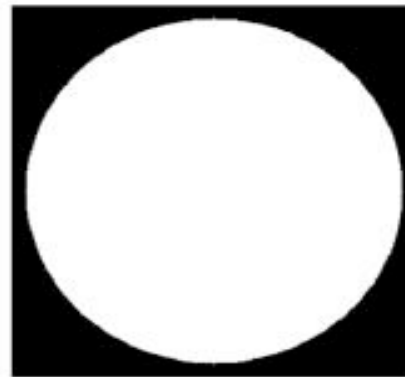
a) Mask



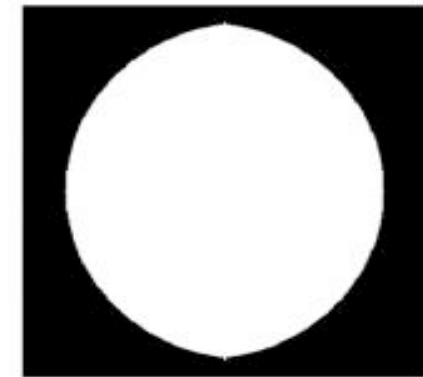
b) Conjugate of Mask Function



c) Pupil



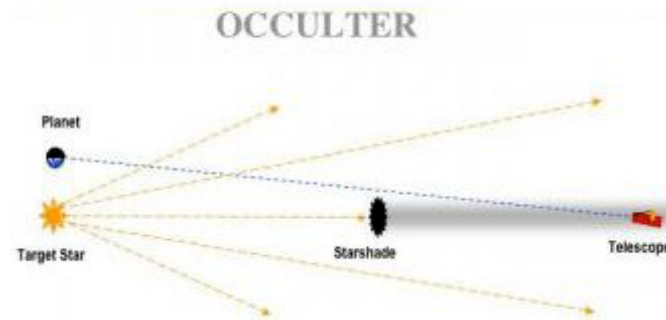
d) Lyot Stop



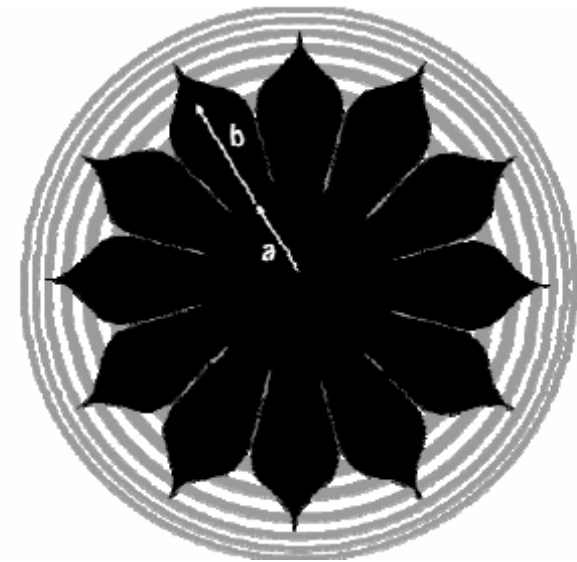
Kuchner and Traub 2002
Kuchner 2005

FIG. 4.—Simplest band-limited mask, analogous to a single-baseline nulling interferometer. (a) Mask ITF $\sin^4(x)$ multiplied by a slow taper. Dark areas are opaque. (b) Conjugate of the mask ATF (eq. [13]). This occulting mask can be used with any aperture shape, but for the circular aperture shown in (c), the corresponding Lyot stop is (d).

External Occulter - Flying Sunshades



A properly placed and shaped occulter can drop a deep shadow of starlight over a telescope while allowing planet light to pass unimpeded.



Cash et al. 2005 SPIE 5899 274
Cash 2006, Nature

A paper by Olivier Guyon in 2006 changed the development of coronagraphs.....

Guyon et al. (2006) ApJSS 167 81

THE ASTROPHYSICAL JOURNAL SUPPLEMENT SERIES, 167:81–99, 2006 November

© 2006. The American Astronomical Society. All rights reserved. Printed in U.S.A.

THEORETICAL LIMITS ON EXTRASOLAR TERRESTRIAL PLANET DETECTION WITH CORONAGRAPHS

O. GUYON,¹ E. A. PLUZHNIK,¹ M. J. KUCHNER,² B. COLLINS,³ AND S. T. RIDGWAY⁴

Received 2006 May 25; accepted 2006 July 7

ABSTRACT

Many high-contrast coronagraph designs have recently been proposed. In this paper, their suitability for direct imaging of extrasolar terrestrial planets is reviewed. We also develop a linear algebra based model of coronagraphy that can both explain the behavior of existing coronagraphs and quantify the coronagraphic performance limit imposed by fundamental physics. We find that the maximum theoretical throughput of a coronagraph is equal to 1 minus the nonaberrated noncoronagraphic PSF of the telescope. We describe how a coronagraph reaching this fundamental limit may be designed, and how much improvement over the best existing coronagraph design is still possible. Both the analytical model and numerical simulations of existing designs also show that this theoretical limit rapidly degrades as the source size is increased: the “highest performance” coronagraphs, those with the highest throughput and smallest inner working angle (IWA), are the most sensitive to stellar angular diameter. This unfortunately rules out the possibility of using a small IWA ($< \lambda/d$) coronagraph for a terrestrial planet imaging mission. Finally, a

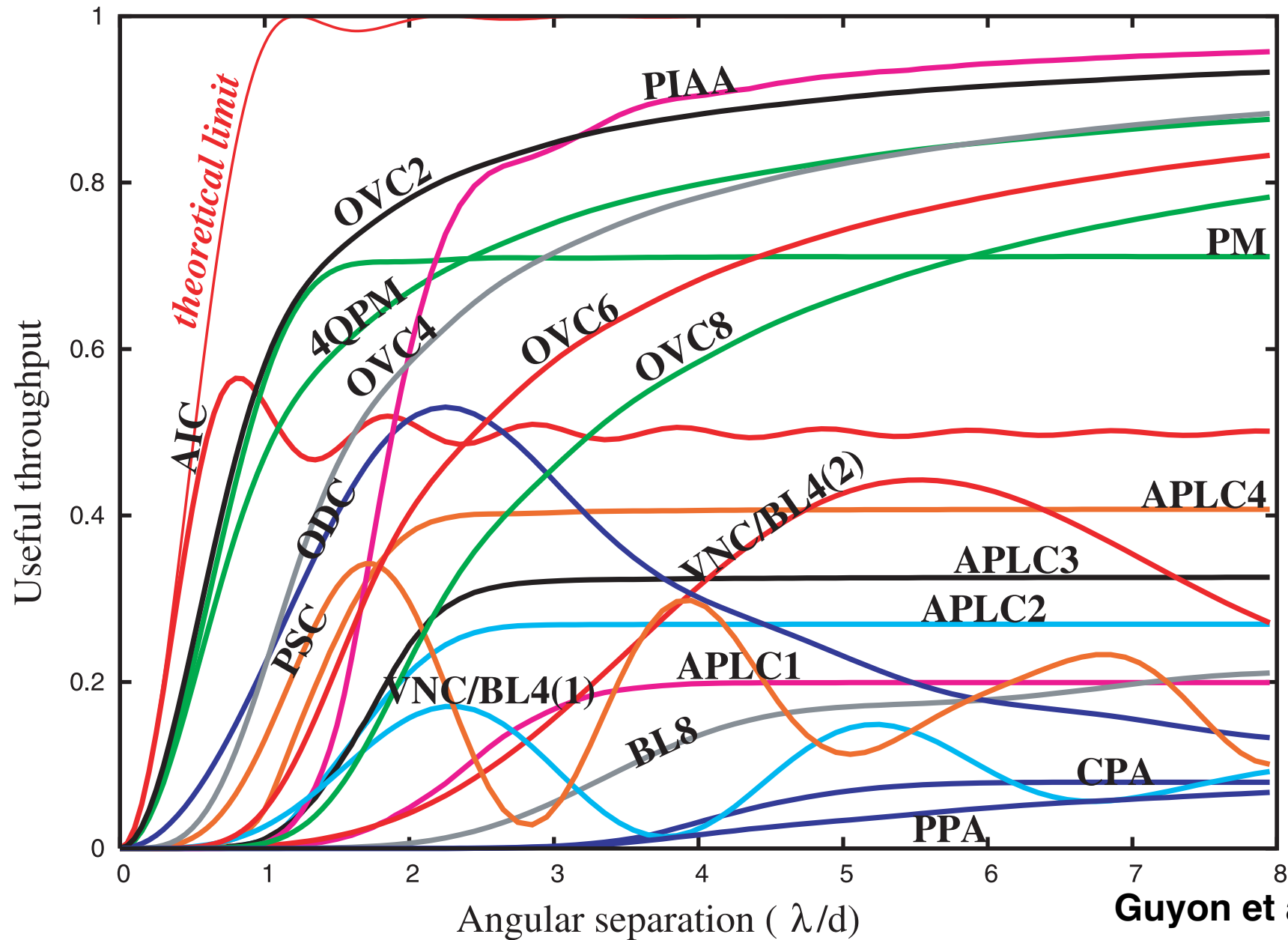
Small IWA means we are looking closer to the stars

OR

We can use a smaller telescope aperture

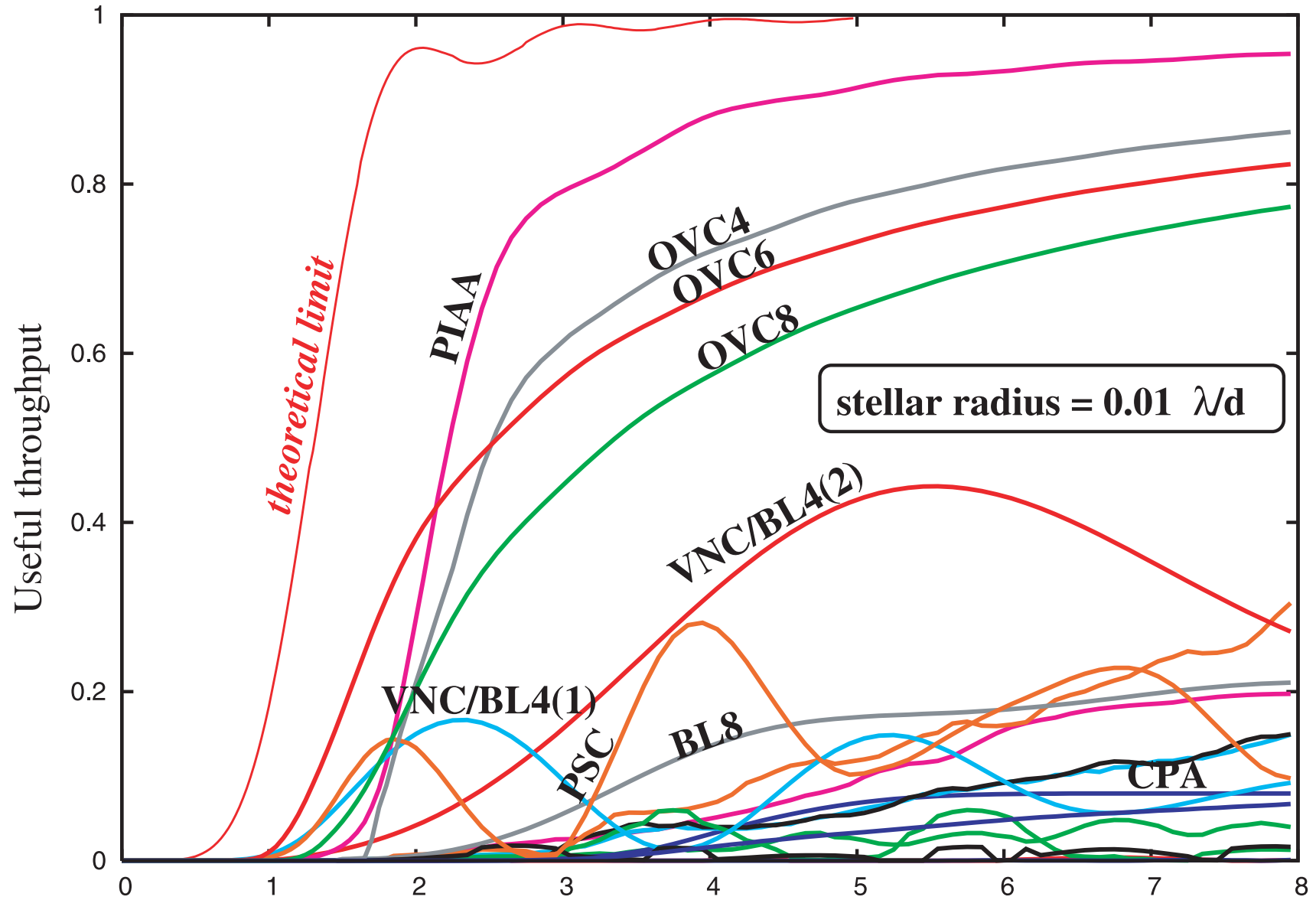
Coronagraph	Abbreviation	Reference
“Interferometric” Coronagraphs		
Achromatic Interferometric Coronagraph.....	AIC	Baudoz et al. (2000)
Common-Path Achromatic Interferometer-Coronagraph	CPAIC	Tavrov et al. (2005)
Visible Nulling Coronagraph, X-Y shear (fourth-order null) ^a	VNC	Mennesson et al. (2003)
Pupil Swapping Coronagraph.....	PSC	Guyon & Shao (2006)
Pupil Apodization		
Conventional Pupil Apodization and Shaped-Pupil ^b	CPA	Kasdin et al. (2003)
Achromatic Pupil Phase Apodization.....	PPA	Yang & Kostinski (2004)
Phase Induced Amplitude Apodization Coronagraph.....	PIAAC	Guyon (2003)
Phase Induced Zonal Zernike Apodization	PIZZA	Martinache (2004)
Improvement on the Lyot Concept with Amplitude Masks		
Apodized Pupil Lyot Coronagraph.....	APLC	Soummer et al. (2003a, 2003b)
Apodized Pupil Lyot Coronagraph, N steps	APLCN	Aime & Soummer (2004)
Band-limited, fourth-order ^a	BL4	Kuchner & Traub (2002)
Band-limited, eighth-order.....	BL8	Kuchner et al. (2005)
Improvement on the Lyot Concept with Phase Masks		
Phase Mask	PM	Roddier & Roddier (1997)
4 Quadrant Phase Mask.....	4QPM	Rouan et al. (2000)
Achromatic Phase Knife Coronagraph.....	APKC	Abe et al. (2001)
Optical Vortex Coronagraph, topological charge m	OVC m	Palacios (2005) Guyon et al. (2006)
Angular Groove Phase Mask Coronagraph	AGPMC	Mawet et al. (2005)
Optical Differentiation	ODC	Oti et al. (2005)

Guyon developed the idea of a 'theoretical limit' coronagraph



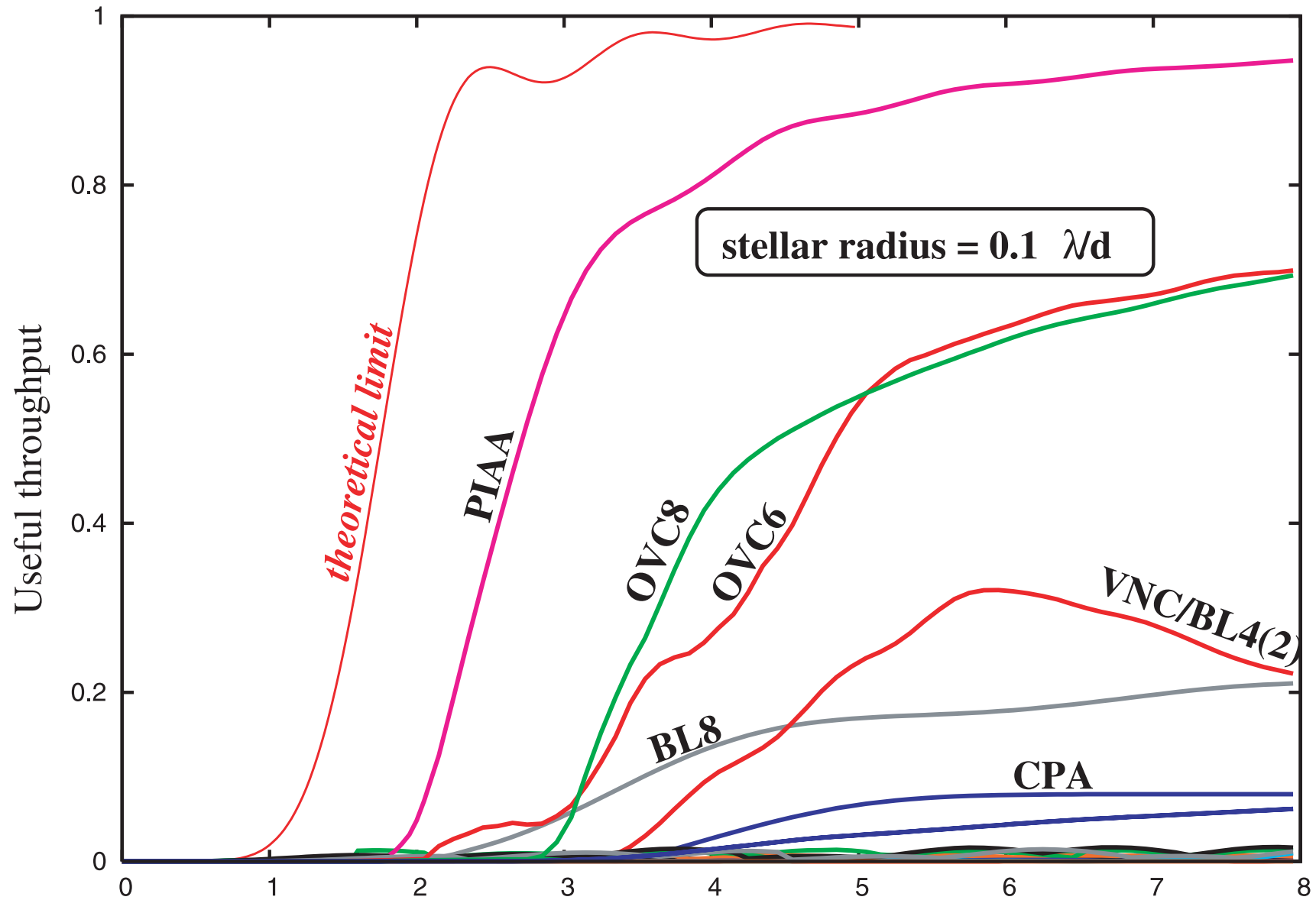
Guyon et al. (2006)

...but nearby stars are not point sources



Guyon et al. (2006)

...and many lose their effectiveness rapidly



Guyon et al. (2006)

We now focus on a much smaller family which can give high contrast at IWA of less than 5 diffraction widths

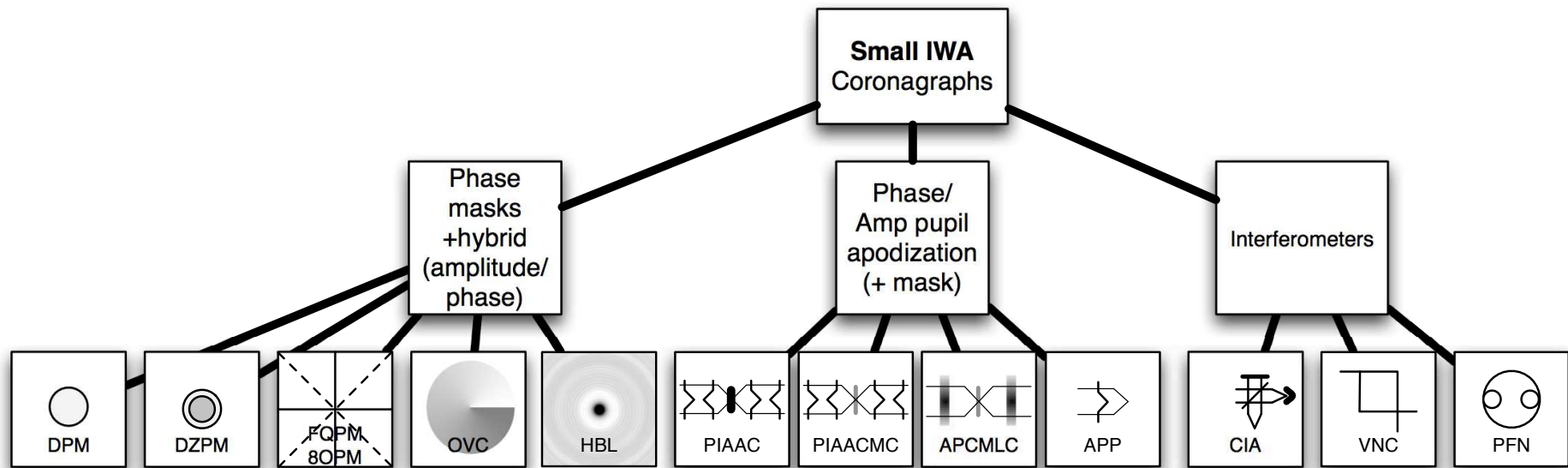
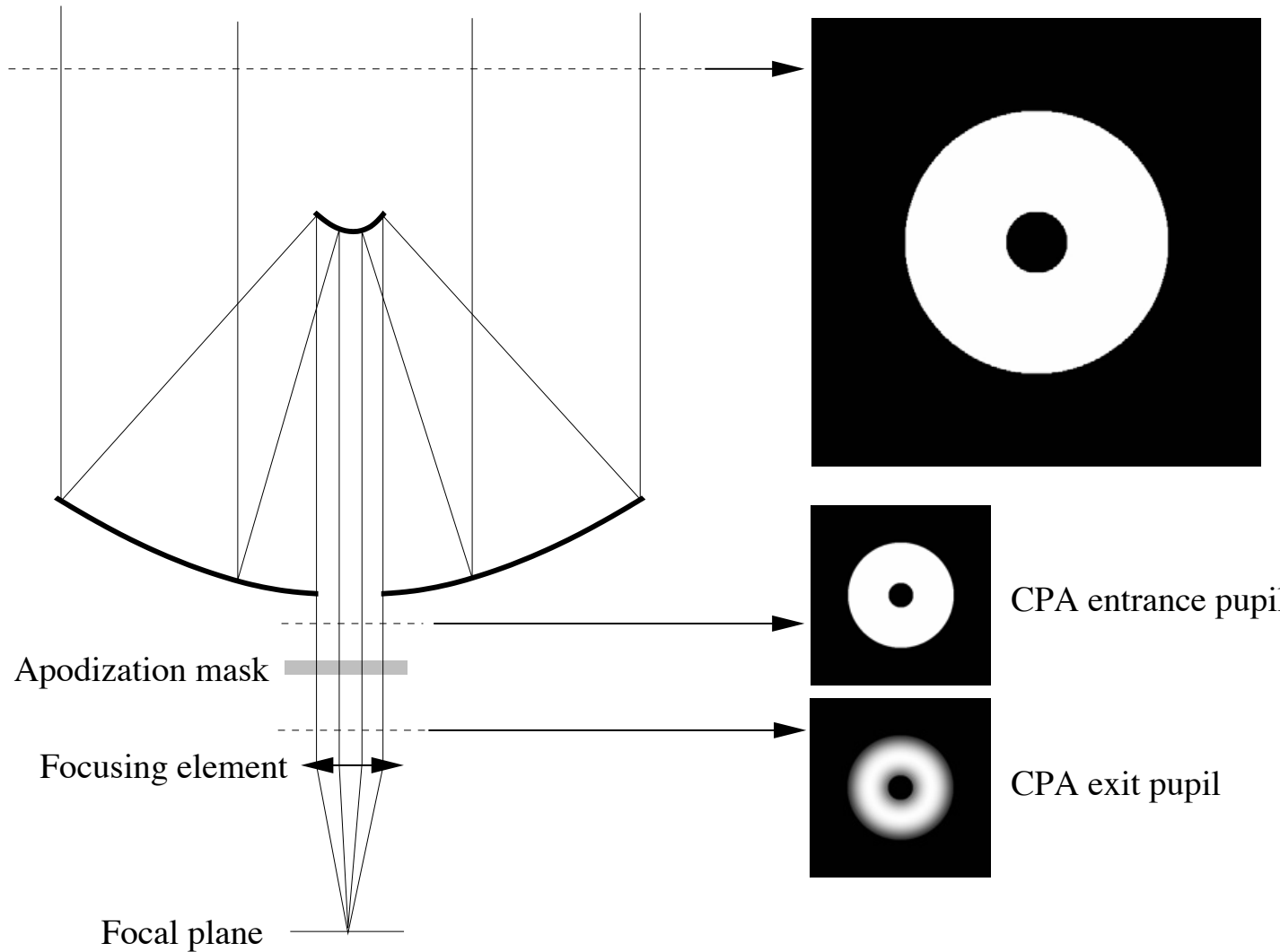


Figure 4. The family tree of small-angle coronagraphs (representative cases included). DPM: disk phase mask. DZPM: dual zone phase mask. FQPM/8OPM: four-quadrant phase mask, 8 octant phase mask. OVC: optical vortex coronagraph. HBL: hybrid band-limited. PIAAC: phase induced amplitude apodization. APP: apodizing phase plate. CIA: “coronagraphe interferentiel achromatique”. VNC: visible nuller coronagraph. PFN: Palomar fiber nuller. Common to all these concepts is some sort of phase manipulation, either in the focal plane or in the pupil plane, or both. Three main families can be pointed out: phase masks, phase/amplitude pupil apodization + focal plane masks (phase and/or amplitude), and interferometers.

Classical Pupil Apodization

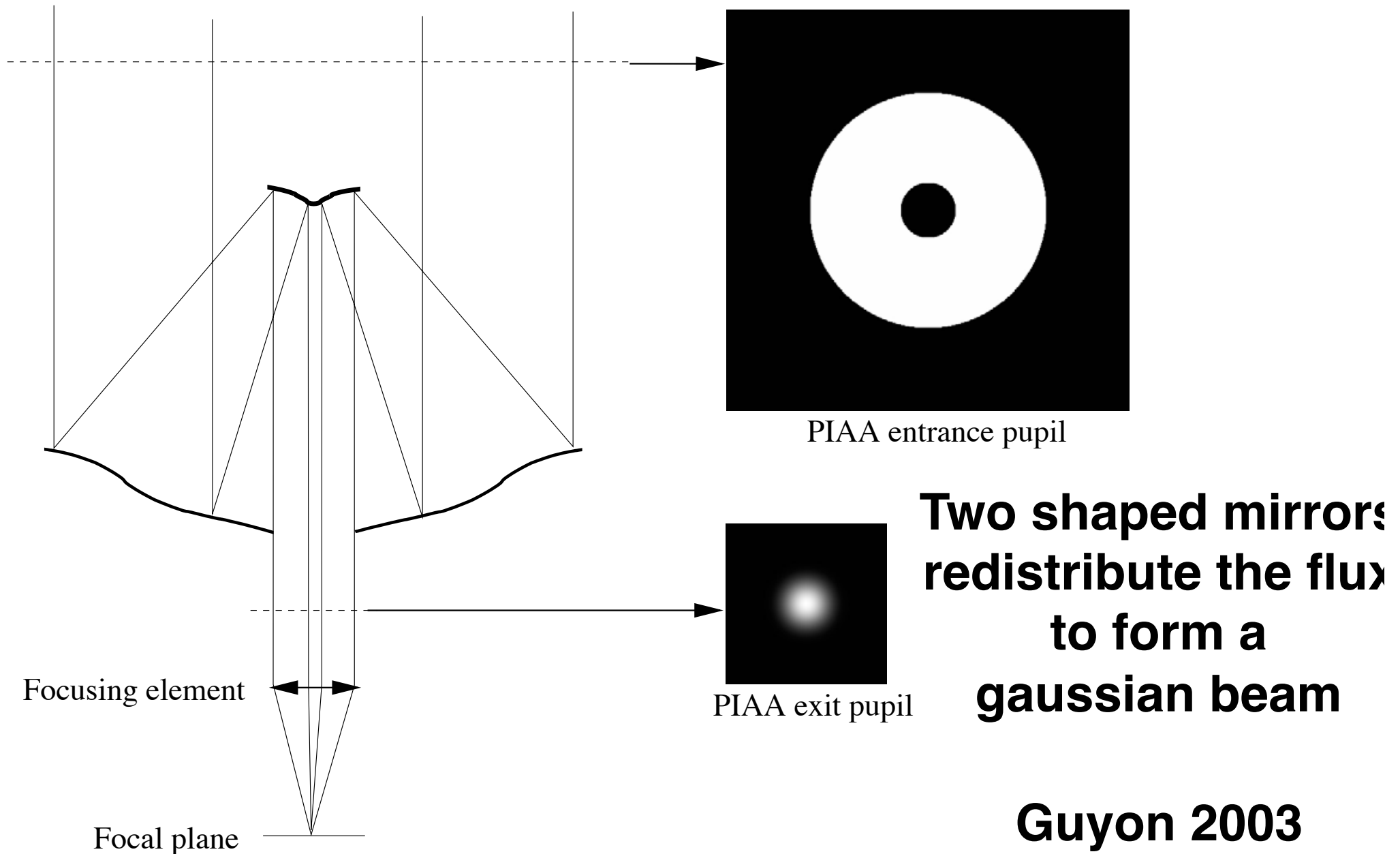


Apodization is done with an optic and lens to form a focused image

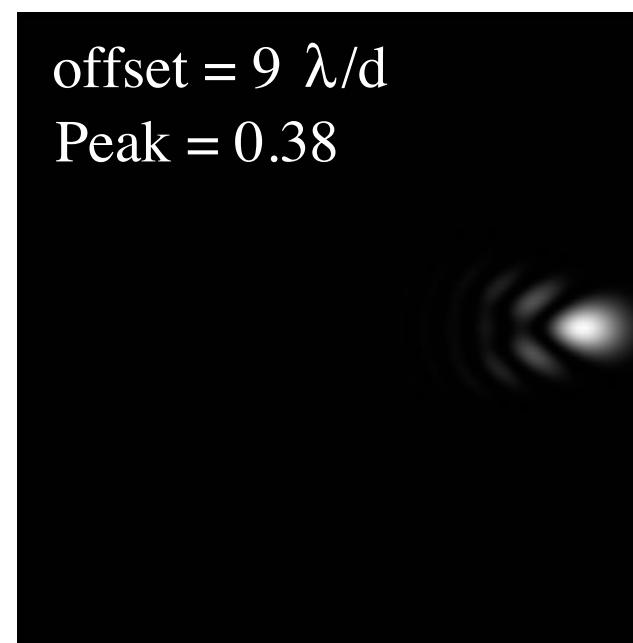
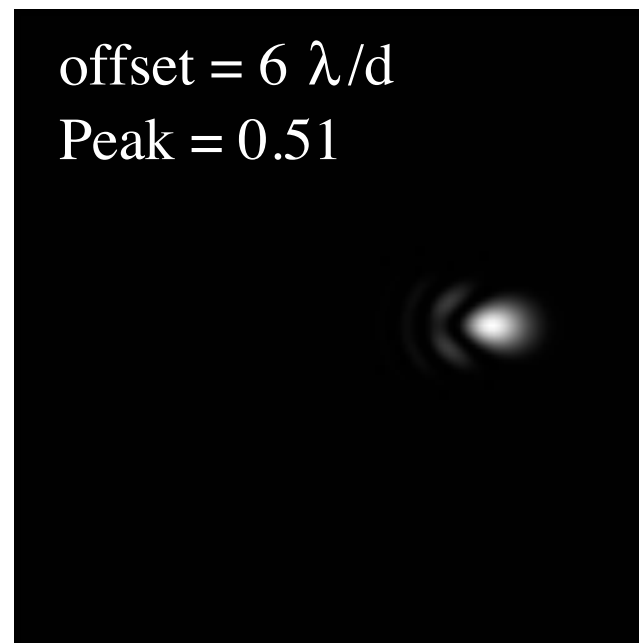
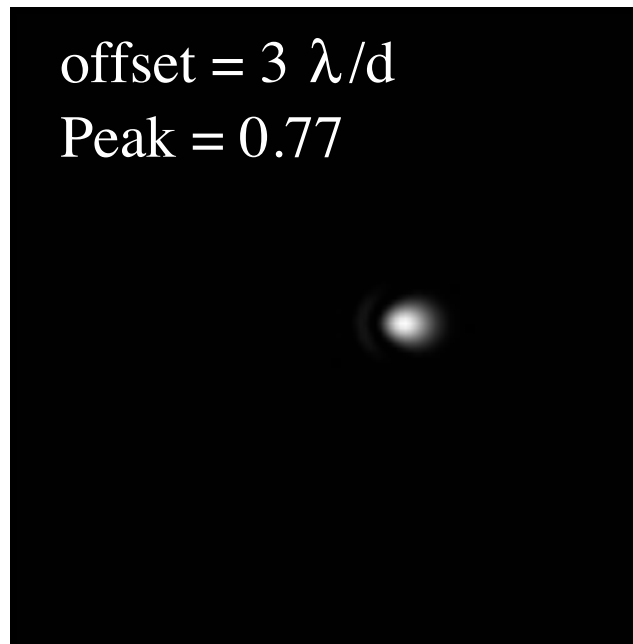
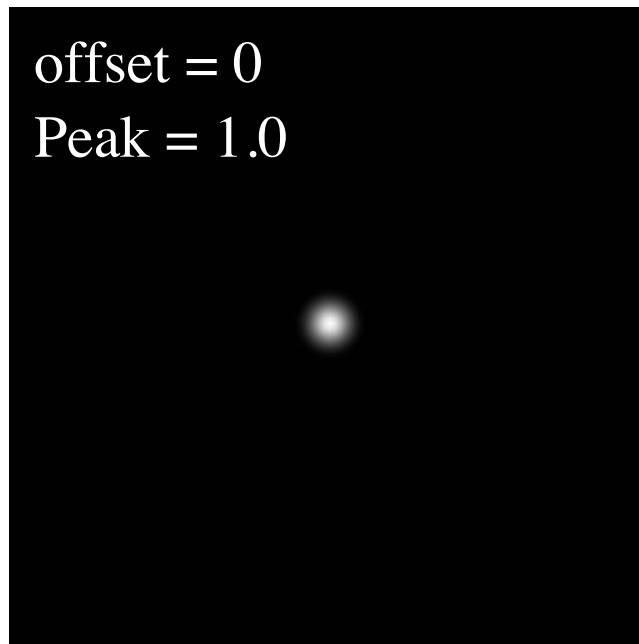
CPA entrance pupil

CPA exit pupil

Phase Induced Amplitude Apodization



Phase Induced Amplitude Apodization



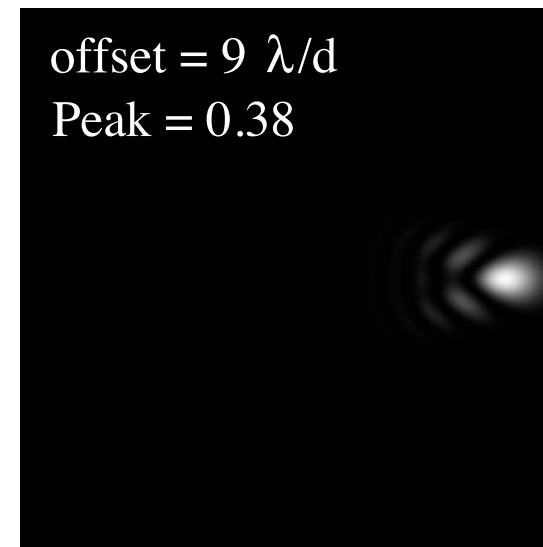
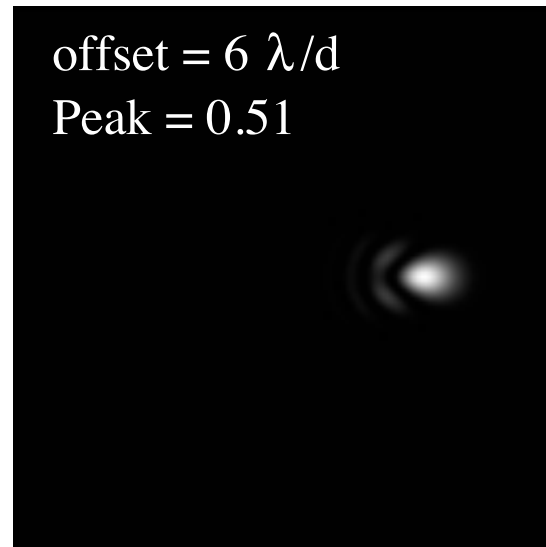
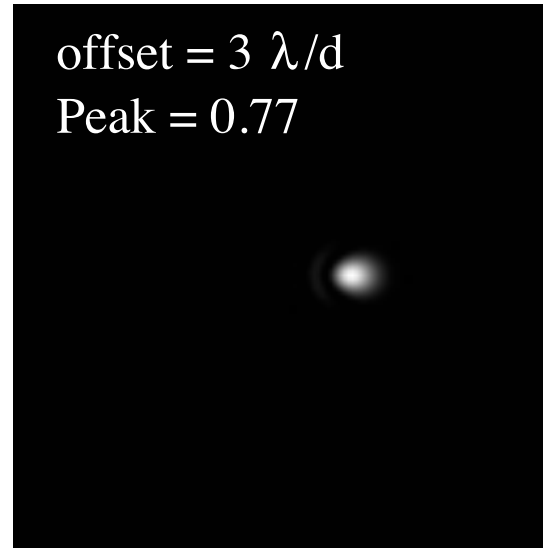
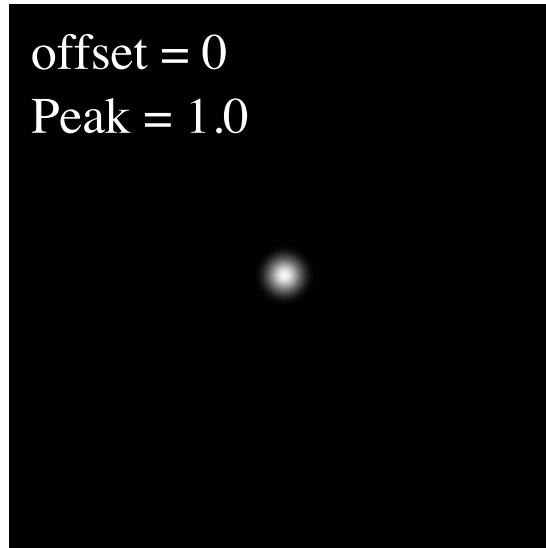
**On-axis PSF
is GAUSSIAN**

**Off-axis is
very aberrated**

Guyon 2003

Phase Induced Amplitude Apodization

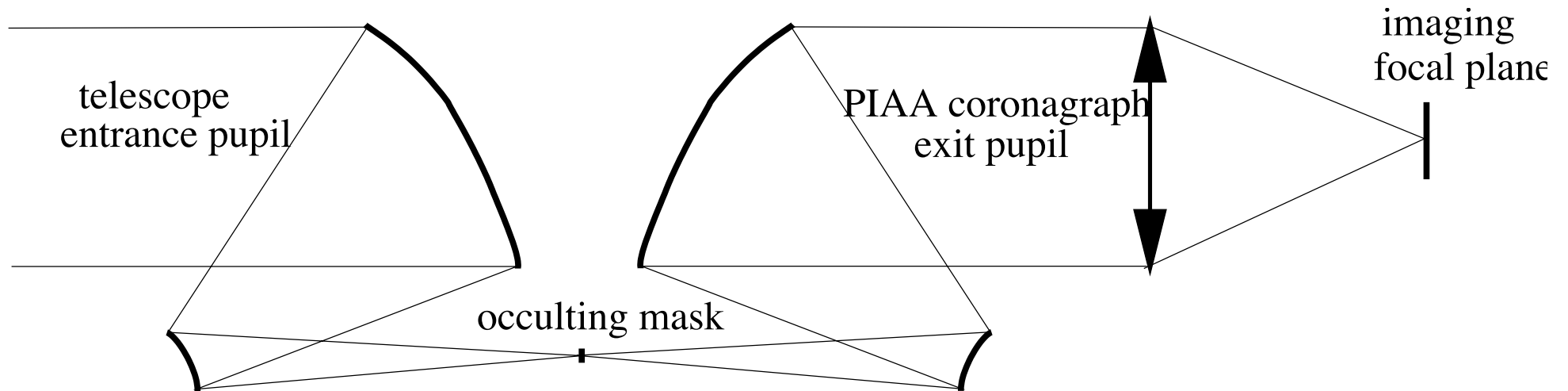
Mask off the central PSF and then an inverse PIAA
recombines the planet images



Guyon 2003

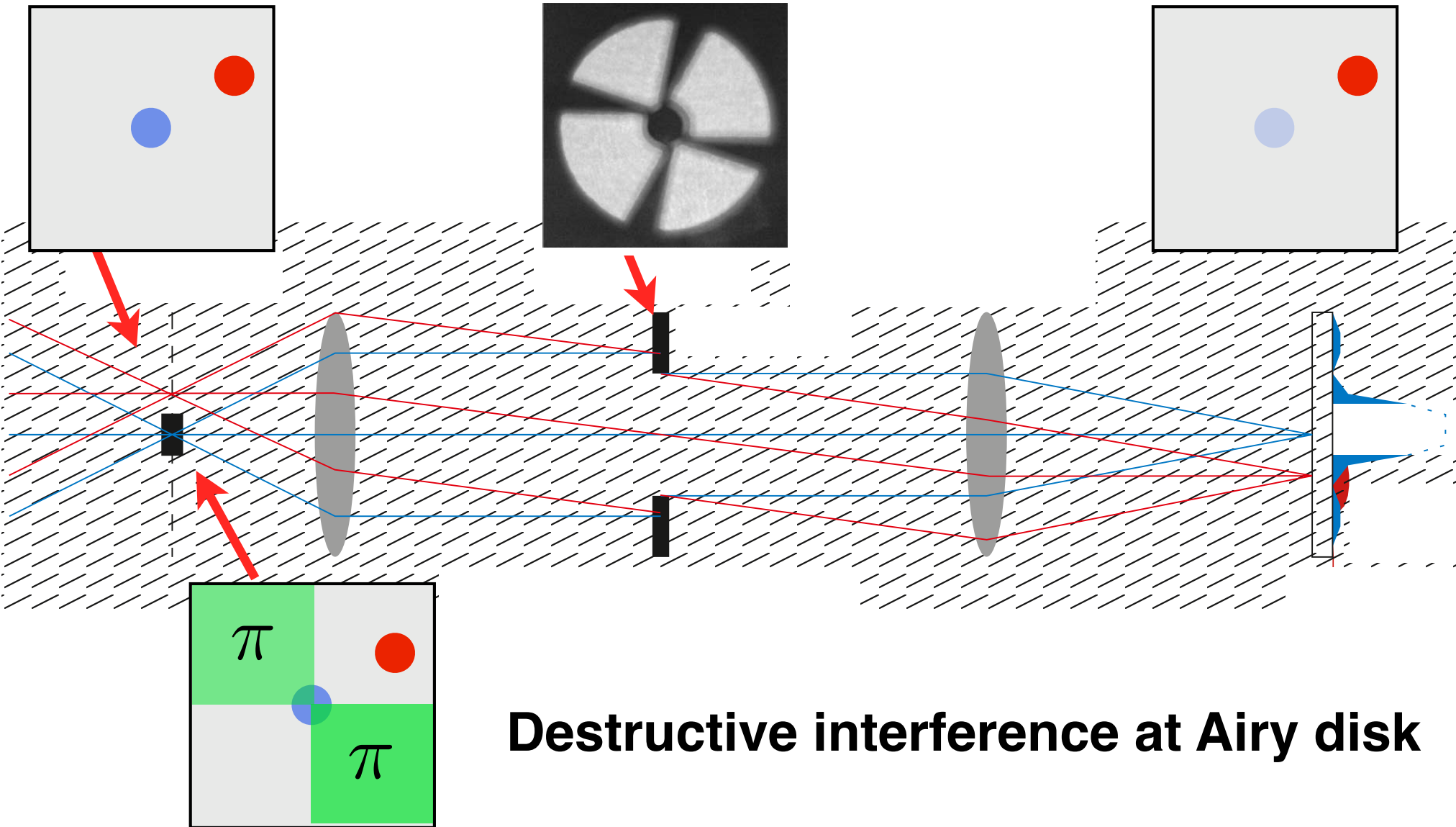
Phase Induced Amplitude Apodization

Mask off the central PSF and then an inverse PIAA
recombines the planet images



Guyon 2003

Four Quadrant Phase Mask (4QPM)



PSF with 2 and 4 Quadrant Mask

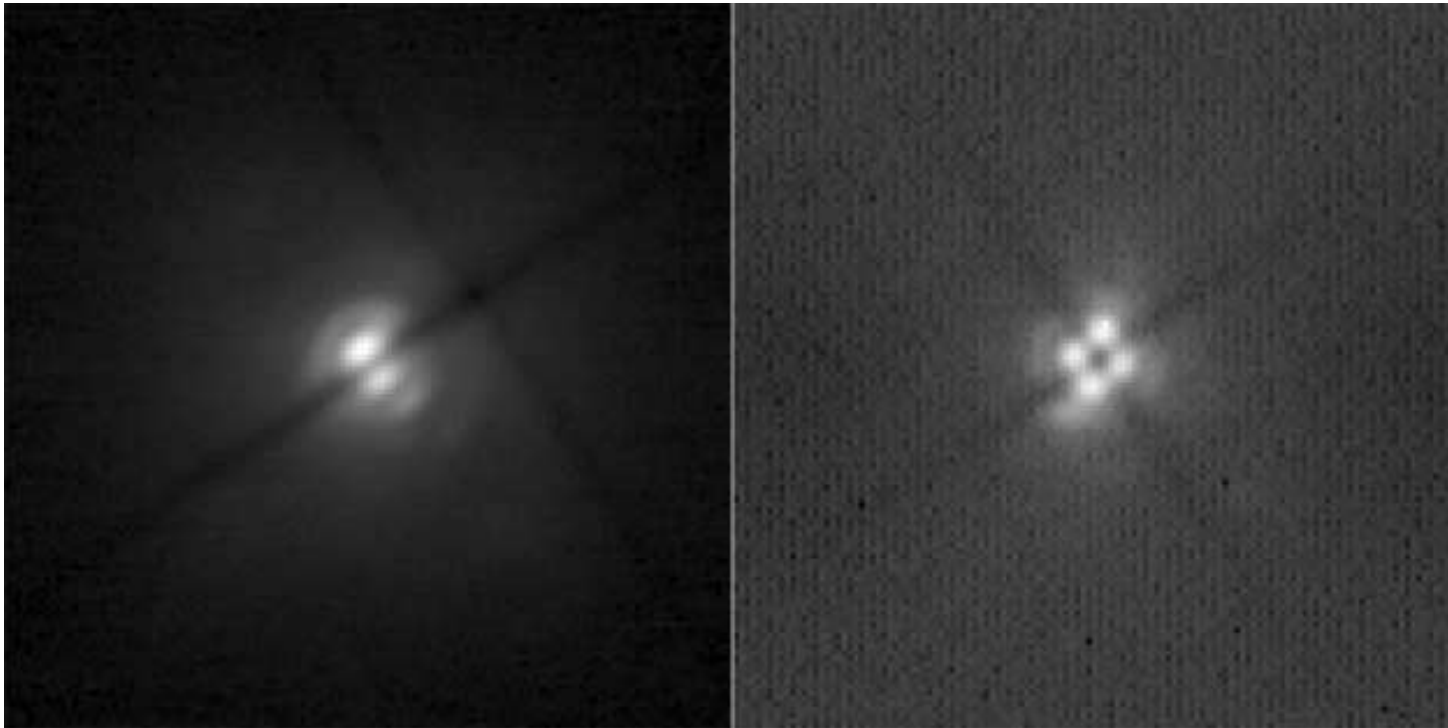
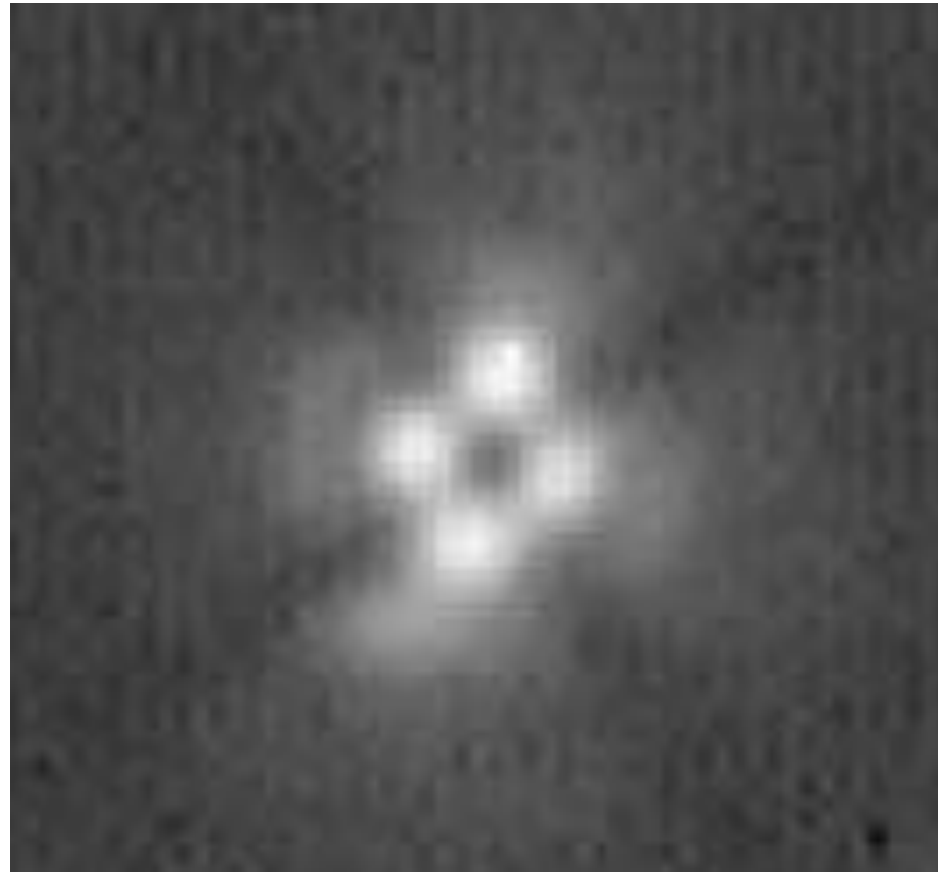


FIG. 3.—Two-quadrant (*left*) and four-quadrant (*right*) images of residuals for HD 32305 obtained in the K_s band. The intensity scale is not identical on both images. For comparison, the PSF peak attenuation is 3.9 on the two-quadrant image and 8.1 on the four-quadrant image.

Problems: PSF has blank edges

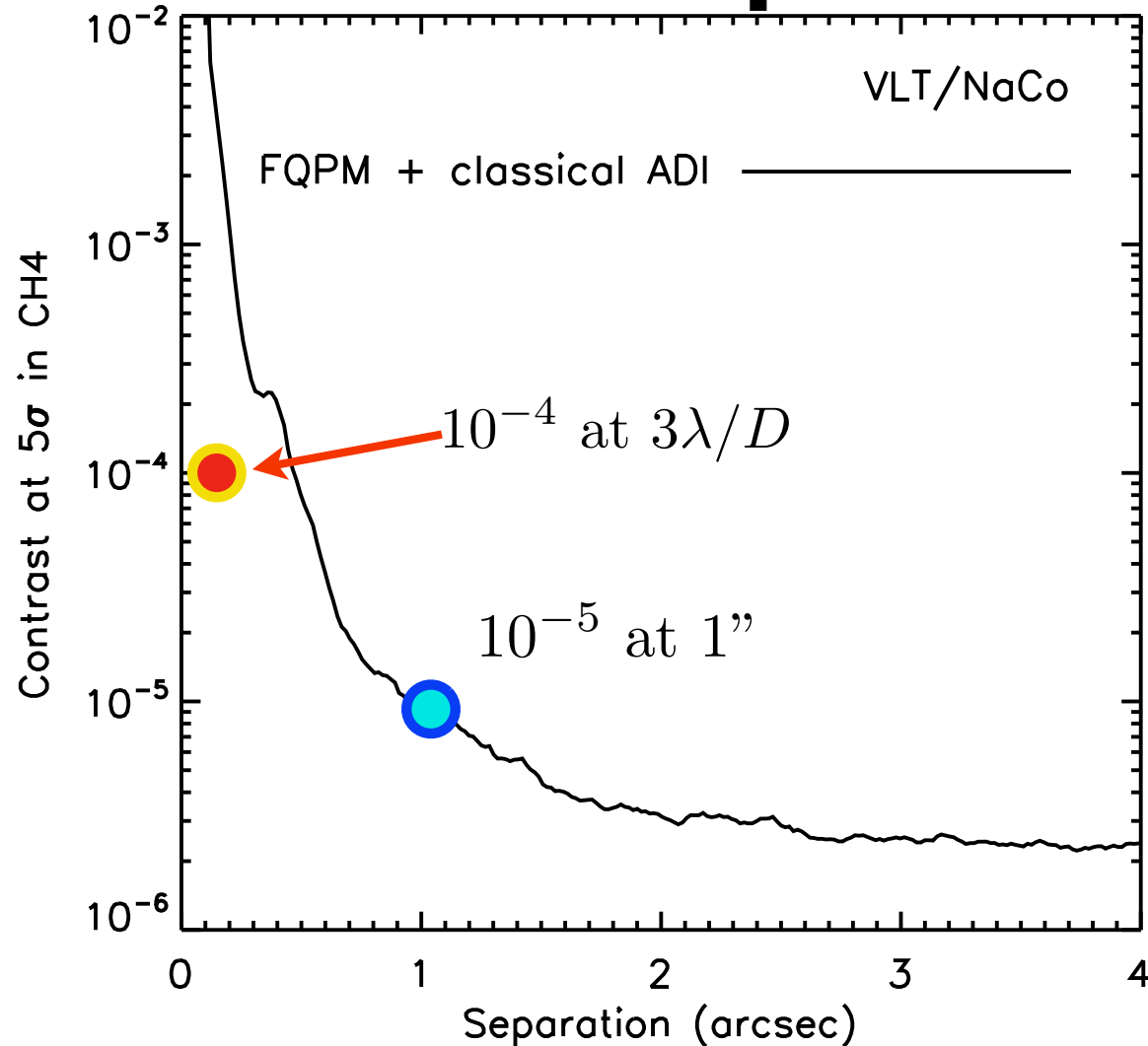


4QPM on a double star



FIG. 9.—HIP 1306 PSF (*left*) and FQPM image (*right*). The exposure time is 60 s for the coronagraphic image and 4 s for the PSF. Not a linear intensity scale ($I^{0.5}$). FOV is $1''.25$. North is up.

4QPM measured performance

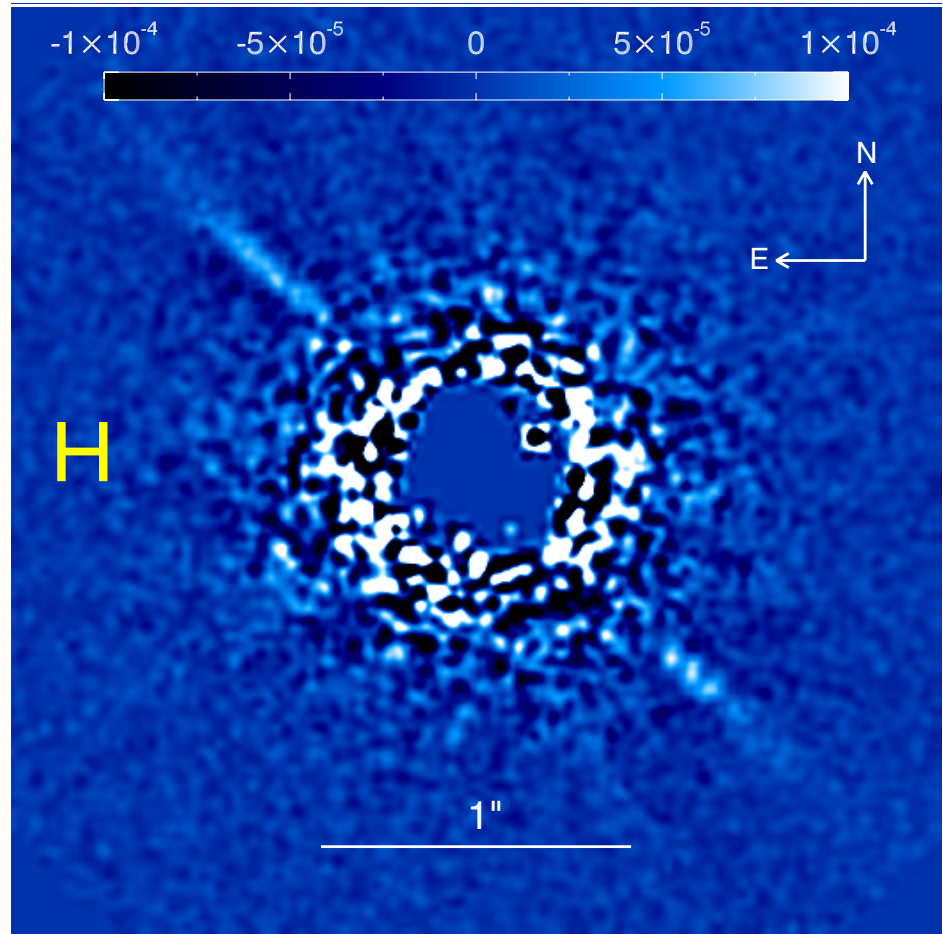
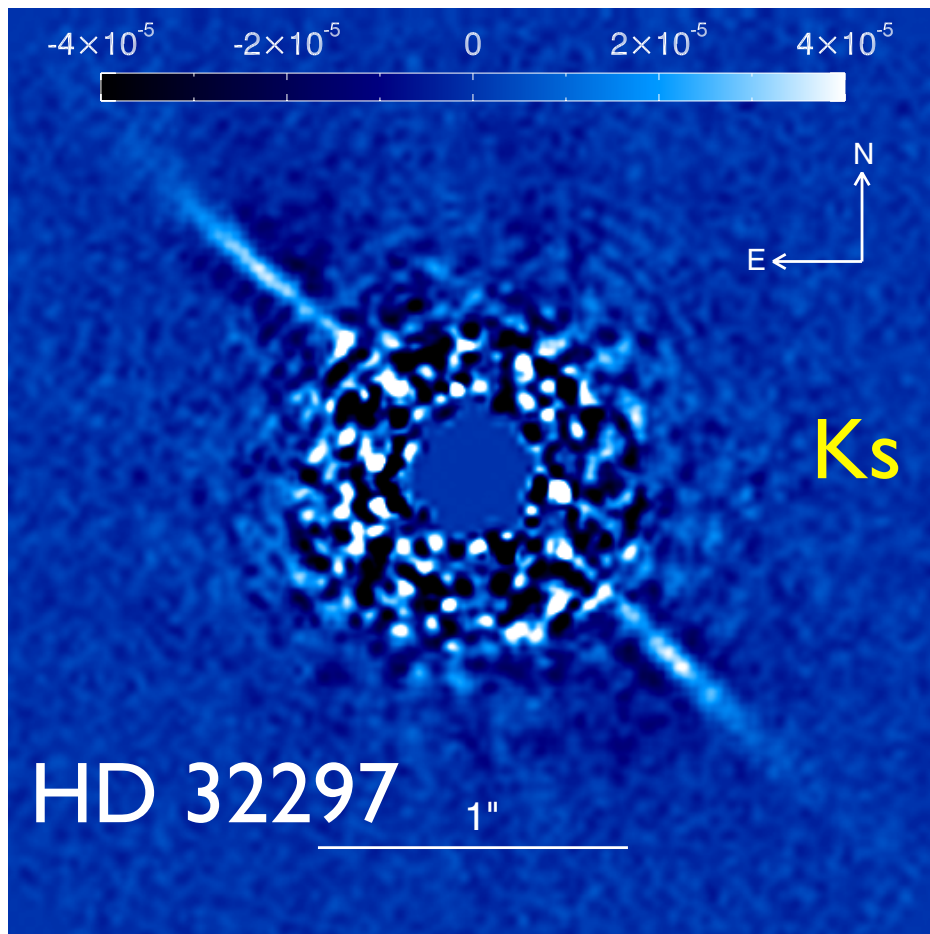


Anne-Lise Maire PhD Thesis (2012)

Observatoire de Paris

Characterisation des exoplanetes par imagerie depuis le sol et l'espace

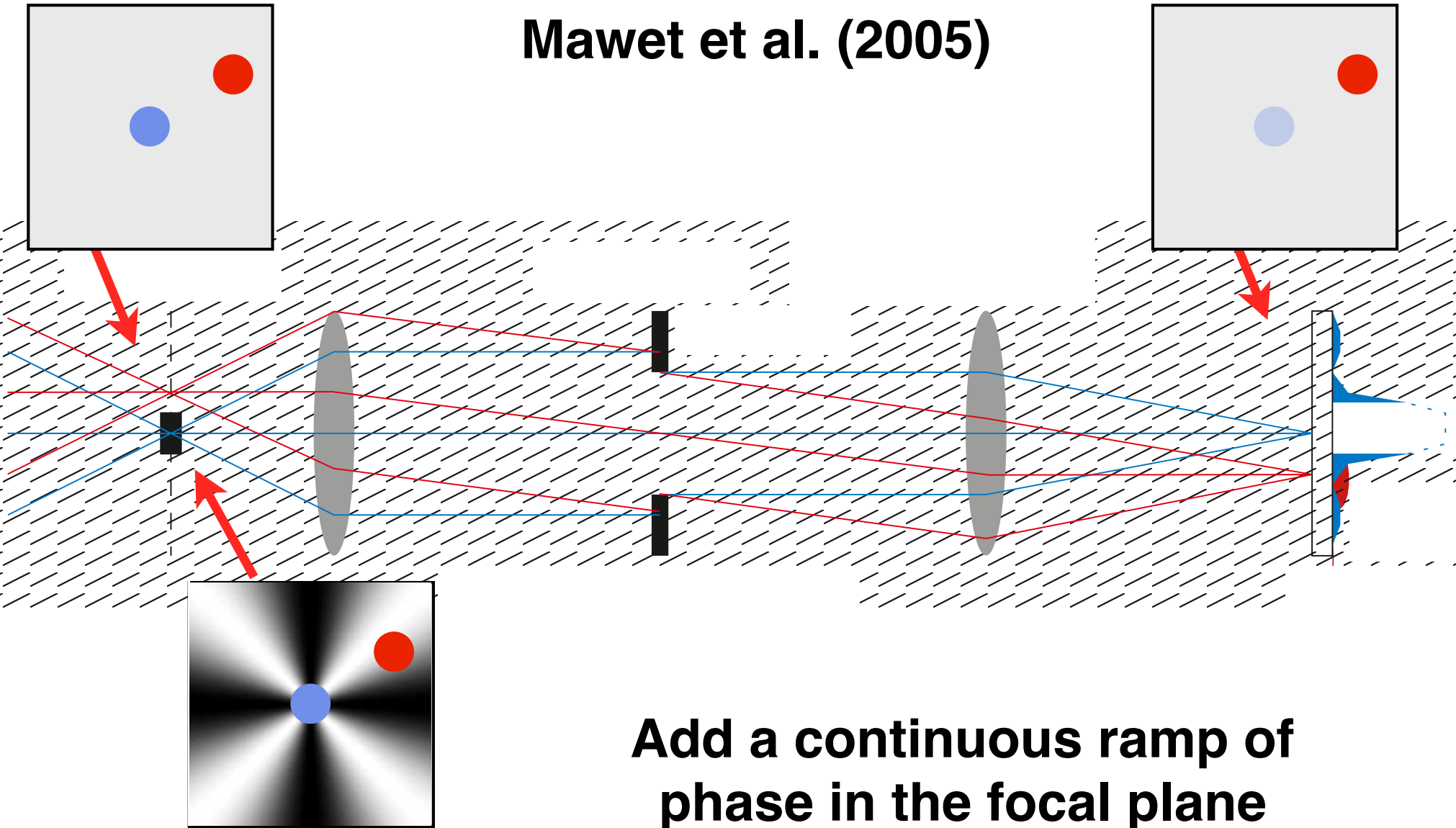
Imaging Disks



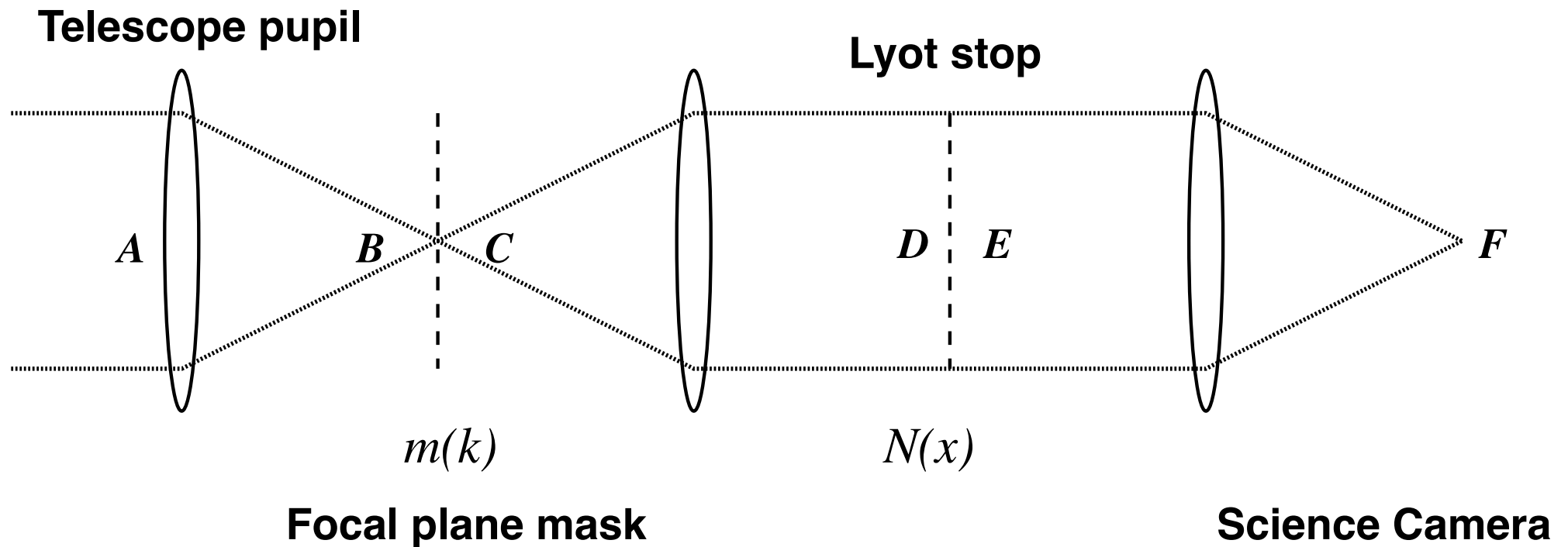
Boccaletti et al. (2012)

Annular Groove Phase Mask

Mawet et al. (2005)

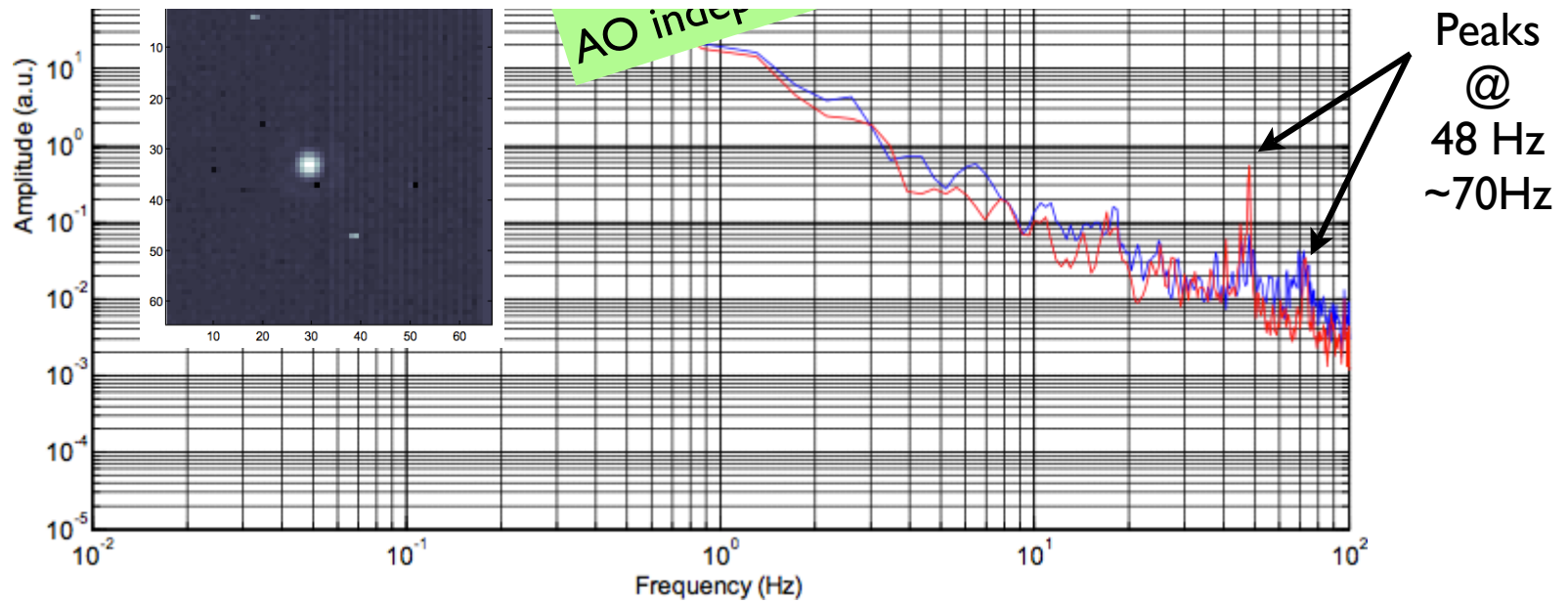


Focal plane coronagraphs are sensitive to telescope shake



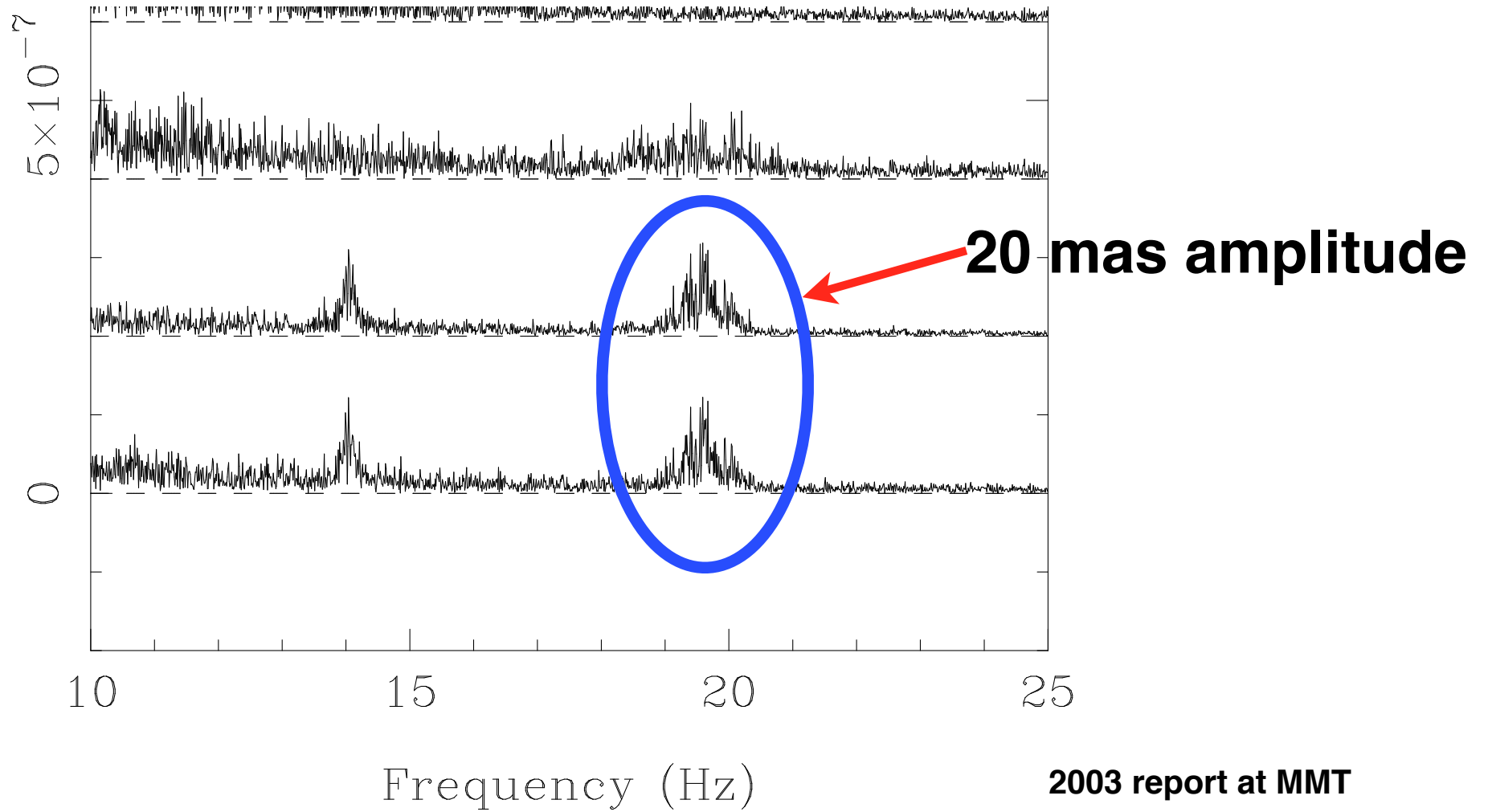
Telescope Vibrations

CONICA
L' imaging
200 Hz
(5 ms)



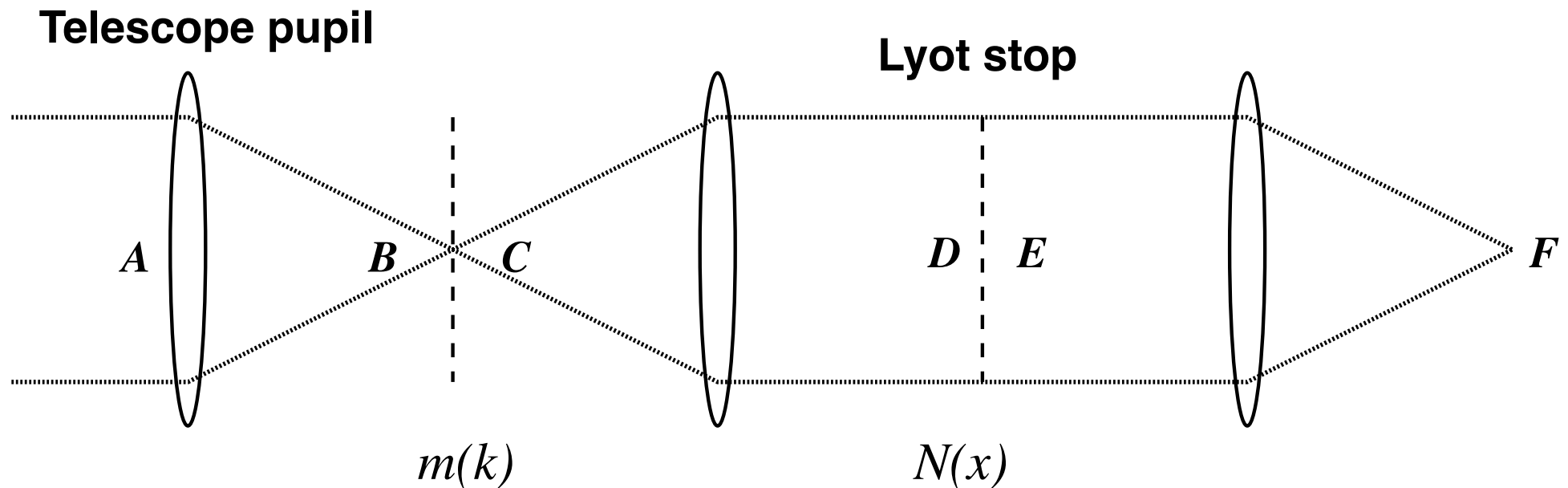
Girard et al. (2012) SPIE

Telescope Vibrations



2003 report at MMT

Pupil plane coronagraphs are NOT sensitive to shake!

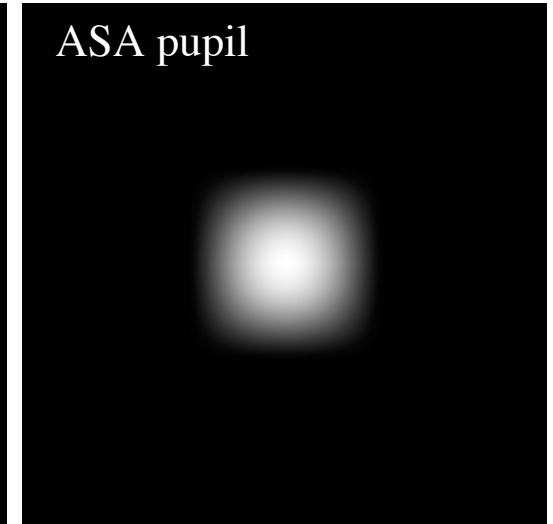
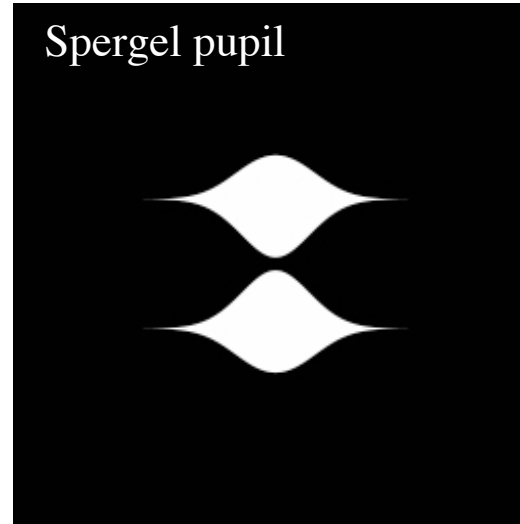
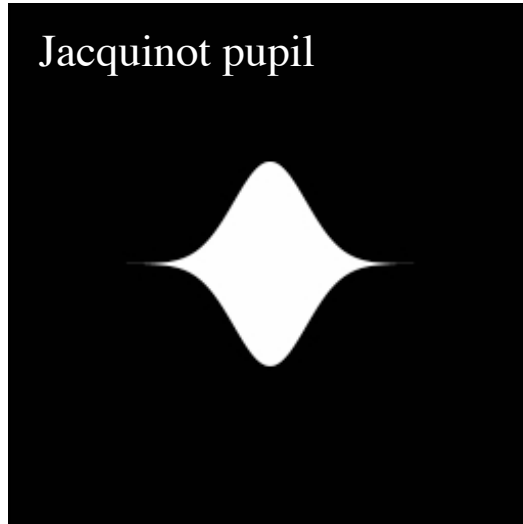


They modify the shape of the telescope PSF to have a dark region

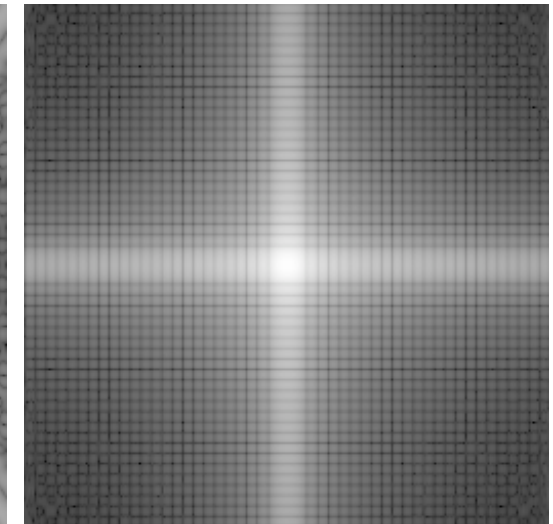
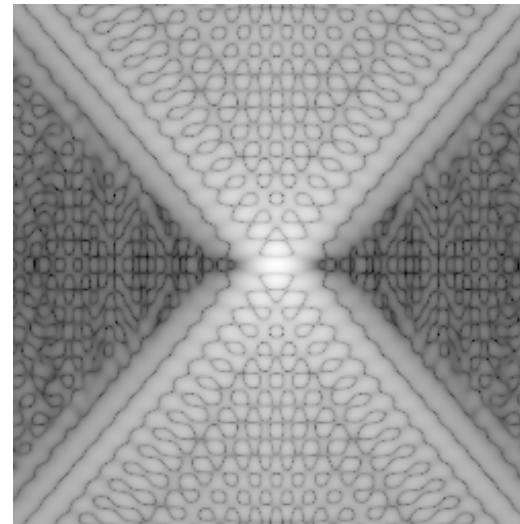
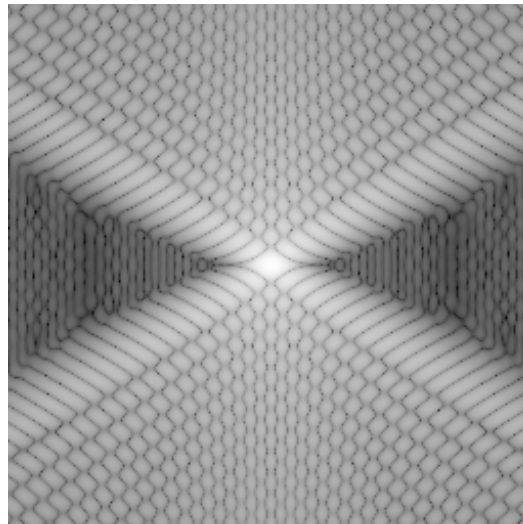
Classical Pupil Apodization

Modify the telescope pupil through **AMPLITUDE** and/or **PHASE** to remove the effects of diffraction

Pupil



PSF



Jacquinot & Roizen-Dossier 1964

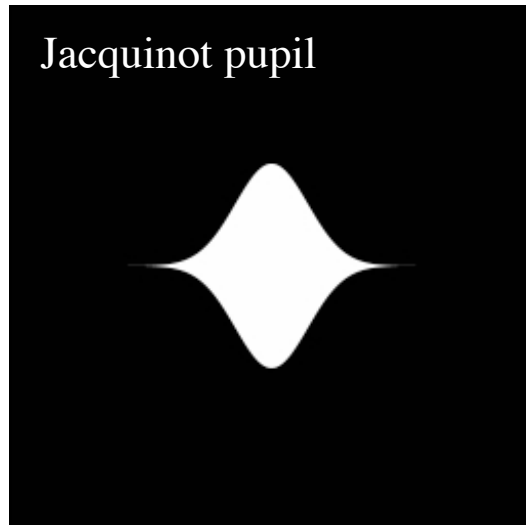
Spergel 2001

Classical Pupil Apodization

Most have very low throughput (~ 0.1 to 0.3) and limited field of view

Jacquinet & Roizen-Dossier 1964

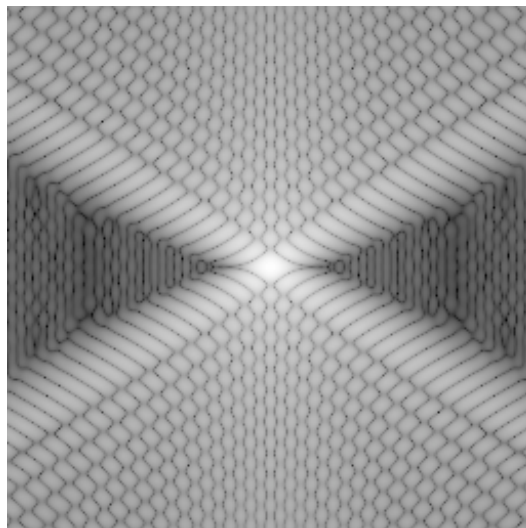
Pupil



$$|y| < R \times \left(e^{-\left(\frac{\alpha x}{R}\right)^2} - e^{-\alpha^2} \right) \quad (7)$$

where R is the radius of the pupil, x and y are the D coordinates in the pupil plane, and $\alpha = 2$. The pupil transmission is equal to 0 everywhere else.

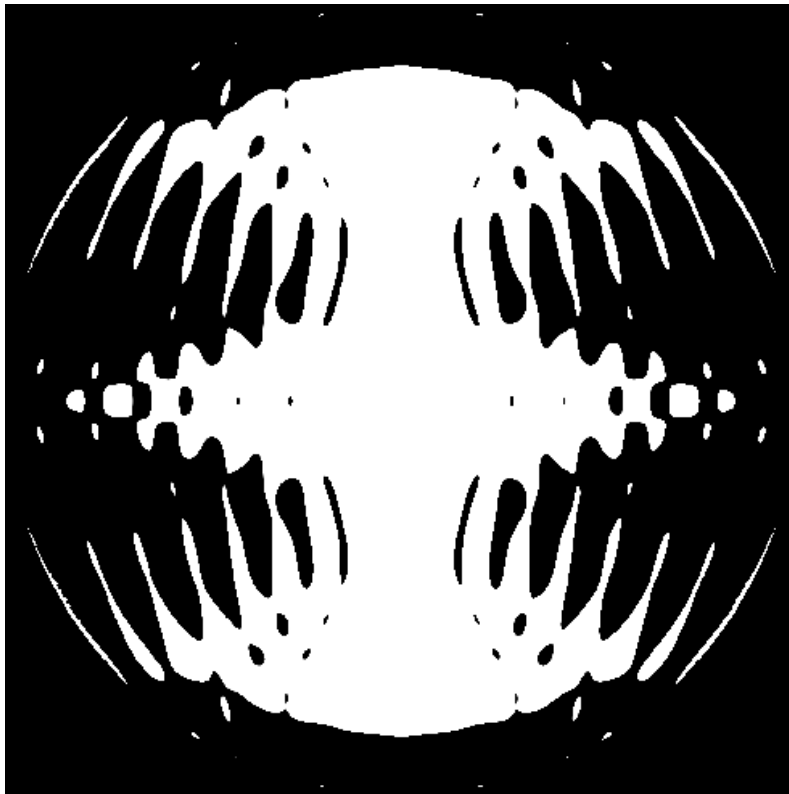
PSF



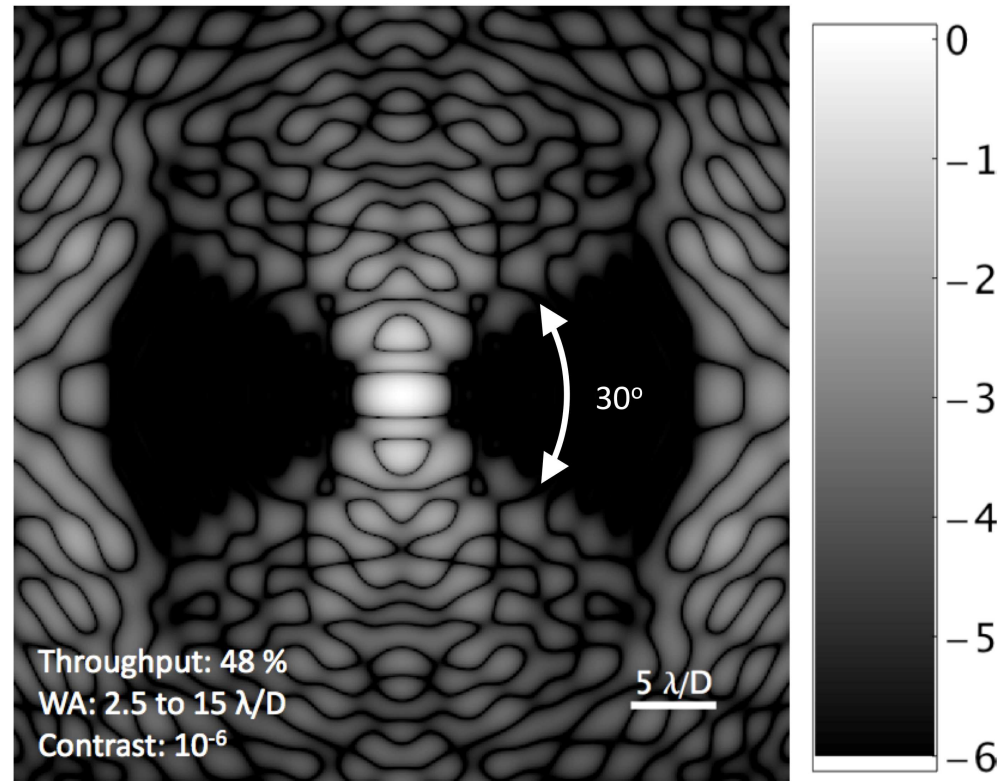
Optimized Pupil Apodizations

Developed by Carlotti, Vanderlei and Kasdin

Pupil

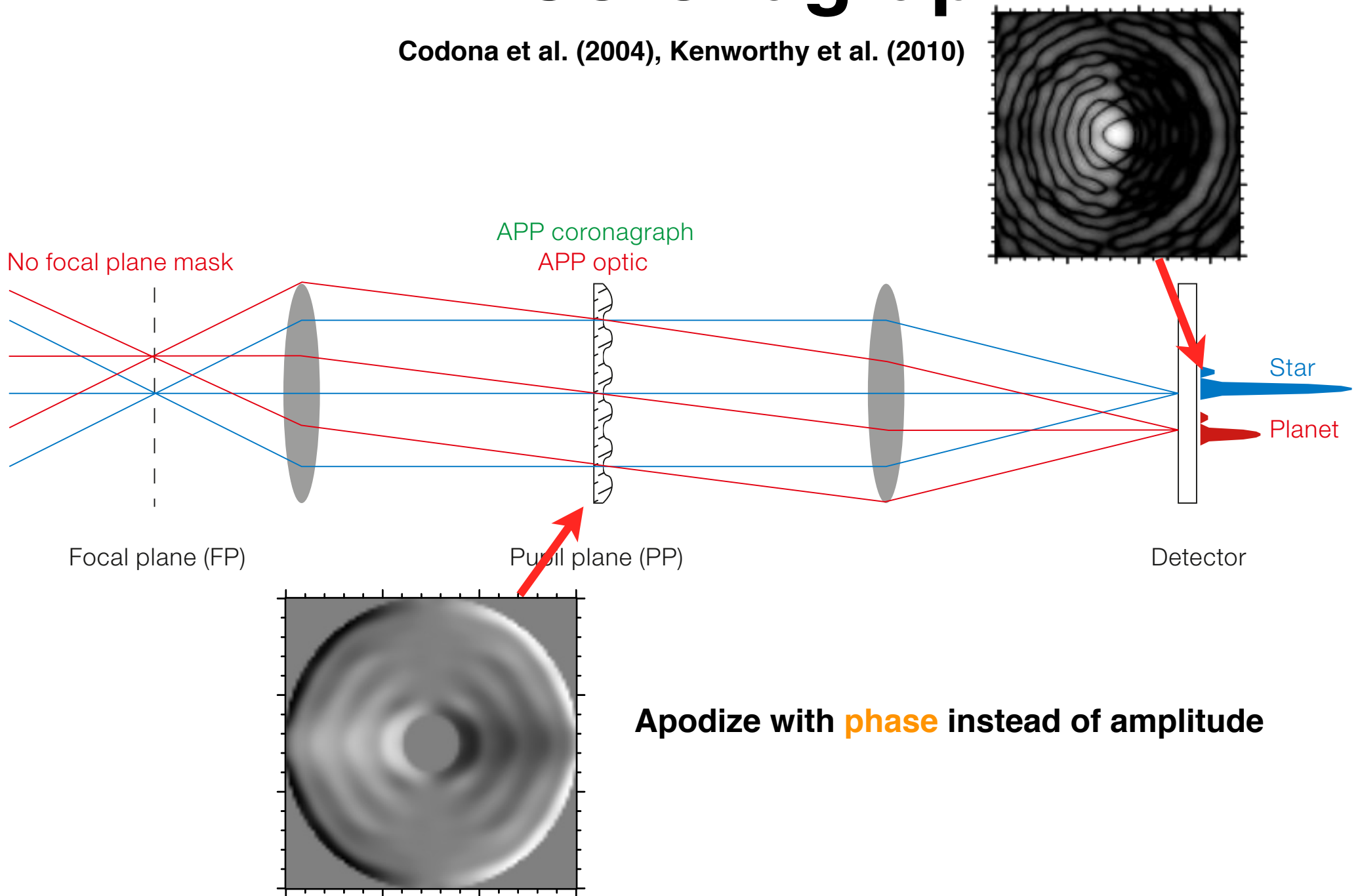


PSF



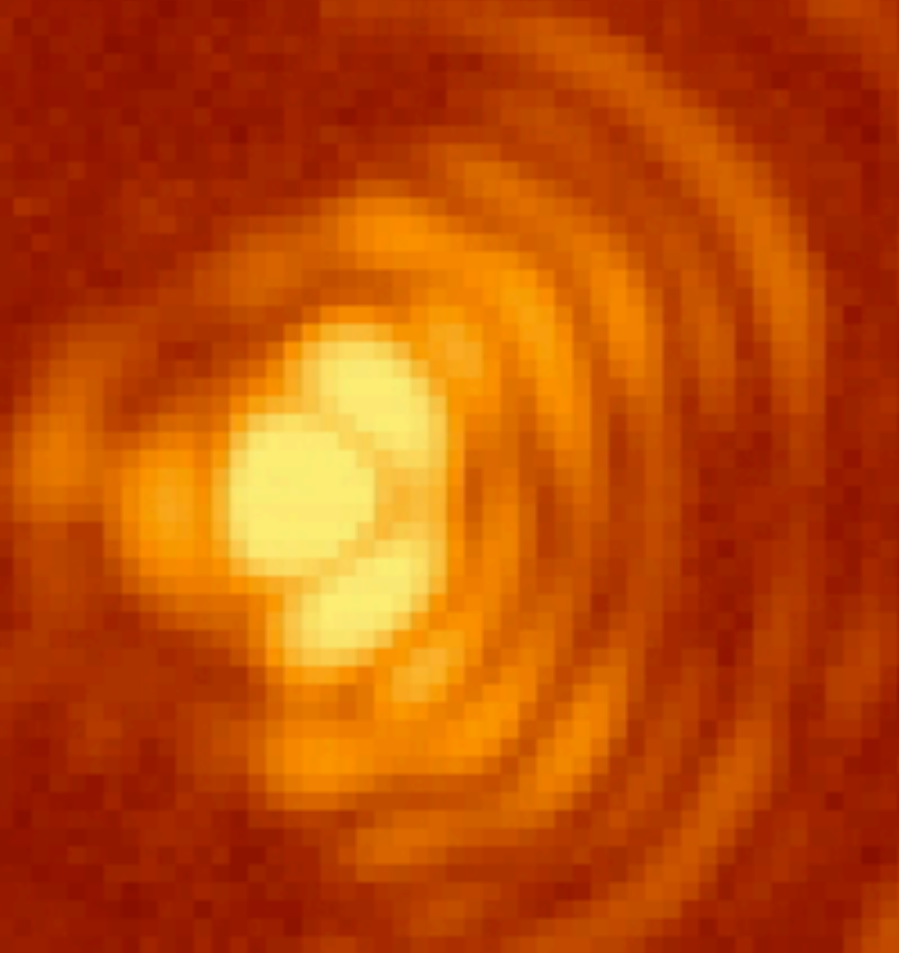
APP Coronagraph

Codona et al. (2004), Kenworthy et al. (2010)



**APP Coronagraph performance not degraded
by tip-tilt vibrations or pupil wander**

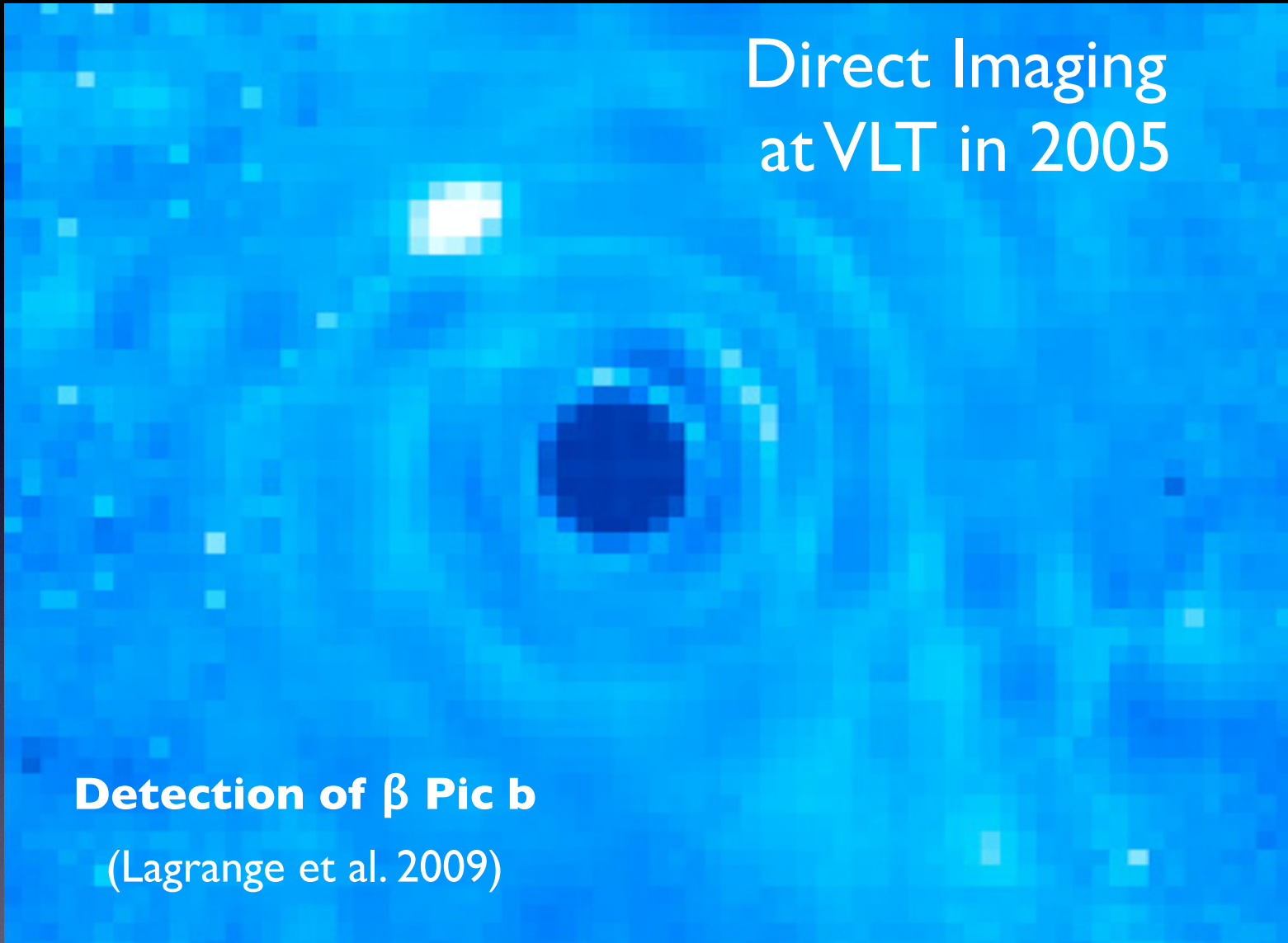
VLT/NaCo 4 microns at real time speed

A real-time coronagraph image showing a bright yellow star with a dark central spot and concentric rings of light, set against a dark red background. The image is centered and occupies the middle portion of the slide.

Direct Imaging at VLT in 2005

Detection of β Pic b

(Lagrange et al. 2009)



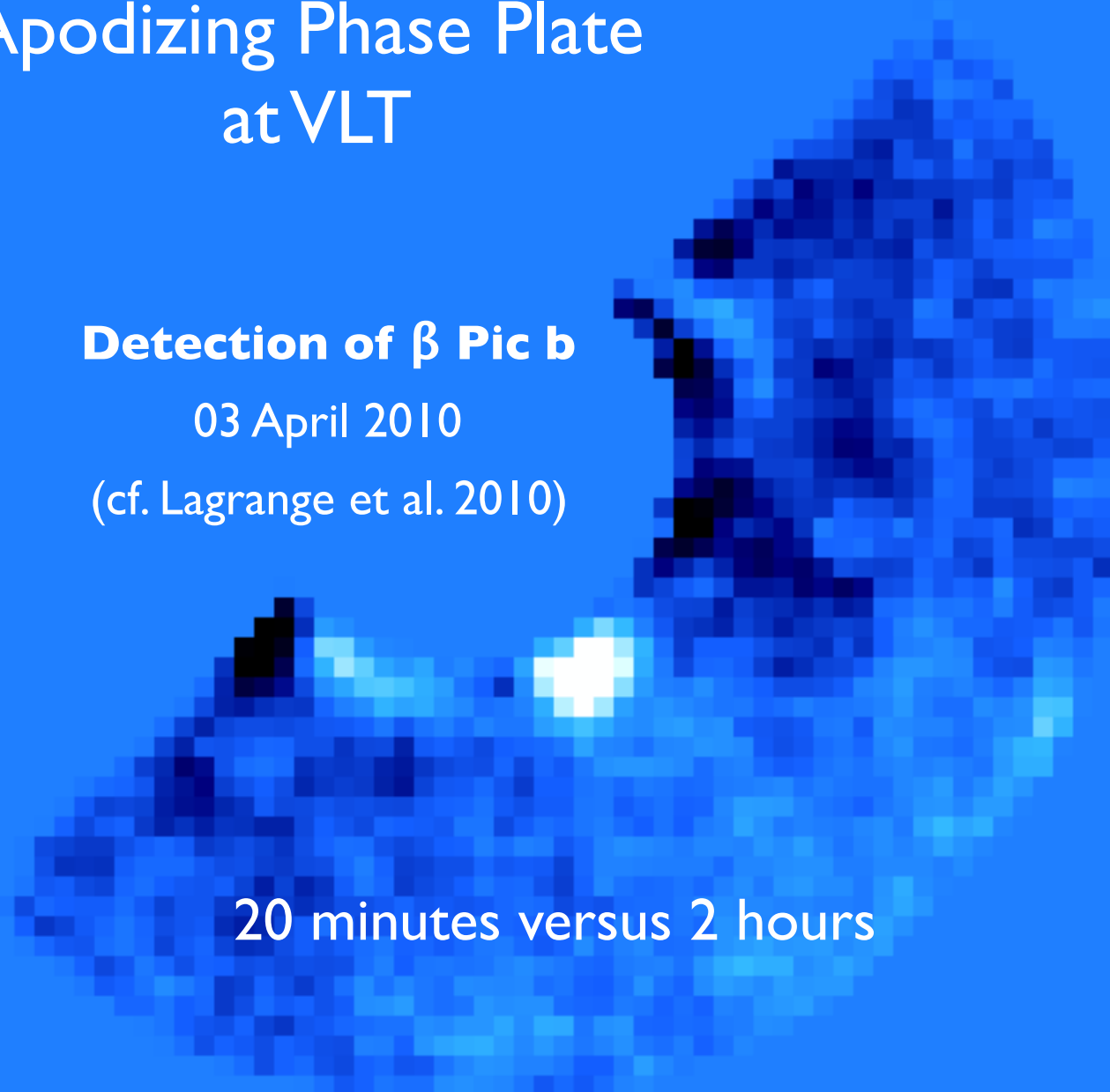
Apodizing Phase Plate at VLT

Detection of β Pic b

03 April 2010

(cf. Lagrange et al. 2010)

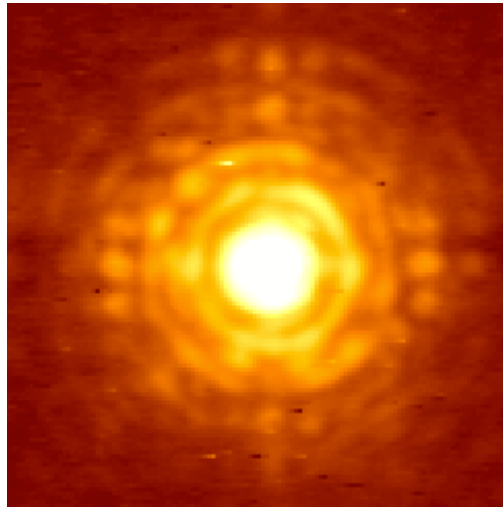
20 minutes versus 2 hours

The image is a blue-toned astronomical photograph of the star system beta Pic. It shows a bright central star (beta Pic A) with a fainter companion (beta Pic B) to its left. A small, dark object, identified as the planet beta Pic b, is visible to the right of the main star. The background is filled with a noisy, pixelated pattern of blue and white, representing the star's light and the detection process.

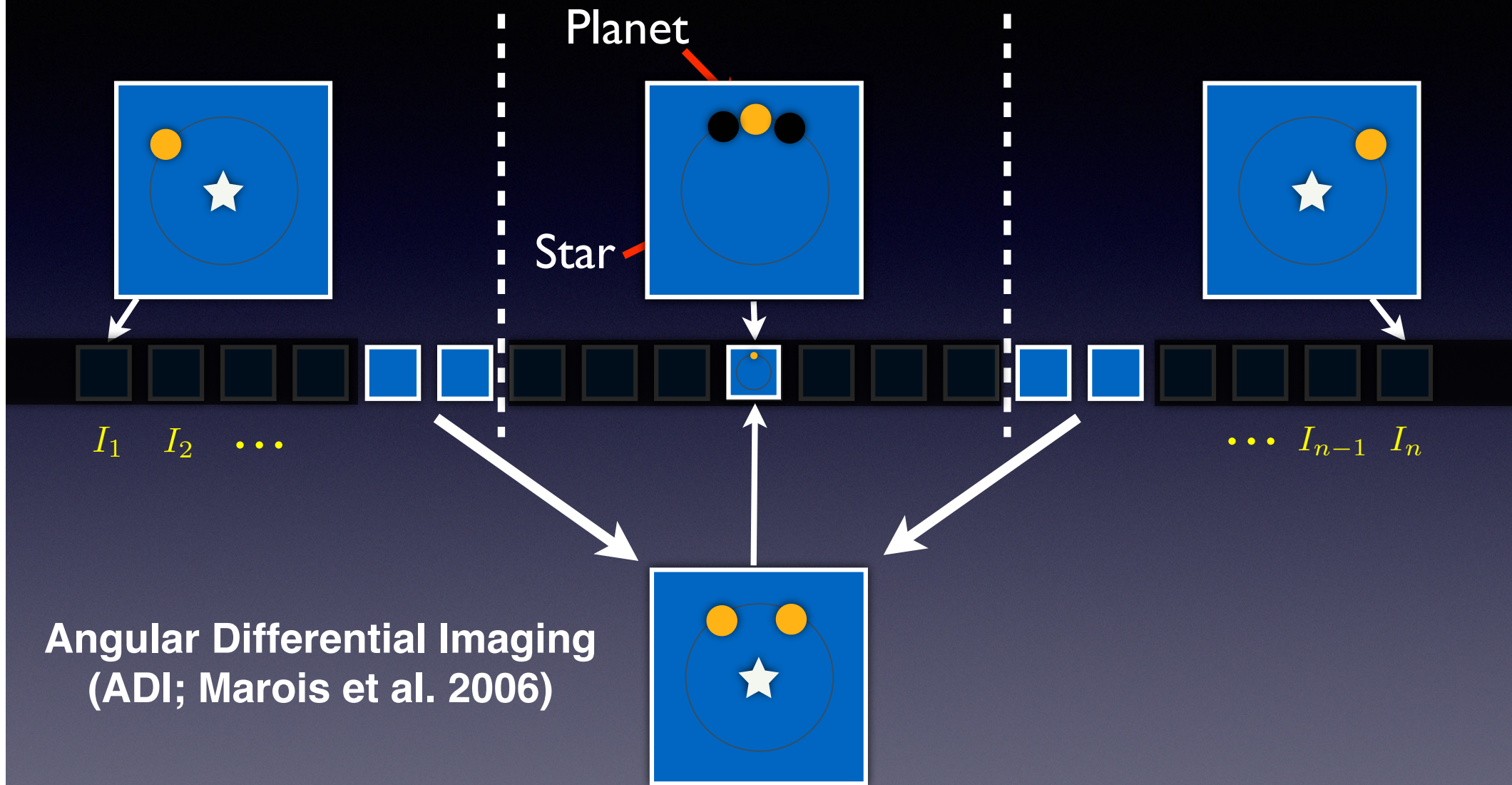
Quanz et al. (2010)

What do we want?

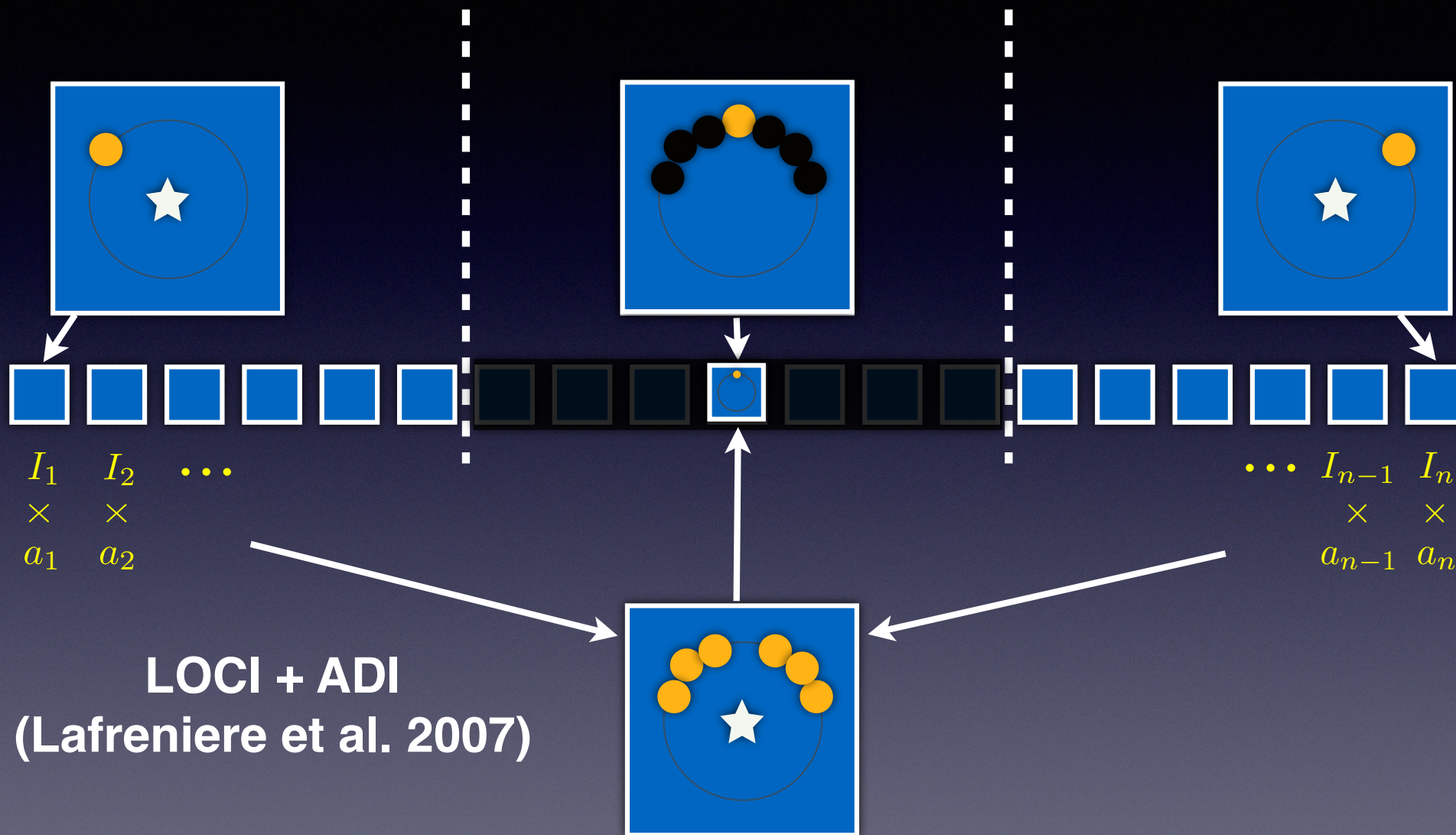
**The instrumental PSF
for each Science Camera Image**



Approximating the Science PSF

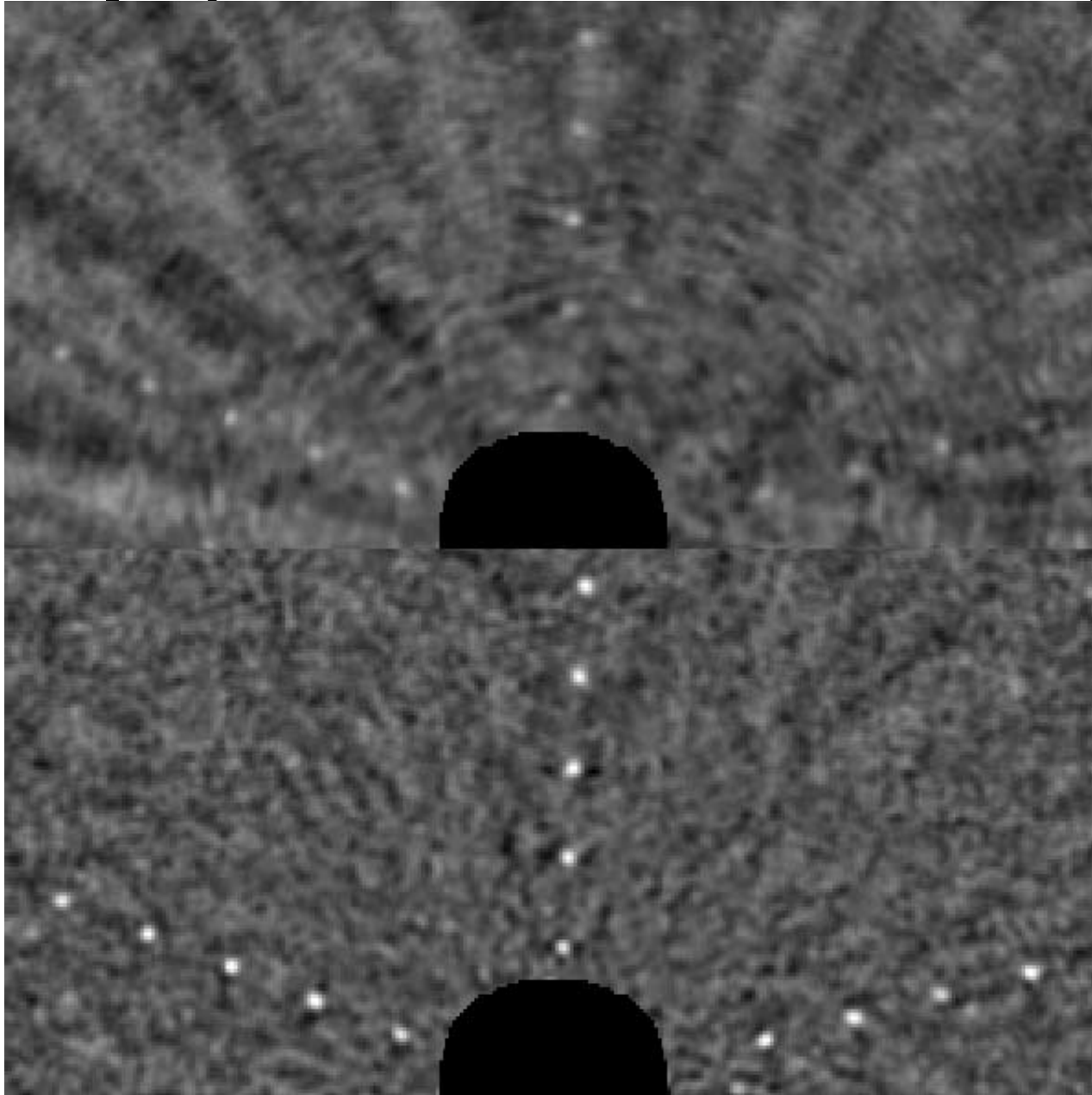


Approximating the Science PSF



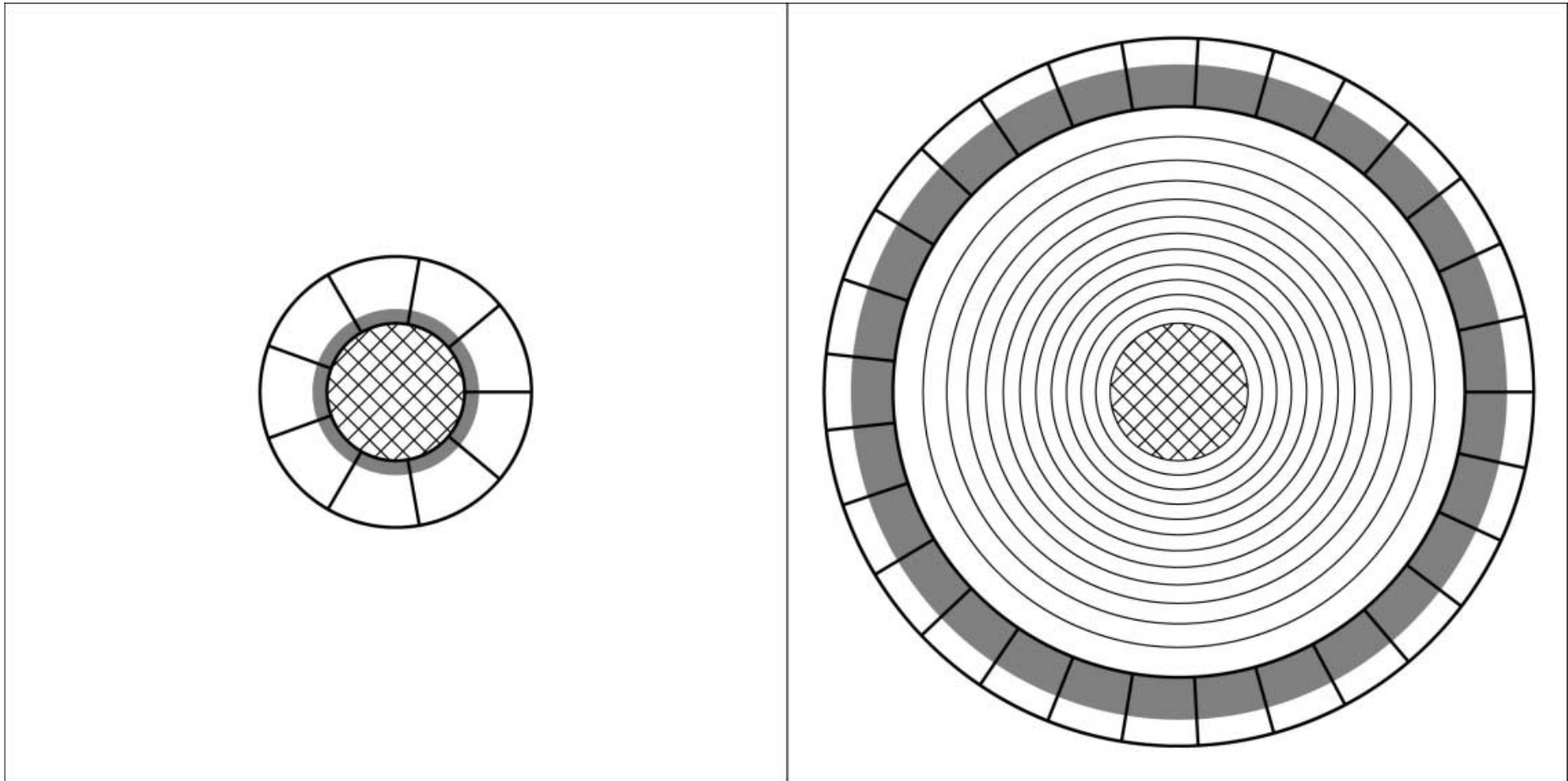
LOCI

Locally Optimised Combination of Images



LOCI

Locally Optimised Combination of Images

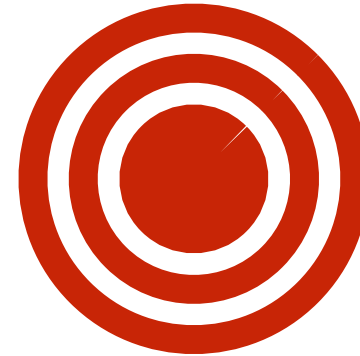


Optimization region geometry a challenge

Stars and Planets



Typically $1e4$ to $1e9$
times brighter than
planet



Spatially separate
from the star
Photons are
incoherent from the
stellar photons

Diversity and Algorithms

Diversity: The property that differentiates planets from speckles
(e.g. Angular, Temporal, Spectral....)

and

Algorithm: The method used to combine the images to make a PSF based on the Diversity
(e.g. LOCI, PCA)

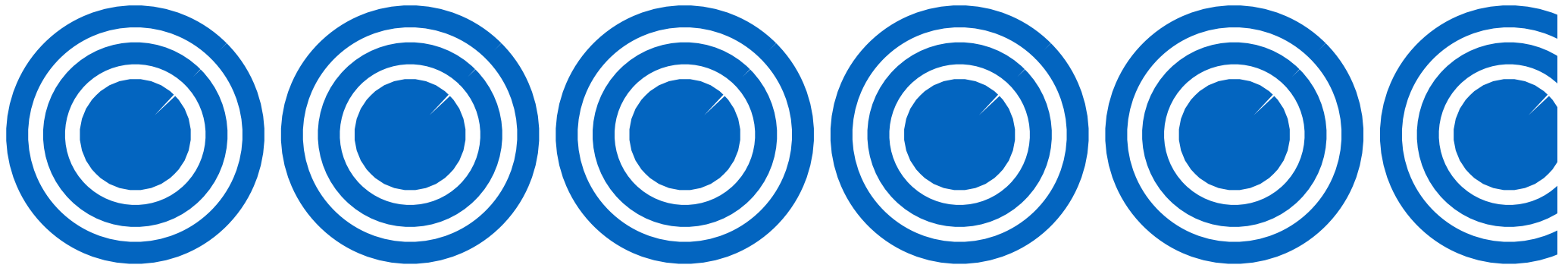
Diversity and Algorithms

**So you can have:
ADI-LOCI, SDI-KLIP, and combinations
of different diversities as well!**

Diversity and Algorithms

Name	Diversity/Algorithm	Paper
ADI	Angular Differential Imaging	Marois 2006
LOCI	Locally Optimised Combination of Images	Lafreniere 2007
ANDROMEDA		Mugnier 2008
SOSIE	ADI/SSDI/RSDI and LOCI	Marois 2010
PynPoint	Principal Component Analysis	Amara 2012
KLIP	Principal Component Analysis	Soummer 2012
DLOCI	Damped LOCI	Pueyo 2012
TLOCI	Template LOCI	Marois 2014
MLOCI	Matched LOCI	Wahhaj 2015
SADI	SDI+ADI	Rameau 2015

Diversity



I_1

I_2

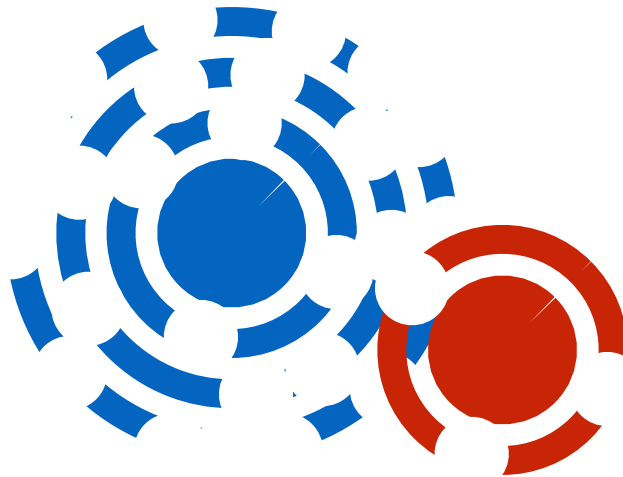
I_3

...

I_n where $n = 1, 2, 3, \dots, N$

Angular Diversity

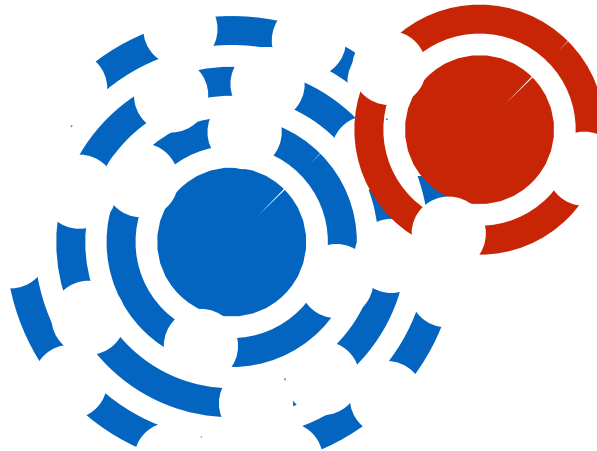
$$I_n = I(\theta_n, t_n)$$



The telescope optics are fixed with respect to the science detector and the sky rotates around

Angular Diversity

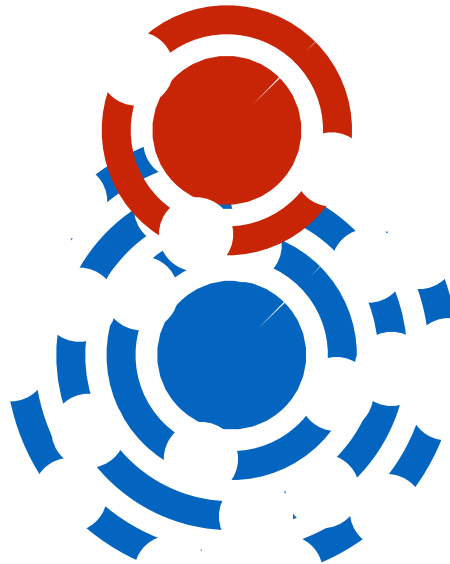
$$I_n = I(\theta_n, t_n)$$



The telescope optics are fixed with respect to the science detector and the sky rotates around

Angular Diversity

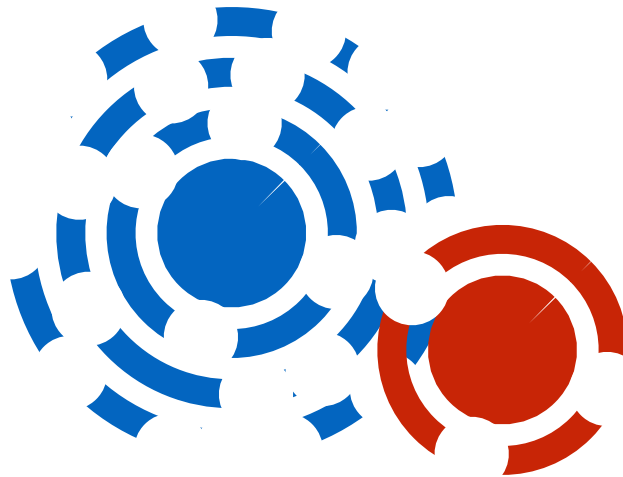
$$I_n = I(\theta_n, t_n)$$



The telescope optics are fixed with respect to the science detector and the sky rotates around

Spectral Diversity

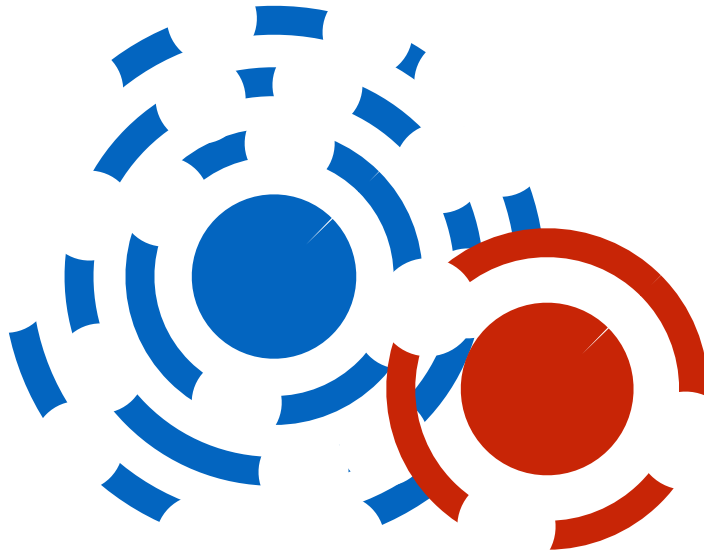
$$I_1 = I(\lambda_1)$$



**PSF scales as $\frac{\lambda}{D_{tel}}$ but the planet remains
in the same position**

Spectral Diversity

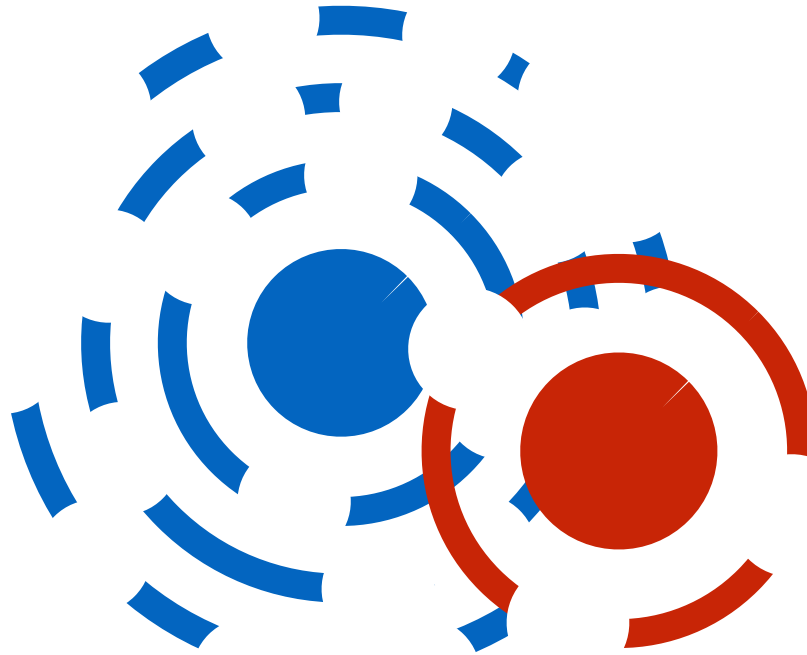
$$I_2 = I(\lambda_2)$$



**PSF scales as $\frac{\lambda}{D_{tel}}$ but the planet remains
in the same position**

Spectral Diversity

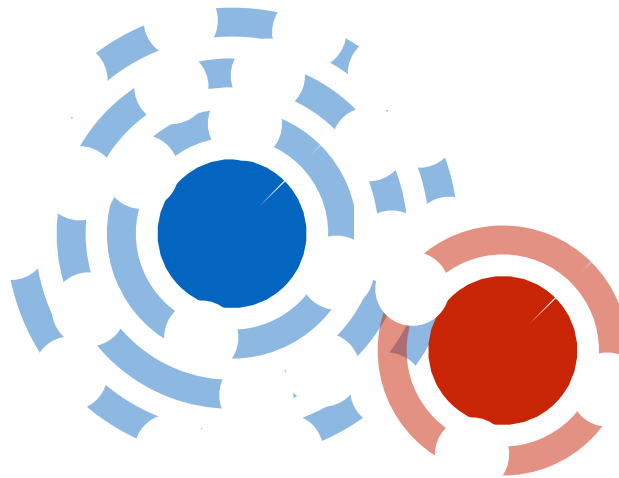
$$I_n = I(\lambda_n)$$



**PSF scales as $\frac{\lambda}{D_{tel}}$ but the planet remains
in the same position**

Intensity Diversity

Gladysz 2008,2009,2010



$$\langle I(r < \lambda/D) \rangle \neq \langle I(r > \lambda/D) \rangle$$

**Airy core intensity has different statistics
from the speckle halo statistics**

Intensity Diversity

Gladysz 2008,2009,2010

**Different AO correction
gives different shaped
histograms**

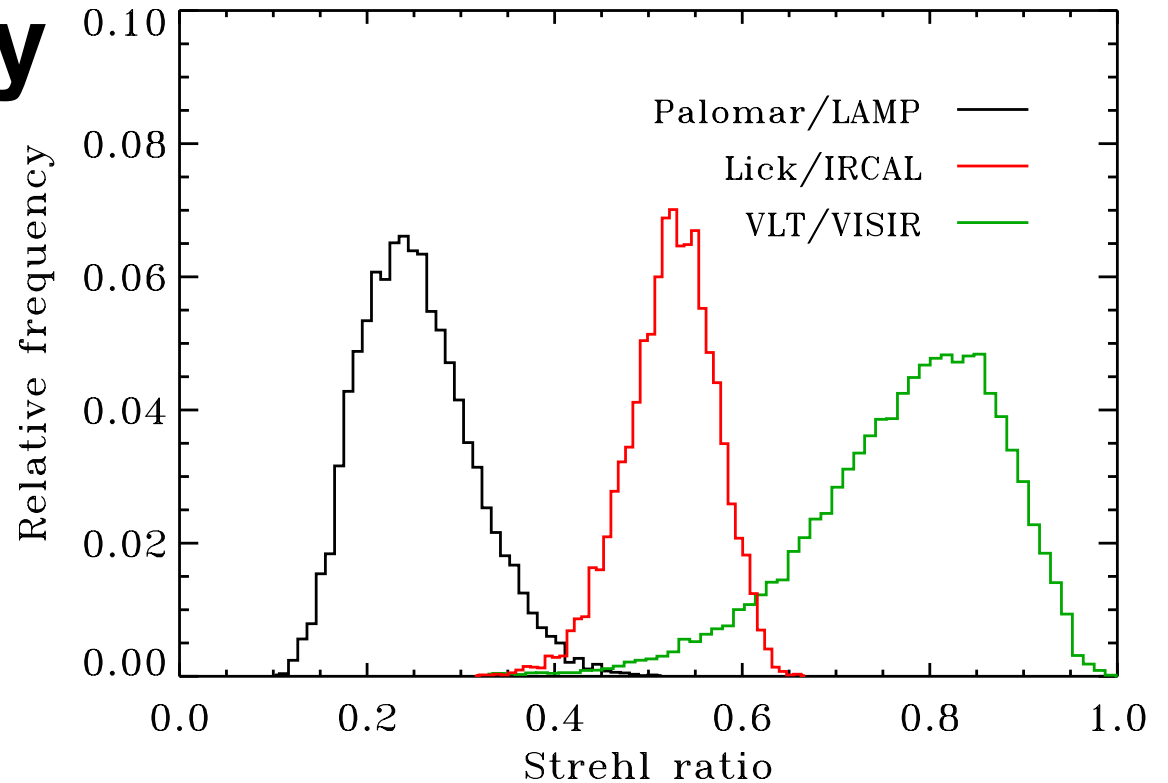
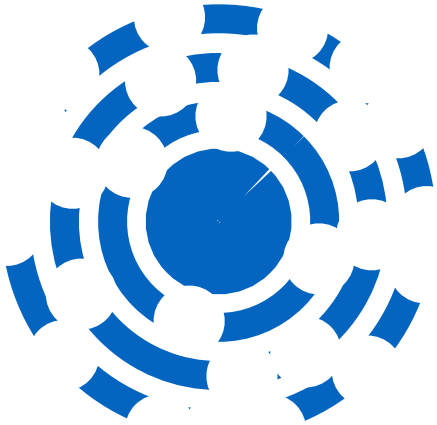
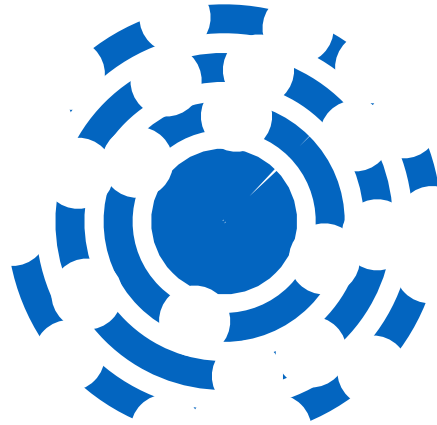


Fig. 1. (Color online) Histograms of the “instantaneous” SRs measured on 5 m Hale Telescope at the Palomar Observatory (LAMP detector, wavelength $0.95 \mu\text{m}$, 10^4 images, exposure time 20 ms, natural guide star AO), 3 m Shane Telescope at the Lick Observatory (IRCAL detector, $2.2 \mu\text{m}$, 10^4 images, exposure time 22 ms, natural guide star AO), and 8 m Very Large Telescope at the Paranal Observatory (VISIR detector, $10 \mu\text{m}$, $3 \cdot 10^4$ images, exposure time 10 ms, no AO compensation). We define instantaneous SR as ratio of peak value of a single short exposure to that of the diffraction-limited image. Data courtesy of Nicholas Law (University of Toronto) and Eric Pantin (CEA Saclay).

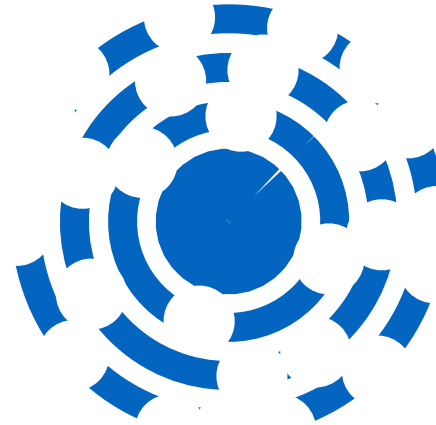
PSF Library



$$I_1 = I(\text{Star 1})$$



$$I_2 = I(\text{Star 2})$$



$$I_3 = I(\text{Star 3})$$



...

**Use other stars in the same field of view
AND/OR in the same night**

Algorithms

We want the science PSF for all images m

$I_{(m, \text{science PSF})}$ for $m = 1, 2, 3, \dots, N$

...but that doesn't exist as there's a planet/
disk in all the images!

We approximate by **linearly combining** all
the PSF images and the challenge is to find
the best coefficients so that

$$I_{(m, \text{science PSF})} \approx I_{(m, \text{PSF estimate})}$$

$$I_{(m, \text{PSF estimate})} = a_{(1, m)} \cdot I_1 + a_{(2, m)} \cdot I_2 + a_{(3, m)} \cdot I_3 + \dots$$

A linear combination of all the PSFs

$$I_{(m,\text{science PSF})} \approx I_{(m,\text{PSF estimate})}$$

where

$$I_{(m,\text{PSF estimate})} = a_{(1,m)} \cdot I_1 + a_{(2,m)} \cdot I_2 + a_{(3,m)} \cdot I_3 + \dots$$

...or more compactly....

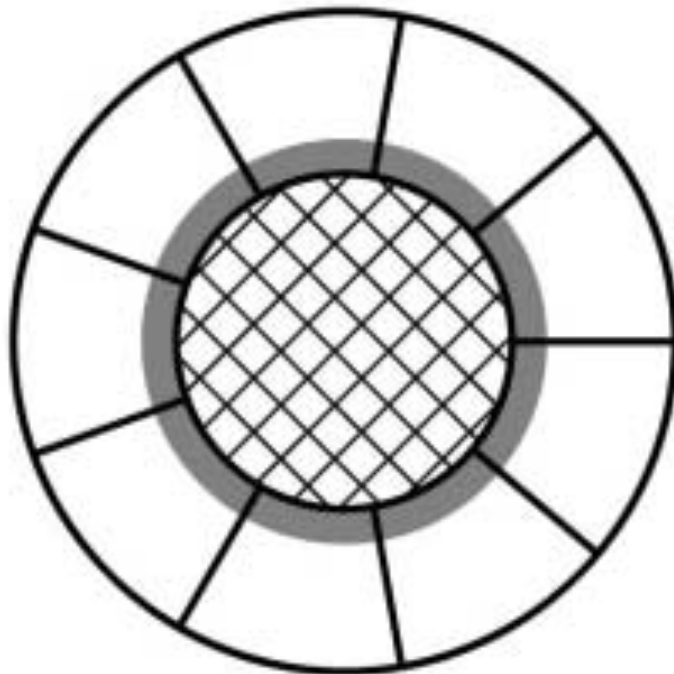
$$I_{(m,\text{PSF estimate})} = \sum_N^{n=1} a_{(n,m)} \cdot I_n$$

We need to determine all the values of $a_{(n,m)}$

Locally Optimised Combination of Images (LOCI) Lafreniere et al. (2007)

PSF is cut into small radial and azimuthal wedges

A linear combination of all the science PSFs is chosen to
minimise the R.M.S. within a small area

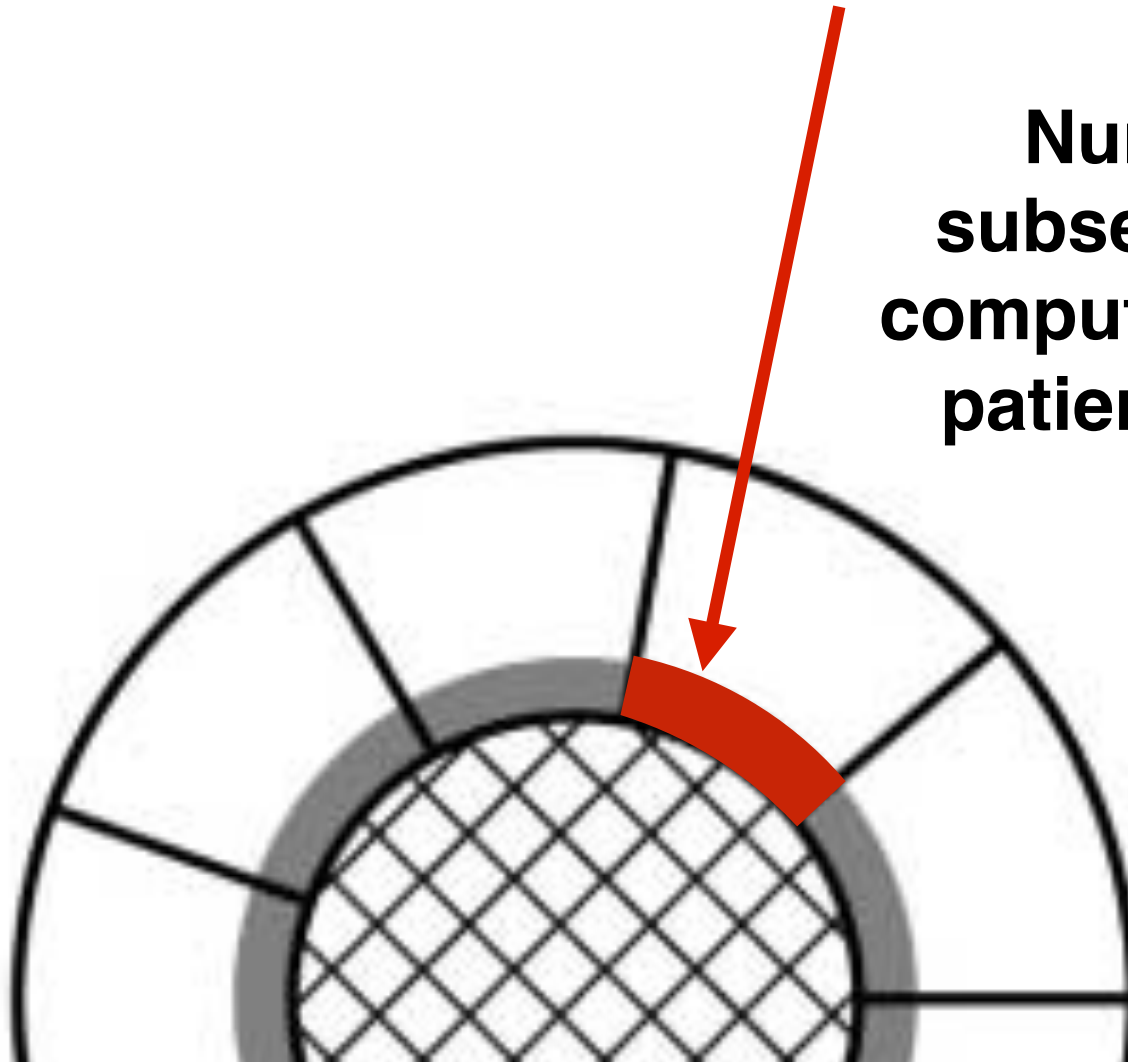


Example of 9
wedges at a given
radius around a
central star

LOCI

For each wedge subsection S^T

Number of wedge subsections limited by computer power and your patience in doing this!



LOCI

and Optimisation subsection O^T

$$A = N_A \pi \left(\frac{W}{2} \right)^2, \quad (1)$$

where W is the full width at half-maximum (FWHM) of the PSF; N_A thus corresponds to the number of “PSF cores” that fit in the optimization subsection.

Size of O^T is determined by how many diffraction patches can fit in it - minimises the self-subtraction problem



Linear combination

You determine what a coefficients will minimise

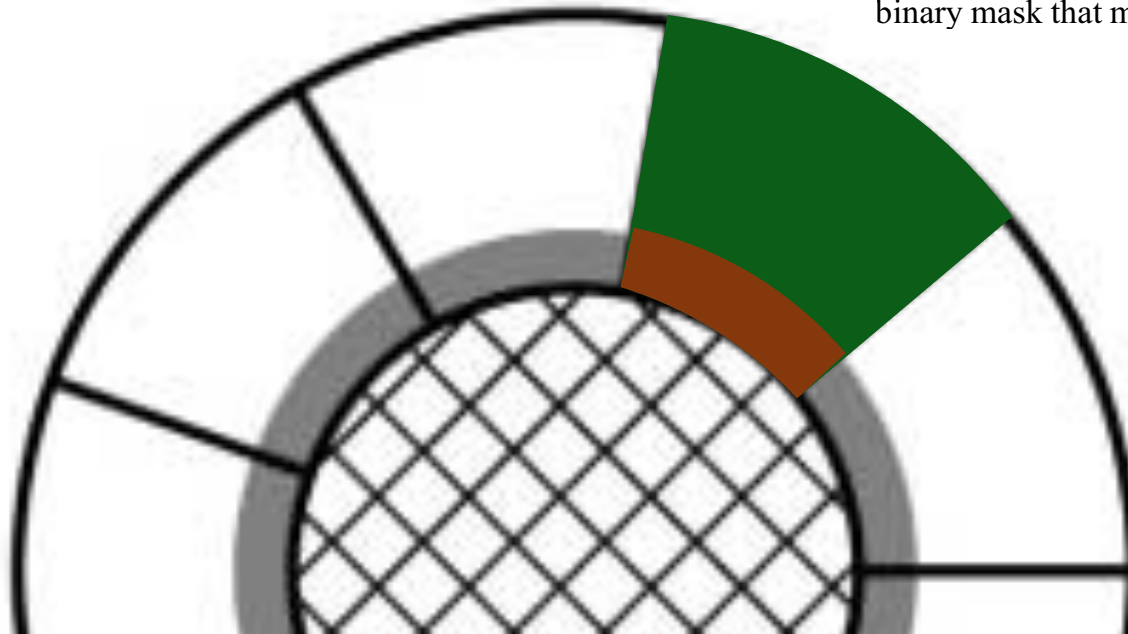
The reference PSF for the optimization subsection is then constructed according to

$$O^R = \sum_{k \in K} c^k O^k, \quad (3)$$

where the coefficients c^k are to be determined by the algorithm. They are computed by minimizing the sum of the squared residuals of the subtraction of O^R from O^T , which is given by

$$\sigma^2 = \sum_i m_i (O_i^T - O_i^R)^2 = \sum_i m_i \left(O_i^T - \sum_k c^k O_i^k \right)^2, \quad (4)$$

where i denotes a pixel in the optimization subsection and m is a binary mask that may be used to ignore some pixels. The quan-

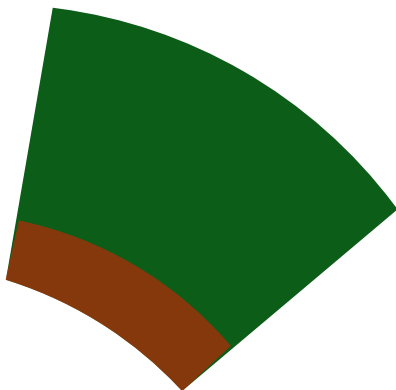


Multiple parameters to “tune up”

TABLE 1
PARAMETER VALUES USED FOR OPTIMIZATION

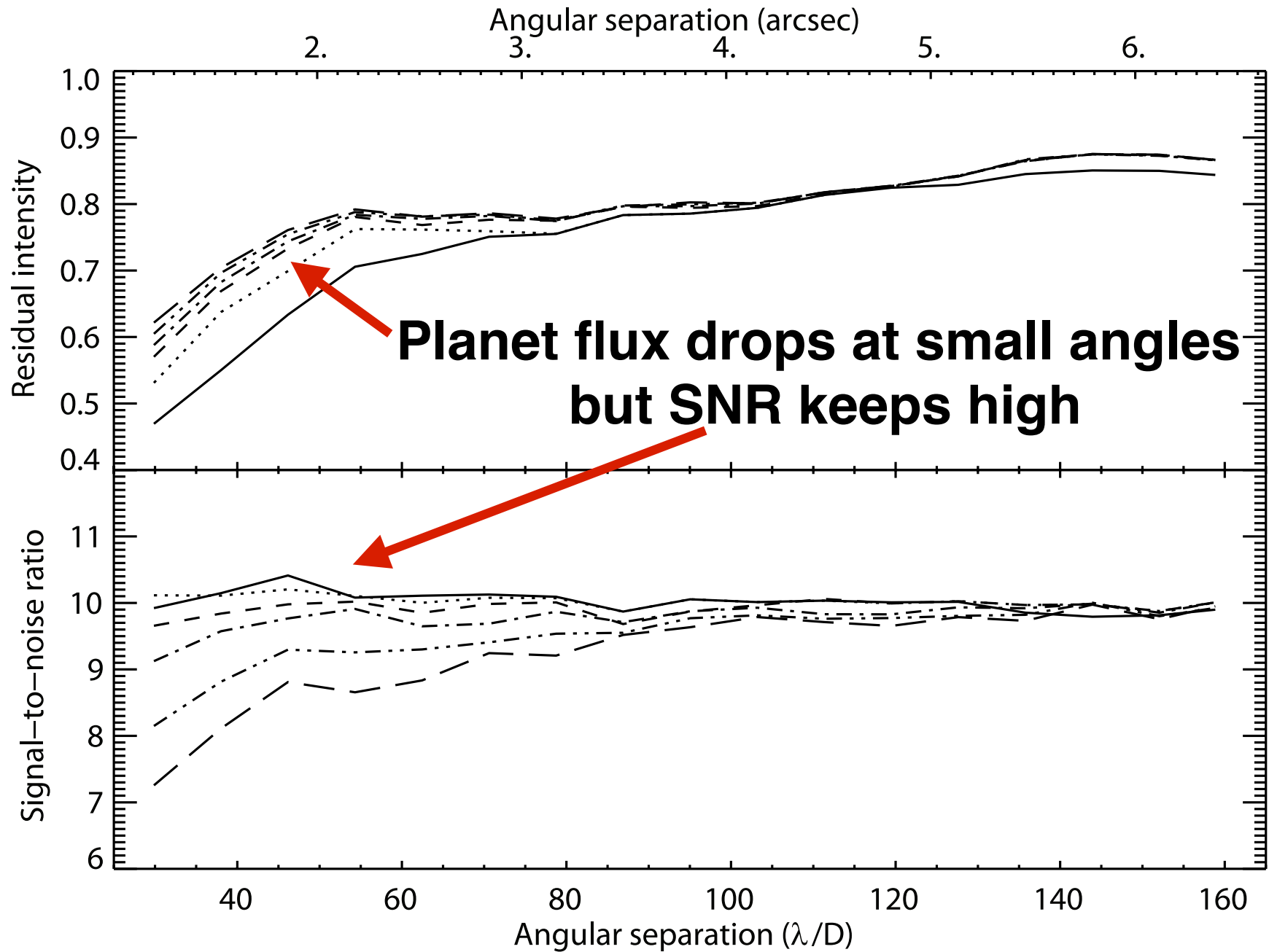
Parameter	Trial Values	Adopted Value	
N_δ	0.25, 0.5, 0.75, 1.0, 1.5, 2.0	0.5	FWHM shift
N_A	50, 100, 150, 300, 500	300	# of FWHM
g	0.5, 1.0, 2.0	1.0	ratio of width to height
dr	1.5, 3, 6, 9, 15, (1.5–15) ^a	(1.5–15) ^a	Width of annuli

^a We use $dr = 1.5$ for separations less than $60\lambda/D$ and $dr = 15$ for larger separations.

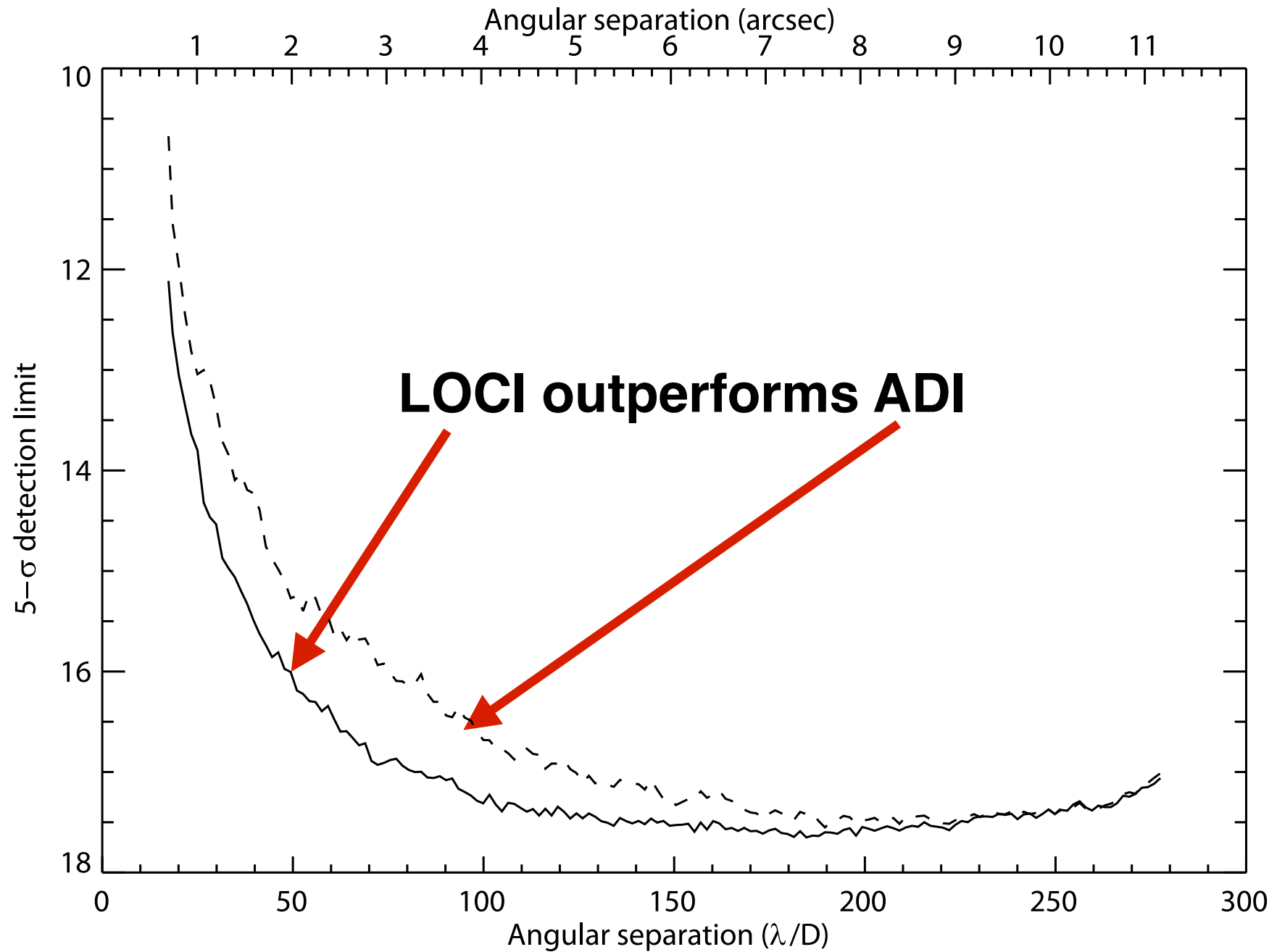


LOCI has several parameters that need to be optimised for each data set and for each planet radial distance. This is a BIG parameter space to explore.....

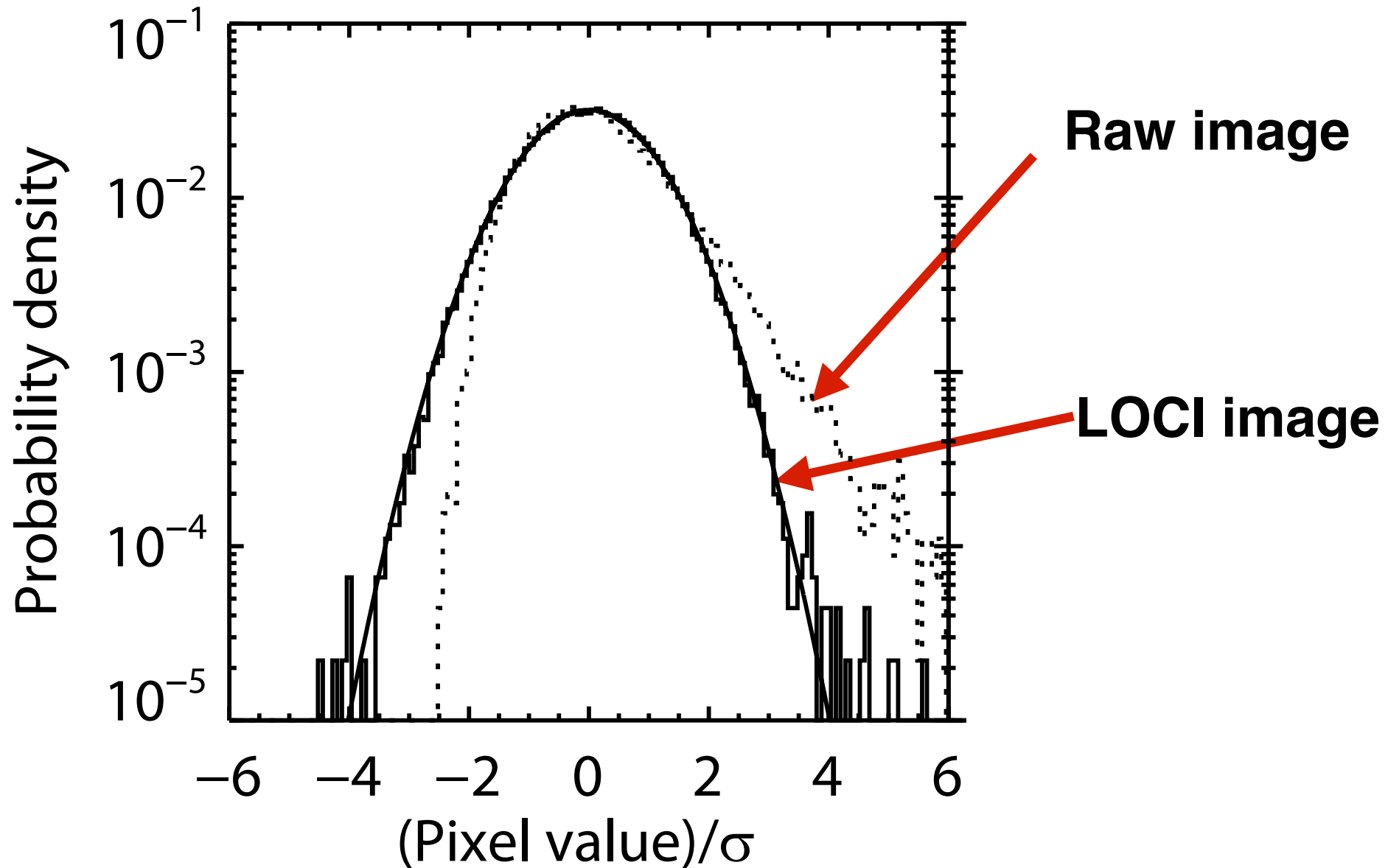
Self-subtraction



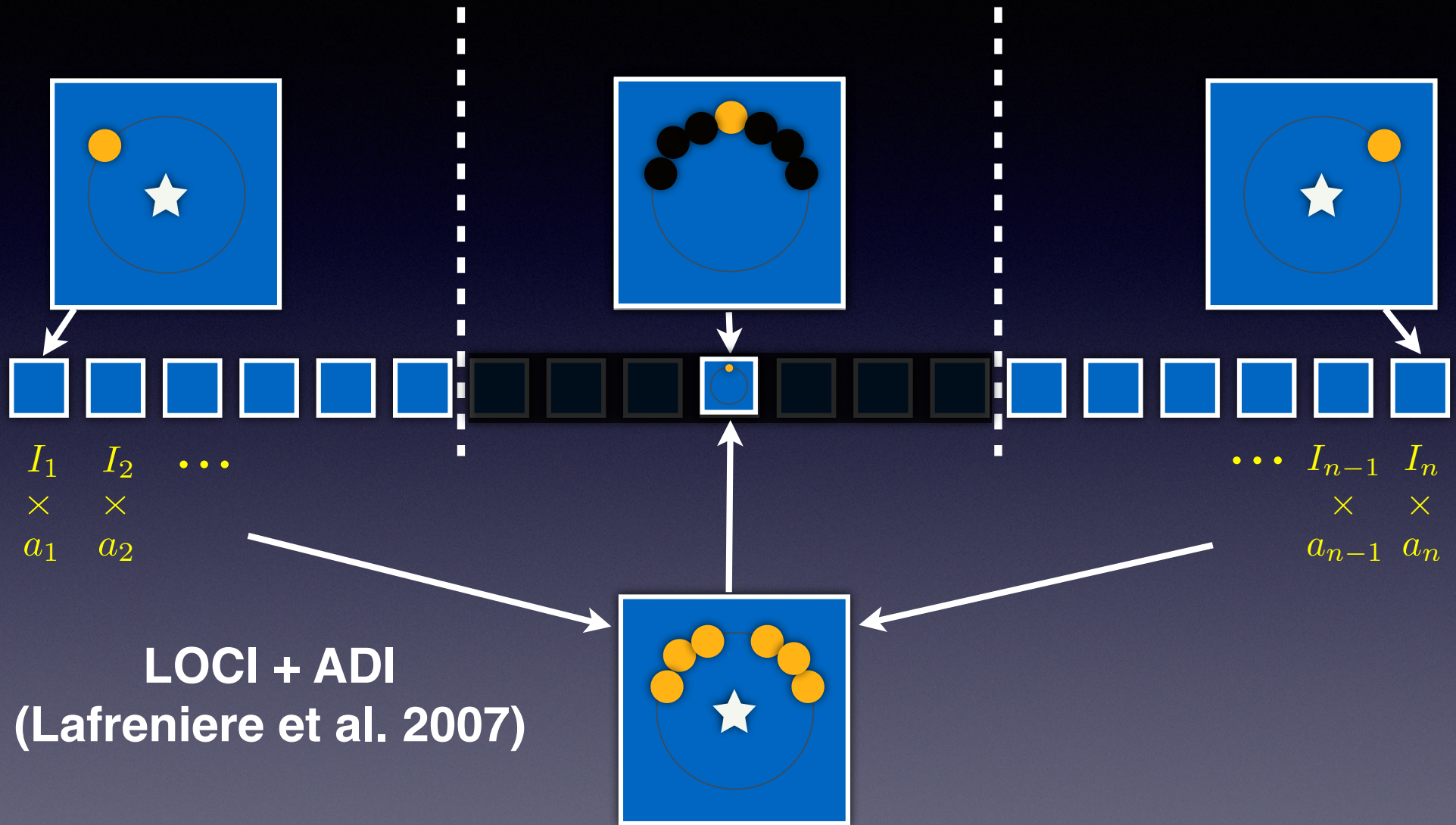
LOCI gain over ADI



Statistical distribution of LOCI pixels is closer to Gaussian



Approximating the Science PSF



PynPoint / KLIP

Amara and Quanz 2012 / Soummer et al. 2012

Any science image can be thought of as a linear combination of an orthogonal basis set formed from all the science images.

$$I(\vec{x}) = \sum a_i \phi_i(\vec{x}), \quad (1)$$

where $I(\vec{x})$ is the image of the PSF, $\phi(\vec{x})$ is a given basis and a_i is the coefficient for each basis function.

Instead of small wedges, the whole stack of images is taken and a Principal Component Analysis (PCA) is performed on it.

Singular Value Decomposition (SVD)

Take stack of input images, and subtract off the mean from all of them, then form a 2-D array \mathbf{S} where each row i is the unravelled version of image i .

means that \mathbf{S} has dimensions $\mathbf{M} \times \mathbf{N}$, where \mathbf{N} is the number of pixels in an image and \mathbf{M} is the number of images in a stack. We calculate the SVD such that

$$\mathbf{S} = \mathbf{U}\mathbf{W}\mathbf{V}^{\mathbf{T}}, \quad (4)$$

where \mathbf{W} is a diagonal matrix with positive (or zero) elements. In this decomposition, \mathbf{V} is a matrix containing the PCA elements that form an orthogonal basis set (\mathbf{U} and \mathbf{V} are column-orthogonal matrices).

SVD example

Input is a set of images of faces:



http://www.eos.ubc.ca/research/cdsst/Tad_home/eigenfaces.html

Produce orthogonal eigenmodes

After SVD, output looks like this:



http://www.eos.ubc.ca/research/cdsst/Tad_home/eigenfaces.html

eigenfaces!

Can now use the eigenfaces and linearly fit them to any of the original data using just a few coefficients



http://www.eos.ubc.ca/research/cdsst/Tad_home/eigenfaces.html

PynPoint / KLIP

Amara and Quanz 2012 / Soummer et al. 2012

Now linearly fit each image with just a few of the lowest PCA components (typically 2 to 10)

$$I(\vec{x}) = \sum a_i \phi_i(\vec{x}), \quad (1)$$

where $I(\vec{x})$ is the image of the PSF, $\phi(\vec{x})$ is a given basis and a_i is the coefficient for each basis function.

PynPoint

Amara and Quanz 2012

